Doctoral Dissertation

Micro-fabrication by Different Approaches of Irradiation on Biocompatible Polymer-modified Surfaces

Department of Advanced Nano- and Biosciences

Graduate School of Innovative Life Sciences

UNIVERSITY of TOYAMA

2016

Lifu Li

平成 28 年度 博士学位論文

生体適合性高分子による表面改質
および微細加工に関する研究

生命融合科学教育部 先端ナノ・バイオ科学専攻

氏　　名　　李 黎夫

指導教員　　遠田 浩司

CONTENTS

Chapter 1

Introduction

1. 1 General introduction

Materials interface is a place which contacts with outside and another substance, and belongs to a very important property of materials. Researches on the chemical/physical phenomena of interface and its functional expression have been emphasized and developed in a wide range of advanced fields, including materials science and life science. Interface shows completely different properties according to the different bulks, and the analysis of interface is very complicated as W. Puli (1900~1958, 1945 year Nobel Prize in Physics) said, "God made solids, but surfaces were invented by Devil".[1] Recently, it has become possible to elucidate the various properties of interfaces by the exercise ingenuity in the field of molecular design. However, advanced analytical techniques and equipment remain to be developed.

With the development of science and technology, it is necessary that the performance and functionality of materials have also become diversified, and simple materials are not enough to cope with the complicated application for the advanced researches. Therefore, many studies on the surface modification methods and techniques have been developed, such as the introduction of polymer with various functionalities, which increase the functions of the material surface. The polymer materials are well known that it can change significantly the interaction with surrounding environment or the characteristics of configured material itself, by various functional groups in the molecule units. Therefore, it is possible to control the interesting

physical properties of the soft-interfaces between the polymeric material and the gas or liquid. The technique is not only industrially applied, but also in various bioscience-related fields.

Recently, studies of polymeric material in the medical and biological fields has been attracting, and biomaterials are used in the medical field and biotechnology, have become to be widely recognized as the special substance, which can be applied in the living body. As the biomaterial is usually introduced into the living body and it is usually required to have high compatibility with the living body, the development of biomaterial has become very indispensable for the advances of medicine. In fact, many researches and developments have been conducted for modification techniques on the surface of medical materials/biomaterials by functional polymer. These techniques are applied in a wide range from an artificial organ indwelled in the body, to the treatment instrument or testing devices in the body, such as intravascular catheters, guidewires and biosensors. Various characteristics including thrombus formation suppression capability of the material surface, friction resistance ability in the body and specific cognitive ability, are required as an effective method to improve QOL (Quality of life) of the medical field, which means stress reduction, improvement of inspection accuracy and surgery operability. It is known that the zwitterionic-polymer-coated surface of the material mimics the structure of lecithin in the cell membrane and has both positive and negative charge in molecule units. As a result, it has the properties to suppress protein/cell nonspecific adsorption/adhesion and can inhibit the thrombus formation due to the biocompatibility and hemocompatibility. Furthermore, it has been expected to be applied in biomaterials.[2-4] In terms of cell membrane imitation, the sugar-carrying macromolecule that mimics the structure/function of sugar chains on cell surfaces is also included in its category, and utilized as a purpose to investigating the specific recognition ability of glycosylic acceptor at the solution-polymer interfaces.[5,6]

The one of the approach using surface modification with cell membrane-mimic polymer is the “surface patterning”, by which proteins and cell patterning is also possible for preparation.

Therefore, the development of various functional materials can be expanded into the analysis tools of individual functions/interactions of intercellular, multi-screening cell array of drugs.

Although many approaches have been proposed until now, the patterning by ultraviolet (UV) or ion beam (IB) could be mentioned because of excellent convenience and precision.[7,8] In the case of UV irradiation, UV irradiation apparatus and the photo mask for the purpose is required, but it is possible to produce a complex pattern of submicron order. On the other hand, IB irradiation, by utilizing gallium ion beam device for general microfabrication, is possible to produce a micro-pattern in a range from submicron order to several nanometers.

As mentioned above, the functional materials would be created when combined with the biocompatible polymer and light patterning for surface modification. In this thesis, the author examined the surface modification by UV/IB irradiation and the patterning of biological substances on the surface modified by a polymer consisting of Poly[2-deoxy-2-*N*-(2-methacryloyloxyethyl)aminocarbamyl *D*-glucose] (PGUMA, one type of the sugar-bearing polymers) or Poly[1-carboxy-*N*,*N*-dimethyl-*N*-(2-methacryloyloxyethyl) methanaminium hydroxide inner salt] (PCMB, one type of the zwitterionic polymers).

1.2 Self-Assembled Monolayer (SAM)

Self-assembled monolayer (SAM) means as organized membrane spontaneously formed by only immersing the substrate in a solution of the target molecule. Either organosulfur SAM using organic sulfur such as alkanethiols and organosilane SAM using a silane-coupling agent, has been most widely studied.

SAMs have been studied by a large number of scientists and are applied in various fields such as coating of the metal nano-particles/silica particles, surface modification, and molecular sensing.[9-13] For example, Whitesides et al. used alkanethiols and thiolatedoligoethylene glycol to form the interface, which suppresses the non-specific adsorption of proteins and cells.[14, 15] The main formation process of SAM is shown below. It should also been noted that there are still many problems about SAM, such as what is the driving force of self-organization, and how the SAM grows.

The main reaction of alkanethiols SAM is resulting in a chemical adsorption (Au-S bond in case of gold) with a metal surface while arranged in a certain extent such as by hydrophobic interaction of the carbon chain in solution. Furthermore, as the main reaction of the silane-coupling agent, the Si-O-R bond is hydrolyzed to silanol group by water, and partially becomes oligomeric via the condensation reaction. Then, it is adsorbed on the mineral surface via the hydrogen bonding, and cause the dehydration condensation reaction by drying treatment of the inorganic material to become a strong chemical bond.

(a)

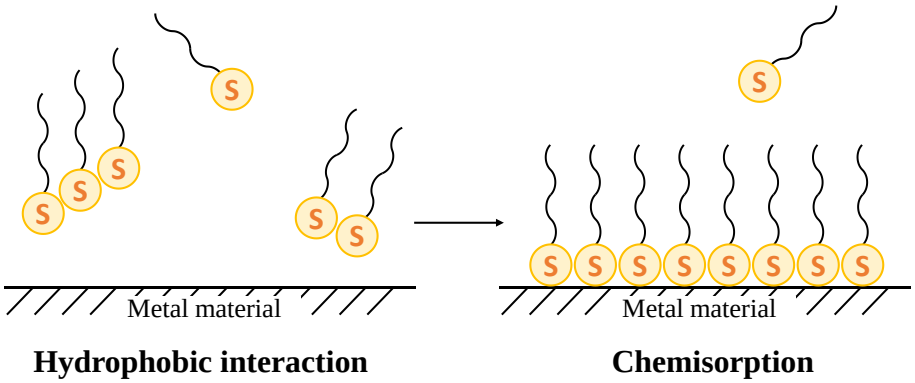

Hydrophobic interaction **Chemisorption**

(b)

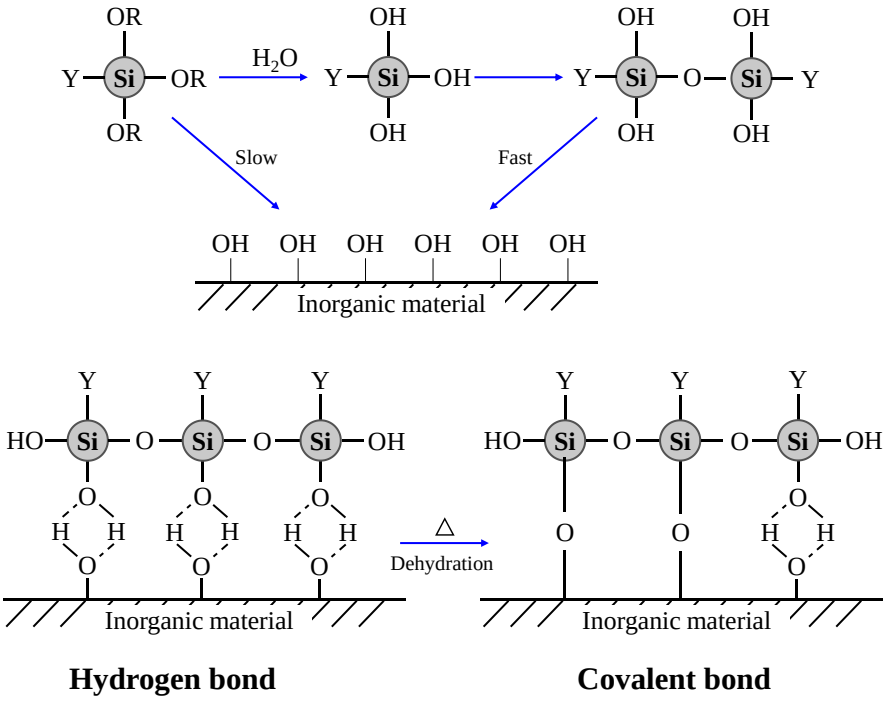

Hydrogen bond **Covalent bond**

Figure 1-1. Formation of self-assembled monolayer (SAM). (a) Organosulfur SAM and (b) Organosilane SAM.

1.3 Polymer Brush

The polymer chains, which are self-assembled into the interfaces, are classified into a type of SAM in a broader sense. The structure/physical properties are believed to strongly depend on the graft density. Generally, the polymer chains become coiled when the graft density is low. However, when the graft density is raised to a region where the polymer chains contact each other, it can get a structure that extend from the surface in the vertical direction due to osmotic effects. This state is called as polymer brush, which has become an important research area in academic fields because the properties such as the adhesiveness/friction characteristic/dispersibility will become possible to control this state.

Method to form a polymer brush in two-dimensional interface is usually classified into two types: (1) the extrapolating graft derived from the preformed polymer chain with a functional group such as thiol or disulfide binding to the surface via physical adsorption or covalent bonding ("grafting-to" method); (2) the surface-initiated graft is polymerized from the surface-confined initiator ("grafting-from" method).

In particular, the study of "grafting-from" method has been conducted actively in various fields as an effective method of surface modification/functionalization, because the relatively high grafting density can be expected. However, by the "grafting-to" method, it is difficult to precisely control the chain length and the molecular weight distribution, and the accomplished grafting density may be limited to the area called "semi-dilute polymer brushes".[16-19]

The grafting-from method is also used by a kind of precise living radical polymerization method. The synthesis of "concentrated polymer brushes" grafting at dramatically high density has been actively studied.[20-24] Furthermore, the graft chain is not only found to be highly stretched (oriented) comparable to the fully extended chain in the good solvent, but also this membrane derived from high-density graft has been demonstrated to exhibit unique properties, which cannot be obtained by conventional mere "grafting-to" method. The polymer brushes

prepared by the "grafting-from" method show the large steric repulsion force abnormally/ ultra-low friction characteristic/ size exclusion effect of the brush/ excellent thermodynamic behavior characteristics.

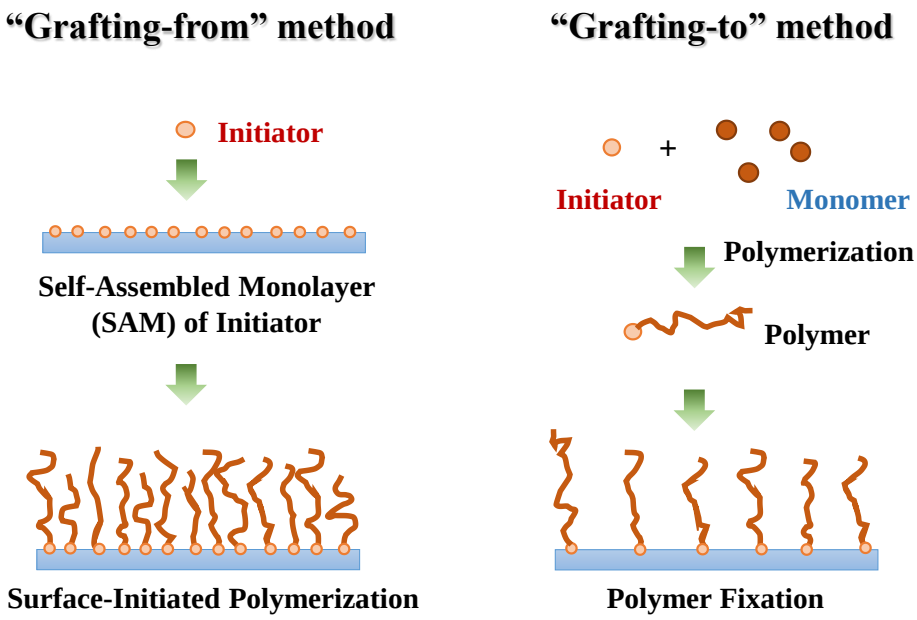

Figure 1-2. Schematic presentation for constructing polymer brushes.

1.4 Atom Transfer Radical Polymerization (ATRP)

Atom transfer radical polymerization (ATRP) is a kind of living radical polymerization (LRP) that has been developed by Jin-Shan Wang, Matyjaszewski (1995) and Sawamoto (1994-5) et al. As precision polymerization method with the convenience/versatility which is easily able to obtain a polymer of different composition (homopolymer, random, block, graft) and shape (linear, star, comb-shaped, multi-branched), it showed rapid progress, and came to be used for the synthesis of a variety of new materials.[25-44]

Although the radicals irreversibly occur in conventional free radical polymerization, the LRP shows reversible radical formation, further controllable polymerization in equilibrium between initiation stage and propagating stage (**Scheme 1-1**). Especially, ATRP is a method using the transition metal complex, and the reaction includes the following: reversible transfer reaction of halogen group from the dormant species (R-X) to the transition metal (M_t^n/Ligand), and a reaction that produces the radical initiating the polymerization and the metal halide (X-M_t^{n+1}/Ligand) advancing one of oxidation state (**Scheme 1-2**). The kinetics are dependent on various factors such as monomer/ initiators/ the concentration of the reaction medium/ compatibility with the ligand, and it becomes ordinary radical polymerization by conventional uncontrolled redox process when the inactivation process is slower than the growth reaction.

According to the ATRP for the surface-initiated graft of polymer chain on the silicon substrate, the Cu(I)X/L complexes pull the halogen atom of α-position immobilized on the silicon substrate at first, and polymerization is initiated. Then, the initiating radical is capped again with halogen atom by a divalent copper complex (Cu(II)X/L) after few monomer addition. Similarly, the graft chain is able to grow aligned substantially in length because the terminal halogen atom of the polymer is repeated reversibly activated/capping with sufficient frequency.

Further, the polymer growing from the free initiator (free polymer) has been reported to have the similar M_n and M_w/M_n values to those of the graft chain, when the free (unfixed) initiator

was added during the polymerization (**Figure 1-3**). [22]

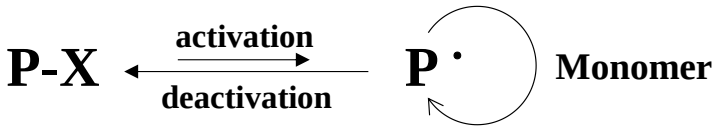

Scheme 1-1. Living Radical Polymerization (LRP).

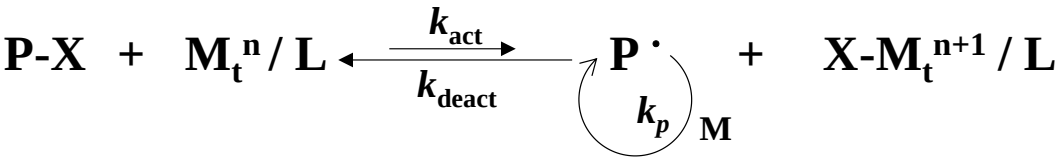

Scheme 1-2. Atom Transfer Radical Polymerization (ATRP).

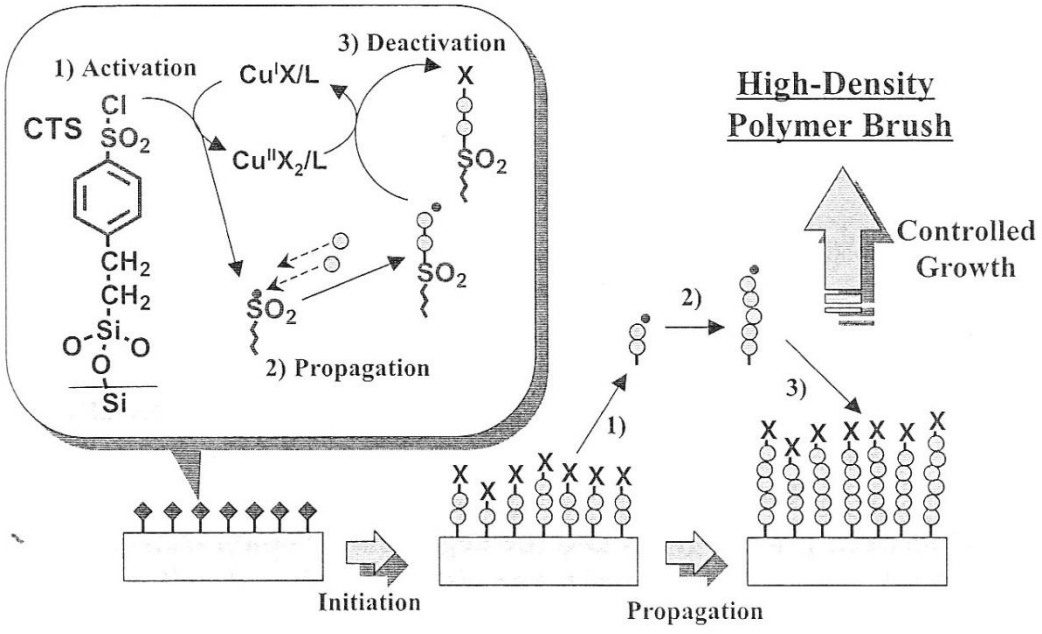

Figure 1-3. Schematic illustration of surface initiated-atom transfer radical polymerization (SI-ATRP). This figure is quoted from reference 20.

1.5 Reversible Addition Fragmentation and Chain Transfer (RAFT) polymerization

The reversible addition fragmentation and chain transfer (RAFT) polymerization belongs to a relatively new category among the living radical polymerization method, which has been found by Rizzardo et al of Commonwealth Scientific and Industrial Research Organization (CSIRO, Australia) (**Scheme 1-3**).[45] The RAFT polymerization has been developed over the past fifteen years because it is able to be applied to wide range of monomer under the variety polymerization conditions.[46-48] In the RAFT polymerization, usual radical polymerization proceeds in the presence of a suitable chain transfer agent (CTA). The chain transfer agent has the substituents R and Z, which affect not only the kinetics, but also the structural control of the product. Generally, dithio ester/ trithiocarbonate/ dithiocarbamate/ dithiocarbonate have been used as a chain transfer agent.

The mechanism of the RAFT polymerization is explained briefly in the following (**Scheme 1-3, (a)-(e)**).

(a) Initiation/Propagation: The growing chain (P_n・) is generated by the addition of radical-yielding initiator to the monomer.

(b) Addition to RAFT agent: Pn・reacts (adds) with the chain transfer agent that has an addable double bond and a substituent group (R) which is desorbed easily as the radical. Then, the radical R・is desorbed (cleaved) from the intermediate 2.

(c) Reinitiation/Propagation: R・reacts with monomer again to generate a new growing chain radical P_m・(chain transfer), and the growing reaction proceeds as it is.

(d) Chain equilibration by reversible addition fragmentation: Because the introduction of the thiocarbonyl group S=C- into polymer terminal enables to pursue the radical addition by the chain transfer, the intermediate 5 can exchange thioester group between growing species as a dormant species.

(e) Termination: Thus, the probability of bimolecular termination is reduced, and the molecular weight and the end group of polymer are precisely controllable.

Such a series of the reaction is called as “addition fragmentation and chain transfer”. The case of each elementary reaction of addition/ cleavage/ chain transfer is reversible and therefore called as “reversible addition fragmentation and chain transfer (RAFT)”, when each elementary reaction of addition/ cleavage/ chain transfer is reversible.

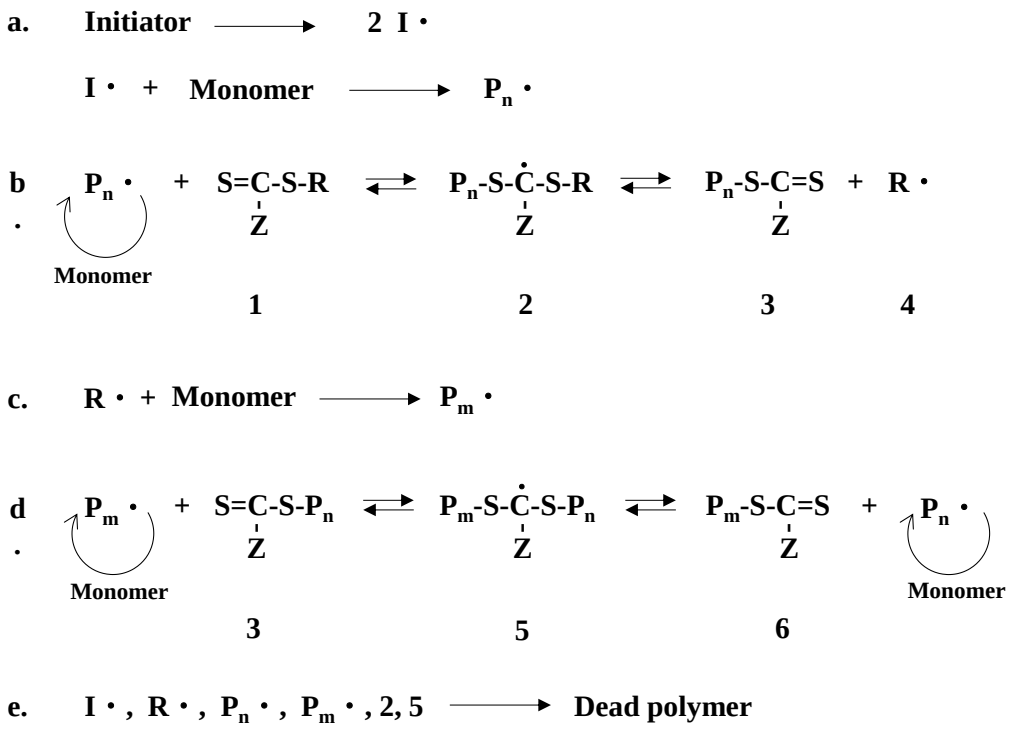

Scheme 1-3. Proposed mechanism of RAFT polymerization.

1.6 Micro-patterning

In recent years, the utilization of polymer patterning has been rapidly developed at wide-ranging fields. The strong interest in the polymer patterning is due to the presence of various synthetic polymers or biopolymers, because various functionality of the polymer can be easily introduced to substrate surface.

The application of patterned polymer surface is broadly classified, (1) Light-emitting displays (LEDs), semiconductor device and fabrication of plastic electronic parts, (2) The bio-pharmaceutical-related research including cell engineering and regenerative medicine, (3) Production of mask and template, (4) Production of optical components such as crystal lattice and (5) Basic research of interface science and combinatorial synthesis.[49]

The microfabrication technology of the polymer surface (lithography) includes photolithography by UV light or X-ray irradiation, electron beam lithography, scanning probe lithography using a scanning tunneling microscope (STM) or atomic force microscope (AFM), and soft lithography. Among them, photolithography is one of the main ways to be used in the patterning of the polymer, particularly in electronic materials. Development of the resist material and photolithography techniques enables the miniaturization of semiconductor elements, and it has been contributed greatly to the semiconductor industry.

Furthermore, by using the micro-fabrication technology cultivated on the semiconductor industry and to control the structure of surface/interface at the molecular level, several studies have been examined to control the cell function. The attempt has been prominent as research trends of regenerative medicine and bio-device. For example, Nishizawa et al. have reported patterned culture technique such as the cell adhesion controlled at single cell level, by patterning a polydimethylsiloxane (PDMS) using soft lithography.[50]

As described above, the microfabrication of the polymer surface occupies an important position in research for cell engineering/ regenerative medicine/ the pharmaceutical field and

optics and electronic materials field.

1-7. References

[1] Jamtveit, B.; Meakin, P. Eds. *Growth, Dissolution and Pattern Formation in Geosystems* **1990,** 291.

[2] Kitano, H.; Tada, S.; Mori, T.; Takaha, K.; Gemmei-Ide, M.; Tanaka, M.; Fukuda, M.; Yohoyama, Y. *Langmuir* **2005**, *21*, 11932.

[3] Fujishita, S.; Inaba, C.; Tada, S.; Gemmei-Ide, M.; Kitano, H.; Saruwatari, Y. *Biol. Pharm. Bull.* **2008**, *31*, 2309.

[4] Tada, S.; Inaba, C.; Mizukami, K.; Fujishita, S.; Gemmei-Ide, M.; Kitano, H.; Mochizuki, A.; Tanaka, M.; Matsunaga, T. *Macromol. Biosci.* **2009**, *9*, 63.

[5] Morokoshi, S.; Ohhori, K.; Mizukami, K.; Kitano, H. *Langmuir* **2004**, *20*, 8897.

[6] Kitano, H.; Gemmmei-Ide, M.; Anraku, Y.; Saruwatari, Y. *Colloids. Surf. B* **2007**, *56*, 188.

[7] Kamada, T.; Yamazawa, Y.; Nakaji-Hirabayashi, T.; Kitano, H.; Usui, Y.; Hiroi, Y.; Kishioka, T. *Colloids. Surf. B* **2014**, *123*, 878.

[8] Suzuki, H.; Li, L.; Nakaji-Hirabayashi, T.; Kitano, H.; Ohno, K.; Matsuoka, K.; Saruwatari, Y. *Colloids. Surf. B* **2012**, *94*, 107.

[9] Ulman, A. *Chem. Rev.* **1996**, *96*, 1533.

[10] Moineau, J.; Granier, M.; Lanneau, G.F. *Langmuir* **2004**, *20*, 3202.

[11] Nomura,K.; Mikuni, S.; Nakaji-Hirabayashi, T.; Gemmei-Ide, M.; Kitano, H.; Noguchi, H.; Uosaki, K. *Colloids. Surf. B* **2015**, *135*, 267.

[12] Nuzzo, R. G.; Allara, D. L. *J. Am. Chem. Soc.* **1983**, *105*, 4481.

[13] Porter, M. D.; Bright, T. B.; Allara, D. L.; Chidsey, C. E. D. *J. Am. Chem. Soc.* **1987,** *109*, 3559.

[14] Bain, C. D.; Troughton, E. B.; Tao, Y. T.; Evall, J.; Whitesides, G. M.; Nuzzo, R. G. *J. Am. Chem. Soc.* **1989**, *111*, 321.

[15] Love, J. C.; Estroff, L. A.; Kriebel, J. K.; Nuzzo, R. G.; Whitesides, G. M. *Chem. Rev.*

2005, *105*, 1103.

[16] Edmondson, S.; Osborne, V. L.; Huck, W. T. S. *Chem. Soc. Rev.* **2004**, *33*, 14.

[17] Zhou, F.; Liu, W.; Xu, T.; Liu, S.; Chen, M.; Liu, J. *J. Appl. Polym. Sci.* **2004**, *92*, 1695.

[18] Sethi, D.; Kumar, A.; Gupta, K. C.; Kumar, P. *Bioconjugate. Chem.* **2008**, *19*, 2136.

[19] Kitano, H.; Hayashi, A.; Takakura, H.; Suzuki, H.; Kanayama, N.; Saruwatari, Y. *Langmuir* **2009**, *25*, 9361.

[20] Tsujii, Y.; Ohno, K.; Yamamoto, S.; Goto, A.; Fukuda, T. *Adv. Polym. Sci.* **2006**, *197*, 1.

[21] Zhang, Z.; Chao, T.; Chen, S.; Jiang, S. *Langmuir* **2006**, *22*, 10072.

[22] Ohno, K.; Koh, K.; Tsujii, Y.; Fukuda, T. *Macromolecules* **2002**, *35*, 8989.

[23] Ohno, K.; Koh, K.; Tsujii, Y.; Fukuda, T. *Angew. Chem., Int. Ed.* **2003**, *115*, 2857.

[24] Matyjaszewski, K.; Miller, P. J.; Shukla, N.; Immaraporn, B.; Gelman, A.; Luokala, B. B.; Siclovan, T. M.; Kickelcik, G.; Vallant, T.; Hoffman, H.; Pakula, H. *Macromolecules* **1999**, *32*, 8716.

[25] Wang, J. S.; Matyjaszewski, K. *J. Am. Chem. Soc.* **1995**, *117*, 5614.

[26] Braunecker, W. A.; Matyjaszewski, K. *Pro. Polym. Sci.* **2007**, *32*, 93.

[27] Kato, M.; Kamigaito, M.; Sawamoto, M.; Higashimura, T. *Macromolecules* **1995**, *28*, 1721.

[28] Kamigaito, M.; Ando, T.; Sawamoto, M. *Chem. Rev.* **2001**, *101*, 3689.

[29] Patten, T. E.; Xia, J.; Abermathy, T.; Matyjaszewski, K. *Science* **1996**, *272*, 866.

[30] Matyjaszewski, K.; Xia, J. *Chem. Rev.* **2001**, *101*, 2921.

[31] Boyes, S. G.; Akgun, B.; Brittain, W. J.; Foster M. D. *Macromolecules* **2003**, *36, 9539.*

[32] Yu, K.; Wang, H.; Han, Y. *Langmuir* **2007**, *23, 8957.*

[33] Lindqvist, J.; Nyström, D.; Östmark, E.; Antoni, P.; Carlmark, A.; Johansson, M.; Hult, A.; Malmström, E. *Biomacromolecules* **2008,** *9*, 2139.

[34] Matsuura, K.; Kitano, H. *Polym. Prep. Jpn.* **2005**, *54*, 1900.

[35] Matsuura, K.; Ohno, K.; Kagaya, S.; Kitano, H. *Macromol. Chem. Phys.* **2007**, *208, 862.*

[36] Lobb, E. J.; Ma, I.; Billingham, N. C.; Armes, S. P.; Lewis, A. L. *J. Am. Chem. Soc.* **2001**,

123, 7913.

[37] Ma, I. Y.; Lobb, E. J.; Billingham, N. C.; Armes, S. P.; Lewis, A. L.; Lloyd, A. W.; Salvage, J. *Macromolecules* **2002**, *35*, 9306.

[38] Ma, I. Y.; Tang, Y.; Billingham, N. C.; Armes, S. P.; Lewis, A. L.; Lloyd, A. W.; Salvage, J. P. *Macromolecules* **2003**, *36*, 3475.

[39] Mu, Q. S.; Lu, J. R.; Ma, Y. H.; Paz de Banez, M. V.; Robinson, K. L.; Armes, S. P.; Lewis, A. L.; Thomas, R. K. *Langmuir* **2006**, *22*, 6153.

[40] Li, Y.; Tang, Y.; Narain, R.; Lewis, A. L.; Armes, S. P. *Langmuir* **2005**, *21*, 9946.

[41] Li, Y.; Armes, S. P.; Jin, X.; Zhu, S. *Macromolecules* **2003**, *36*, 8268.

[42] Chang, Y.; Chen, S.; Zheng, Z.; Jiang, S. *Langmuir* **2006**, *22*, 2222.

[43] Iwasaki, Y.; Akiyoshi, K. *Macromolecules* **2004**, *37*, 7637.

[44] Iwata, R.; Suk-In, P.; Hoven, V. P.; Takahara, A.; Akiyoshi, K.; Iwasaki, Y. *Biomacromolecules* **2004**, *5*, 2308.

[45] Chiefari, J.; Chong, Y. K.; Ercole, F.; Kristina, J.; Jeffery, J.; Le, T. P. T.; Mayadunne, R. T. A.; Meijs, G. F.; Moad, C. L.; Moad, G.; Rizzardo, E.; Thang, S. H. *Macromolecules* **1998**, *31*, 5559.

[46] Mitsukami, Y.; Donovan, M. S.; Lowe, A. B.; McCormick, C. L.; *Macromolecules* **2001**, *34*, 2248.

[47] McCormick, C. T.; Lowe, A. B.; *Acc. Chem. Res.* **2004**, *37*, 312.

[48] In *Handbook of RAFT Polymerization*; Barner-Kowollik, C., et al., Eds.; WILEY-VCH verlag GmbH & Co. KGaA: Weinheim, 2008.

[49] Nie, Z.; Kumacheva, E. *Nature Materials* **2008**, *7*, 277.

[50] Nishizawa, M.; Kagi, H.; Tako, K.; Matsue, T. *Journal of the Surface Science Society of Japan* **2004**, *25*, 290.

Chapter 2

Polymer Brush with Pendent Glucosylurea Groups Constructed on a Glass Substrate by RAFT Polymerization

2.1 Introduction

A ‘‘self-assembled monolayer’’ (SAM) of alkyl thiols and disulfides on gold or silver surfaces has been examined as cell membrane mimetics.[1-4] This is because SAMs can easily be prepared via chemi-sorptive S-Au or S-Ag bonds, and are stable in general.[5-9] Besides, polymer chains accumulated on solid surfaces via covalent or non-covalent bond are usually called ‘‘polymer brushes’’, and they have been extensively studied for functionalization of solid materials. The accumulated polymer chains are, however, not so highly close-packed and well-ordered in comparison with the SAM of aliphatic disulfides or thiols.

Meanwhile, a controlled (or living) radical polymerization has been developed in these fifteen years to obtain well-defined polymers. Of various procedures for pursuing controlled radical polymerization, atom transfer radical polymerization (ATRP)[10-17] and reversible addition fragmentation chain transfer (RAFT) polymerization [18-22] have extensively been examined due to their easiness.

Recently, artificial polymers, which can practically be used in biomedical fields, have largely been developed,[23] partly because of the fatal diseases (bovine spongiform encephalopathy (BSE), Kuru, Creutzfeldt–Jakob disease (CJD), etc.) infected by the intake (BSE and Kuru) and implantation (some of the patients of CJD) of natural polymers. Among the artificial polymers, zwitterionic compounds such as phosphobetaine,[24] sulfobetaine[25-27] and carboxybetaine

polymers[28-30] were found to be highly blood- and biocompatible. For example, the nonspecific adsorption of plasma proteins to the film of phosphobetaine copolymer was very small, and the adsorbed proteins preserved the molecular structure.[31] The suppression of protein adsorption onto the grafted sulfobetaine polymers,[27] and that onto the brushes of various zwitterionic polymers were also reported.[28]

Raman and infrared spectroscopic measurements indicated that the hydrogen-bonded network structure of water in the vicinity of zwitterionic polymers is not largely perturbed,[29,32] which might be crucial for the absence of non-specific adsorption of proteins to the polymers, resulting in the excellent biocompatibility of the polymers.

In addition to zwitterionic polymers, some kinds of nonionic polymeric materials such as poly(2-methoxyethyl acrylate)[33, 34] and poly(ethylene glycol)s[35] have also been found to be biocompatible. In contrast with these polymers, sugar-derivatized polymer (so-called "glycopolymer", is almost always recognized and bound by sugar-binding proteins (lectins and enzymes) specifically,[36,37] and therefore, the glycopolymer is not considered "bio-inert" (no induction of biological responses) in general. However, by the suitable chemical modification (or protection), the sugar residues in the glycopolymer can be converted to a "bio-inert" moiety. Previously it was reported that a conjugation of polymer chain to an amino group in D-glucosamine via a linker chain having an urea group made the sugar residue undetectable for sugar receptors (lectins such as Concanavalin A and wheat germ agglutinin),[38,39] probably because such a conjugation does not exist in nature.

In this chapter, various polymer brushes with many pendent glucosylurea groups have been prepared by the surface-initiated RAFT polymerization using an azo-type radical initiator fixed to a glass plate and a free chain transfer agent (CTA). The combination of a surface-confined azo-type radical initiator and free RAFT agent for the construction of polymer brush was reported previously.[40] Experimental procedures adopted in this work are very convenient to prepare polymer brushes of various compositions for the functionalization of glass, silicon

wafers and many kinds of metallic oxide surfaces. The ATRP method was not adopted due to the presence of "urea group" in the monomer. After reduction of the dithiobenzoate group at the end of the glycopolymer brush with $NaBH_4$ and subsequent coupling with iodoacetic acid, furthermore, the polymer brush has been converted to have a carboxyl end group for the decrease in hydrophobicity of the brush. For comparison, brushes of ionic polymers have also been prepared by the RAFT method.

The polymer brushes have been characterized by using ellipsometry, and contact angle measurements. The biological properties of the brushes have been examined by the non-specific adsorption of proteins using bicinchoninic acid (BCA) method,[41, 42] and the cell adhesion test.[42] Using these methods, valuable information about correlation of the chemical and spatial structure of the brush and non-specific adsorption of proteins and adhesion of cells to the brush surface has been obtained.

2.2 Experimental section

2.2.1 *Materials*

Glucosylureaethyl methacrylate (2-deoxy-2-N-(2'-methacryloyloxyethyl)aminocarbamyl D-glucose, GUMA, **Scheme 2-1 (a)**) was prepared by the coupling of D-glucosamine with 2-methacryloyloxyethyl isocyanate as reported previously.[43,44] 4,4'-Azobis(4-cyanopentanoic acid) (commercial name, V-501, **Scheme 2-1 (b)**) was kindly donated by Wako Pure Chemicals, Osaka, Japan. 4-Cyanopentanoic acid dithiobenzoate (CTA-1, **Scheme 2-1 (c)**) was prepared as previously reported.[19] 2-(2-Carboxyethylsulfanylthiocarbonylsulfanyl) propionic acid (TTC5, **Scheme 2-1 (d)**) was prepared as reported previously.[22] Other reagents were obtained from commercial sources. A Milli-Q grade water was used for preparation of sample solutions.

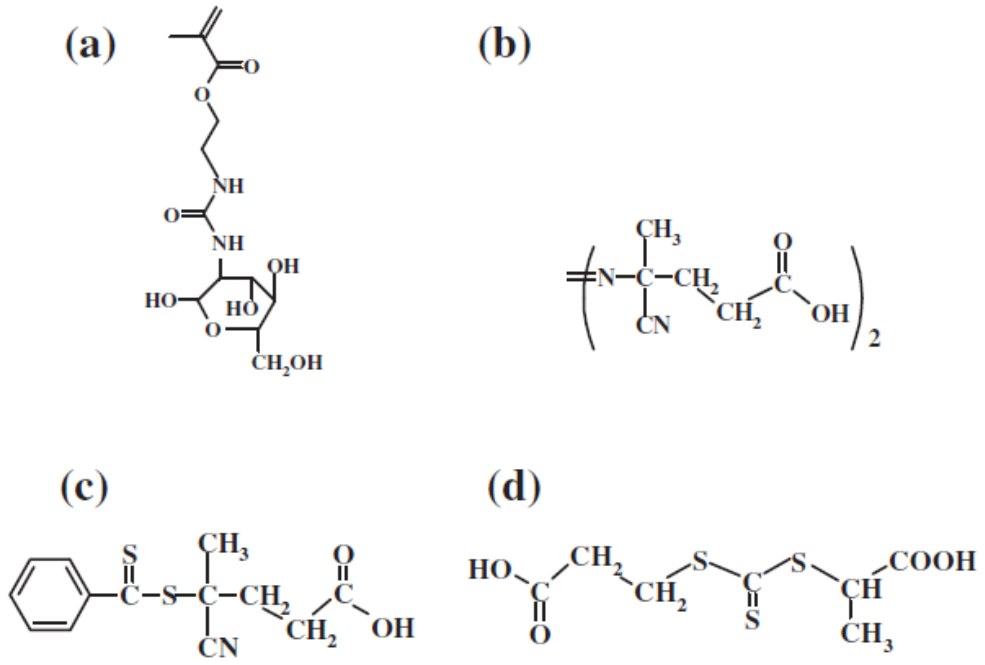

Scheme 2-1. Chemical structure of (a) glucosylureaethyl methacrylate (GUMA), (b) 4,4'-azobis(4-cyanopentanoic acid) (V-501), (c) 4-cyanopentanoic acid-4-dithiobenzoate (CTA-1) and (d) 2-(2-carboxyethylsulfanylthiocarbonylsulfanyl)propionic acid (TTC5).

2.2.2 Synthesis of polyGUMA in liquid phase

GUMA (0.5 g), V-501 (4.2 mg, radical initiator) and CTA-1 (8.4 mg, chain transfer agent) were dissolved in methanol-water mixture (1:3, 3 mL) (GUMA: V-501: CTA-1 = 100:1:2) in a small round bottom flask (**Scheme 2-2**). After passing a N_2 gas for 20 min, the solution mixture was tightly sealed and incubated at 70 ^oC for 6 h. After evaporation of the solvent, the oily mixture was repeatedly washed with ethanol, and after dissolving in water, ultrafiltrated with water (Amicon; membrane, YM 1 (exclusion limit, 1 kD)) to remove unreacted monomers. The

polymer product was finally lyophilized (PGUMA-CTA-1, 0.28 g). The number average molecular weight (M_n) of the polymer was evaluated to be 1.49×10^4 (degree of polymerization (*DP*), 46.1) by the NMR measurements (400 MHz, a-400, JEOL, Tokyo, Japan). The polydispersity of the polymer (M_w/M_n) was determined to be 1.30 by gel permeation chromatography (GPC; column, Wakobeads G-30; mobile phase, 0.1 M NaBr; standard sample, pullulan).

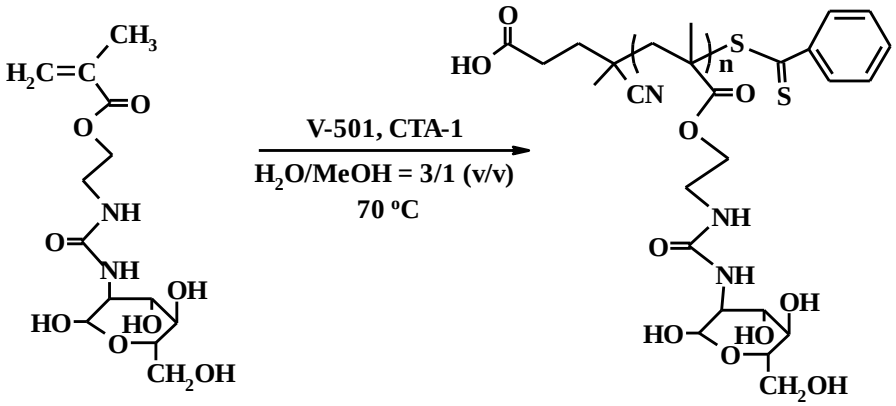

Scheme 2-2. RAFT Polymerization of GUMA in liquid phase.

2.2.3 Accumulation of polymers on a glass substrate (Scheme 2-3)

2.2.3.1 Treatment of the substrate with 3-Aminopropyl)triethoxysilane (APTES)

A glass plate pretreated with a UV/ozone cleaner was soaked in a 10 (v/v) % APTES–ethanol solution for 1 h at room temperature, and washed with Milli-Q water four times. Prior to the

third rinse, the plate was ultrasonified in water for 30 s to remove APTES physically adsorbed. After removal of water droplets on the plate by flushing with N_2 gas, the plate was dried in a drying chamber at 70 ºC for 4 h.

2.2.3.2 Preparation of an initiator-modified glass plate

N-Methylpyrrolidinone (NMP, 40 mL, dried with molecular sieves 4A beforehand) and V-501 (112 mg, 0.40 mmol) were put in a sample vial in which the APTES-modified glass plates had been set on a home-made plate rack made of Teflonr®, and stirred at 0 ºC for 1 h. Water-soluble carbodiimide (WSC, 0.60 g, 3.2 mmol) was added, and the solution was stirred for 1 h at 0 ºC, and at room temperature for 24 h to conjugate V-501 with the amino group on the glass plate. After the reaction, the glass plate was repeatedly rinsed with methanol and Milli-Q water.

2.2.3.3 Construction of the polymer brush by the RAFT polymerization

Construction of a PGUMA-CTA-1 brush

A stirrer chip and the glass plate rack were put into a sample vial. The V-501-modified glass plate was set on the rack, and GUMA (6.7 g, 20.0 mmol), methanol/water (1/3 (v/v), 40 mL), V-501 (56 mg, 0.20 mmol) and CTA-1 (112 mg, 0.40 mmol) were added to the reaction vial. After bubbling of N_2 gas for 30 min, the vial was tightly sealed and incubated in an oil bath at 70 ºC for 6 h. The glass substrate was washed two times with methanol and Milli-Q water and finally dried in *vacuo* (PGUMA–CTA-1 brush). A similar procedure was adopted for the construction of poly(2-methacryloyloxyethyltrimethylammonium chloride) (PolyMOETAC) and poly(methacrylic acid) (PolyMA) brushes, too.

Construction of a PolyMOETAC brush

The general procedures to construct a polymer brush using an azo-type radical initiator and a RAFT agent were shown in **Scheme 2-4** in the text. Ethanol (33.3 mL) and MOETAC (6.7 mL, 40.0 mmol) were put into a sample vial in which the V-501-modified glass plate had been set. V-501 (112 mg, 0.40 mmol) and CTA-1 (560 mg, 2.0 mmol) were added and, after bubbling of N_2 gas for 30 min, the vial was incubated in an oil bath for 6 h at 70 °C. During the incubation, an aliquot of the reaction solution (25 μl) was obtained using a microsyringe at appropriate intervals. The conversion, and reaction ratio of the monomer, log_e ($[M]_o/[M]$), were obtained by ^{1}H NMR. After polymerization, the glass substrate was washed two times with methanol, and Milli-Q water (PMOETAC).

Construction of a PolyMA brush

MA (1.7 mL, 20.0 mmol) and ethanol (34.9 mL) were put into a sample vial in which the V-501-modified glass plate had been set. V-501 (112 mg, 0.40 mmol) and CTA-1 (560 mg, 2.0 mmol) were added, and after passing N_2 gas for 30 min, the solution mixture was incubated in oil bath at 70 °C for 6 h. After the reaction, the glass plate was washed two times with ethanol, and Milli-Q water (PMA).

To increase hydrophilicity of the PolyGUMA brush, the polymer brush-modified glass plate was incubated with $NaBH_4$ solution for several hours ($[NaBH_4]$ = 10 mM in carbonate buffer (pH 8.97)), and subsequently iodoacetic acid was added into a reaction vial ([iodoacetic acid] = 30 mM (final)), and the reacting solution was further stirred for several hours (**Scheme 2-4**).[45] Finally, the brush-modified glass plate was vigorously rinsed with water (PGUMA–COOH brush).

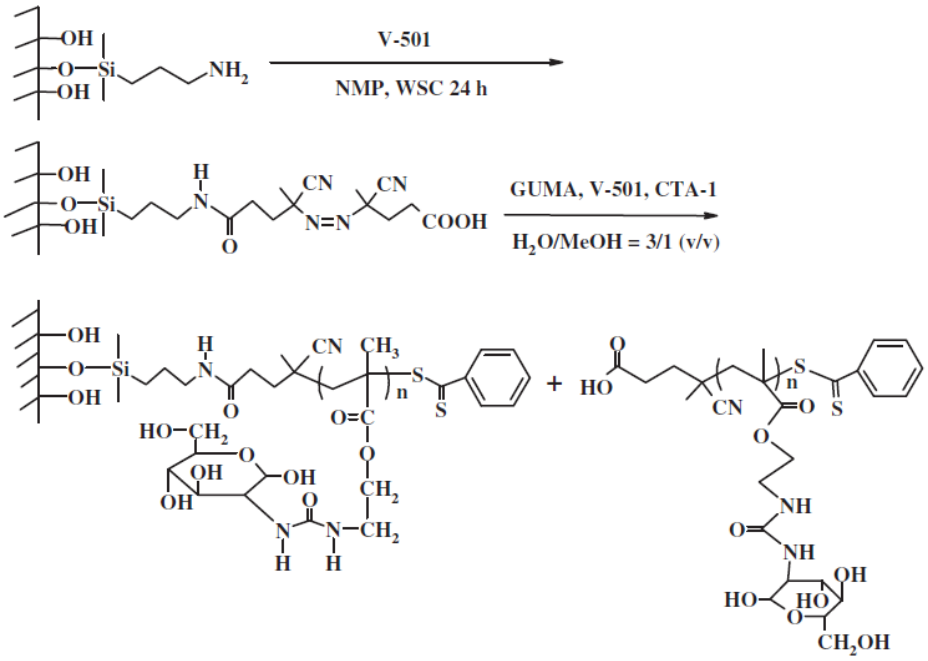

Scheme 2-3. Surface-initiated (SI) RAFT polymerization of GUMA.

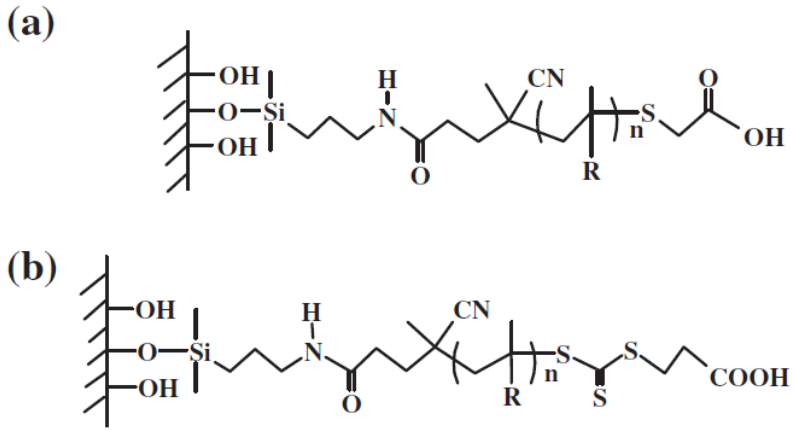

Scheme 2-4. PolyGUMA brush with a carboxyl end group (R, glucosylureaethyloxycarbonyl group) (a) Prepared by the usage of CTA-1 as RAFT agent, subsequent reduction with $NaBH_4$ and coupling with iodoacetic acid (PGUMA-COOH). (b) Prepared by the direct introduction of carboxyl end group using TTC5 as RAFT agent (PGUMA-TTC5).

Construction of a PGUMA-TTC5 brush

Into a sample vial were put a stirrer chip, and the glass plate rack. The V-501-modified glass plate was set on the rack, and GUMA (6.7 g, 20.0 mmol), Milli-Q water (40 mL), V-501 (56 mg, 0.20 mmol) and TTC5 (100 mg, 0.40 mmol) were added to the reaction vial. After bubbling of N_2 gas for 30 min, the vial was tightly sealed and incubated in an oil bath at 70 ^oC for 4 h. The glass substrate was finally washed two times with methanol and water and dried in *vacuo* (PGUMA–TTC5 brush) (**Scheme 2-4 (b)** and **Scheme 2-5**).

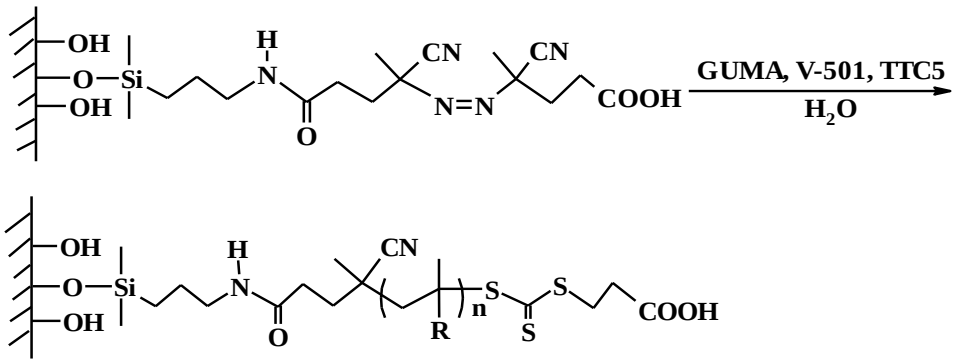

Scheme 2-5. SI-RAFT Polymerization of GUMA using TTC5 (PGUMA-TTC5).
(R, glucosylureaethyloxycarbonyl group.)

2.2.4 Irradiation of ion beam (IB) to the polymer brush.

The polymer brush-modified cover glass was soaked in a 70 vol% ethanol, and dried in a desiccator. An ion beam was irradiated to the PolyGUMA brush on the cover glass using a focused ion beam system (Hitachi FB-2100; ion beam, Ga^+). The acceleration voltage, the diameter of aperture, and the standard beam current were 40 kV, 30 μm and 0.01-0.03 nA, respectively. The dwelling time and the processing time were 10 μs and 30 s, respectively, in the experiments with HEK293 cells, and 10 μs and 60 s, respectively, with HepG2 cells. After the ion beam irradiation, the cover glass was washed with PBS (-) and put in a petri dish (plasma-treated polystyrene; diameter, 60 mm). HEK293 cells and HepG2 cells in Dulbecco's Modified Eagle's Medium (DMEM) containing 10 % FBS and 1 % antibiotics were seeded in the dish ($5x10^5$ cells/dish), and incubated at 37 ºC and 5% CO_2 for 12 h. After rinsing with PBS (-), the medium was changed with the new one, and the glass substrate was further incubated for 24 h. After rinsing with PBS (-), the cover glass was observed with a microscope (DP-71, Olympus, Tokyo, Japan).

2.3 Results and discussion

2.3.1 Construction of a polymer brush on a glass surface

The azo initiator-conjugated glass surface was used for the surface-initiated RAFT polymerization of GUMA (grafting-from method). Both the glass substrate and the reacting solution were characterized 20, 30, 60 and 90 min after onset of the polymerization to obtain the thickness of the polymer brush and the molecular weight of the free polymer, respectively.

The kinetic plot for the polymerization of GUMA produced in liquid phase at the same time was shown in **Figure 2-1 (a)**. The linear relationship between $\log_e ([M]_o/[M])$ vs. time in the figure and the small M_w/M_n value of PGUMA-CTA-1 in **Figure 2-1 (b)** indicated that the polymerization could be pursued in a living manner. M_n of the polymer brush was assumed to be equal to the polymer produced in liquid phase at the same time. Tsujii et al. reported that the M_n values of the graft and free polystyrene were nearly the same through the RAFT polymerization, while the M_w/M_n value of the graft polymer was slightly larger than that of free polymers.[46]

The thickness of polymer brushes increased with the reaction time (**Figure 2-2**), which proves that there were no significant termination reactions occurring during the brush polymerization.[49] Since the radical initiator was covalently fixed to the substrate in this system, there is a possibility that the surface density of the polymer brush depends on the polymerization time, and the half-life and the surface density of the initiator. Baum and Brittain examined the surface-initiated RAFT polymerization of styrene, MMA and N,N-dimethylacrylamide using surface immobilized azo initiator, and found that addition of small amount of untethered (free) initiator to the system facilitated the growth of brushes.[40] Base on their results, the author assumed here that the polymerization almost equally proceeds from the initiation sites on the substrate. **Table 2-1** also shows the characteristics of various polymers prepared by the RAFT

method. M_w/M_n values for all the polymers obtained by GPC showed sufficiently small polydispersity. M_n values in the table were obtained by ^{1}H NMR, and are different from the M_n values by GPC (**Figure 2-1 (b)**), probably because of the non-specific interaction of the filler in the GPC column with the polymer concerned.

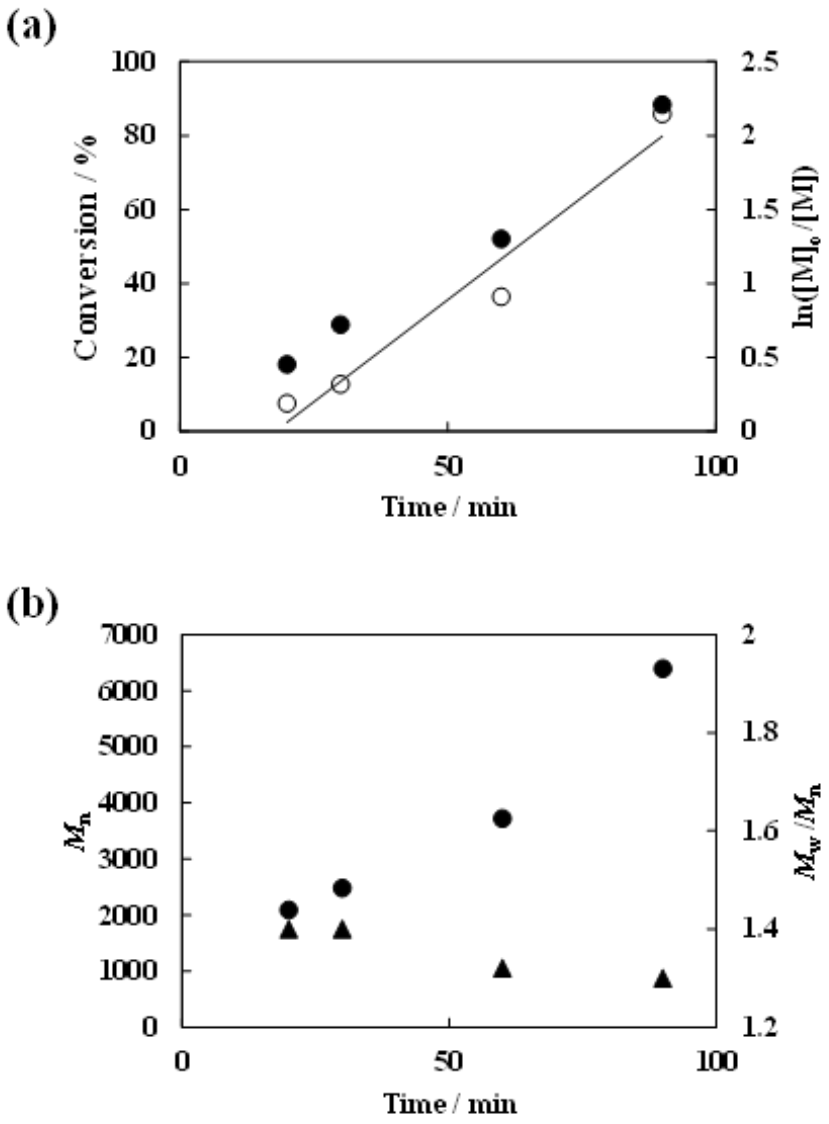

Figure 2-1. Time evolution for polymerization of GUMA at 70 °C. (a) Conversion (○) and log$_e$ ([M]$_o$/[M]) (●). (●) M_n (d) and M_w/M_n (▲). Solvent, methanol and water (1:3 (v/v)).

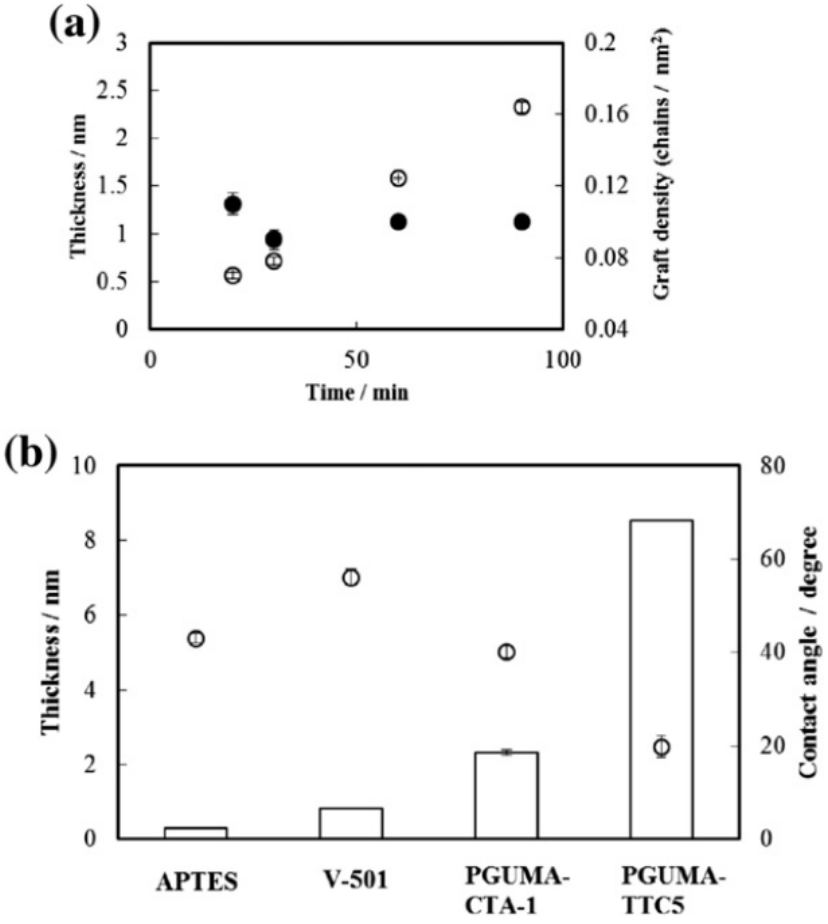

Figure 2-2. (a) Time evolution of thickness (○) and graft density (●) of PGUMA–CTA-1 brush. Solvent, methanol and water (1:3 (v/v)) at 70 ºC. The graft density was obtained by Eq. (1). (b) Thickness (by the ellipsometry) (□) and contact angle (by sessile drop method) (○) of the polymer brushes on the silicon wafers.

To increase hydrophilicity of the PGUMA-CTA-1 brush, the brush-modified glass plate was incubated with 10 mM of $NaBH_4$ and subsequently with iodoacetic acid. The result of the former treatment (**Figure 2-3 (a)** and **Scheme 2-5**) indicates that the reduction with $NaBH_4$ for 2 h was enough to decrease the contact angle. Similarly, the subsequent incubation of the

PolyGUMA brush having a thiol end group with iodoacetic acid for 2 h was enough for the introduction of carboxyl group to the end of the brush (**Figure 2-3 (b)**). The contact angle and ζ-potential measurements indicated that the surface of PolyGUMA brush after these treatments was hydrophilic and almost uncharged (**Table 2-2 and Figure 2-4**). The surface density (σ) of the PolyGUMA brush was evaluated using the data of ellipsometry, and GPC (Eq. (1)).

$$\sigma = \rho \, d \, N_A \times 10^{-21} / M_n \quad (1)$$

where ρ is density of the dry polymer layer, d is the thickness of the polymer brush, and N_A is the Avogadro number. The density for glycopolymer (ρ = 1.0 g/cm^3)[47] was used for the evaluation of r value of PolyGUMA. The σ value for PGUMA-CTA-1 was evaluated to be 0.10 chains/nm^2 which was equal to the criteria of the ‘‘densely’’ packed polymer brush (**Table 2-1**).[12,13]

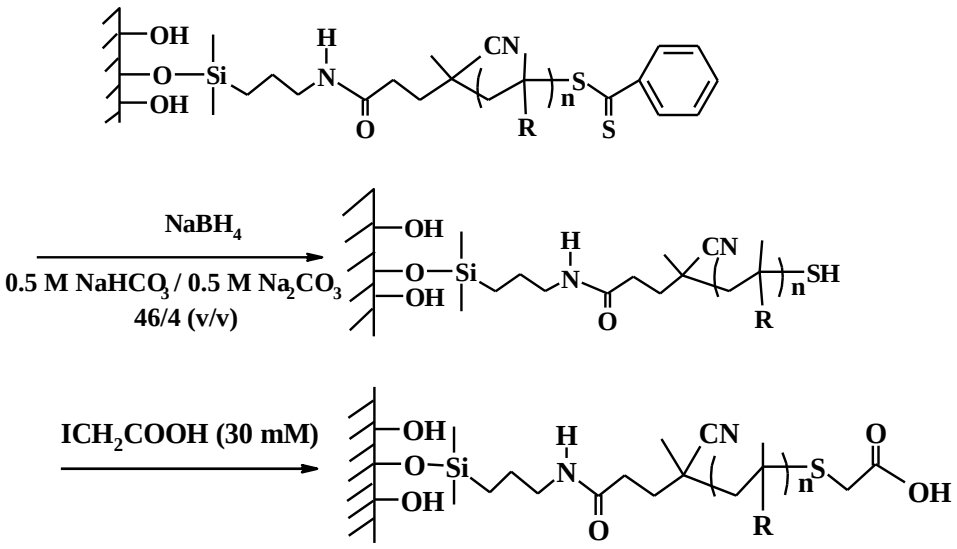

Scheme 2-6. Introduction of carboxyl end group to PGUMA brush by reduction with $NaBH_4$ and subsequent coupling with iodoacetic acid (PGUMA-COOH). R, glucosylureaethyloxycarbonyl group.

Table 2-1. Characteristics of PGUMA brushes and PGUMAs produced in liquid phase.

Sample [a]	Thickness (nm)	$M_{n,\,NMR}$ [b] $\times 10^{-3}$	*DP* [b]	$M_w/M_{n,\,GPC}$ [b]	Graft density (chains/nm^2) [c]
PGUMA-CTA-1 20[d]	0.57	3.1	8.9	1.40	0.11
PGUMA-CTA-1 30[d]	0.71	4.7	14	1.40	0.09
PGUMA-CTA-1 60[d]	1.58	10	30.7	1.32	0.10
PGUMA-CTA-1 90[d]	2.32	14.9	46.1	1.30	0.10
PGUMA-TTC5 240[d]	8.53	16.9	52.4	1.18	0.27

[a] The number at the end of each sample name denotes the polymerization time in min. t*DP* = 50

[b] The values for PolyGUMA simultaneously produced in liquid phase.

[c] Each graft density was calculated using Eq. (1)

[d] Polymerization time, 6 h.

[e] Polymerization time, 4 h.

Table 2-2. Contact angle for polymer brush-modified glass substrates determined by the sessile drop and air-in-water methods.

Sample	Contact Angle / Degrees		
	Sessile Drop [a]	Air-in-Water [a]	Total
Glass	5.4 (±1.0)	162.0 (±1.2)	167.4
APTES	43.0 (± 1.0)	129.6 (±1.6)	172.6
V-501	56.1 (± 1.6)	130.6 (±1.0)	186.7
PGUMA-CTA-1 [b]	40.1 (± 1.4)	145.2 (±1.8)	185.3
PGUMA-COOH [b]	28.5 (± 1.1)	151.3 (±1.5)	179.8
PGUMA-TTC5 [c]	19.8 (± 2.3)	152.3 (± 1.5)	172.1
PMOETAC [b]	24.5 (± 1.2)	151.8 (± 1.7)	176.3
PMA [b]	35.7 (± 0.5)	142.4 (± 1.4)	178.1

[a]. Measurement conditions: Temperature of air, 25.6 ºC; Relative humidity, 40%; Temperature of water, 25.6 ºC.

[b]. Polymerization time, 6 h.

[c]. Polymerization time, 4 h.

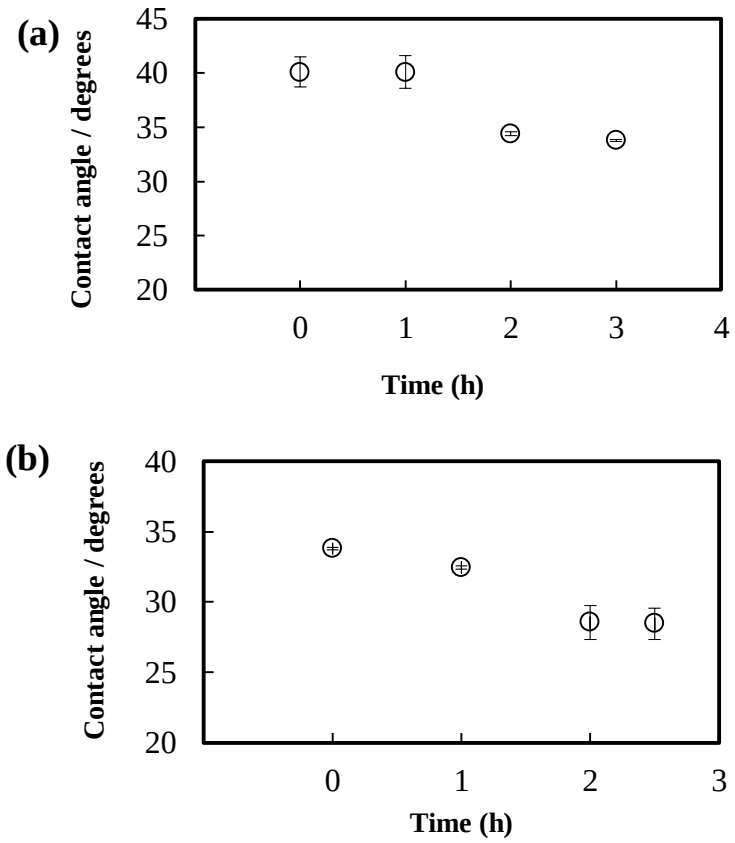

Figure 2-3. Time dependences of contact angle of PolyGUMA brush. (a) At the reduction with $NaBH_4$. (b) At the subsequent incubation with iodoacetic acid.

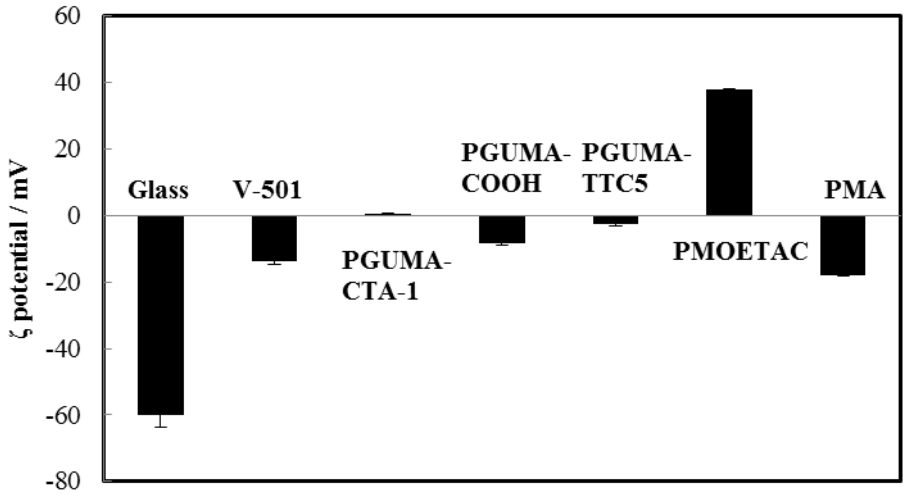

Figure 2-4. Surface ζ-potential of various surfaces.

2.3.2 Non-specific adsorption of proteins

Next, the bicinchoninic acid (BCA) method was used to follow the adsorption of protein to the polymer brush constructed on a glass substrate. To clarify the contribution of electrostatic interaction to the non-specific adsorption of proteins to polymer brushes, BSA and lysozyme were chosen as a probe because their p*I* values are quite different each other (p*I*: BSA, 4.7–4.9; and lysozyme, 11.0).[48,49] At the physiological pH examined here (7.4), the former is negatively charged, while the latter is positively charged.

Figure 2-5 (a) shows that the bare glass strongly adsorbed BSA, whereas BSA was not adsorbed to the surface of the Poly-GUMA brushes (PGUMA-CTA-1 and PGUMA-COOH) to a large extent. This is in good contrast with the significant adsorption of BSA to the cationic polymer brush (PolyMOETAC), which can be ascribed to an electrostatic attraction between the negatively charged BSA and the cationic polymer. It should be mentioned here that BSA adsorbed to the negatively charged PMA brush to some extent. Many factors besides p*I* value affect the adsorption behavior of proteins to solid surfaces. BSA at the pH higher than p*I* is known to adsorb to both negatively and positively charged surfaces, though the net charge of BSA is negative at this pH. For example, the adsorbed amounts of BSA to a SAM of 11-mercaptoundecanoic acid and that to a SAM of 11-aminoundecanethiol were 0.28 and 0.15 μg/cm^2, respectively, in a phosphate-buffered saline (PBS, pH 7.4).[50] Therefore, it is not strange that BSA adsorbed to the brush of PMA to some extent.

The suppression of the nonspecific adsorption of BSA to the PGUMA-CTA-1 brush was, however, still not so satisfactory, due to the low surface density of the brush (0.10 chains/nm^2). To increase surface density of the Poly-GUMA brush, the author used another kind of RAFT agent (TTC5) which has no aromatic group. The σ value of the PolyGUMA brush was increased to a large extent (0.27 chains/nm^2) (**Table 2-1**). TTC5 is a compact molecule and a steric hindrance for the surface-initiated RAFT reaction using TTC5 is smaller than that using CTA-

1. Therefore, the effectiveness of TTC5 in RAFT polymerization might be larger than that of CTA-1, which would enable almost complete reaction using TTC5 in a shorter time than that using CTA-1. Resultantly, the degree of resistance against the non-specific adsorption was significantly increased (**Figure 2-5 (a)**). The similar effective resistance against the non-specific adsorption to the PGUMA-TTC 5 brush was observed for lysozyme (**Figure 2-5 (b)**).

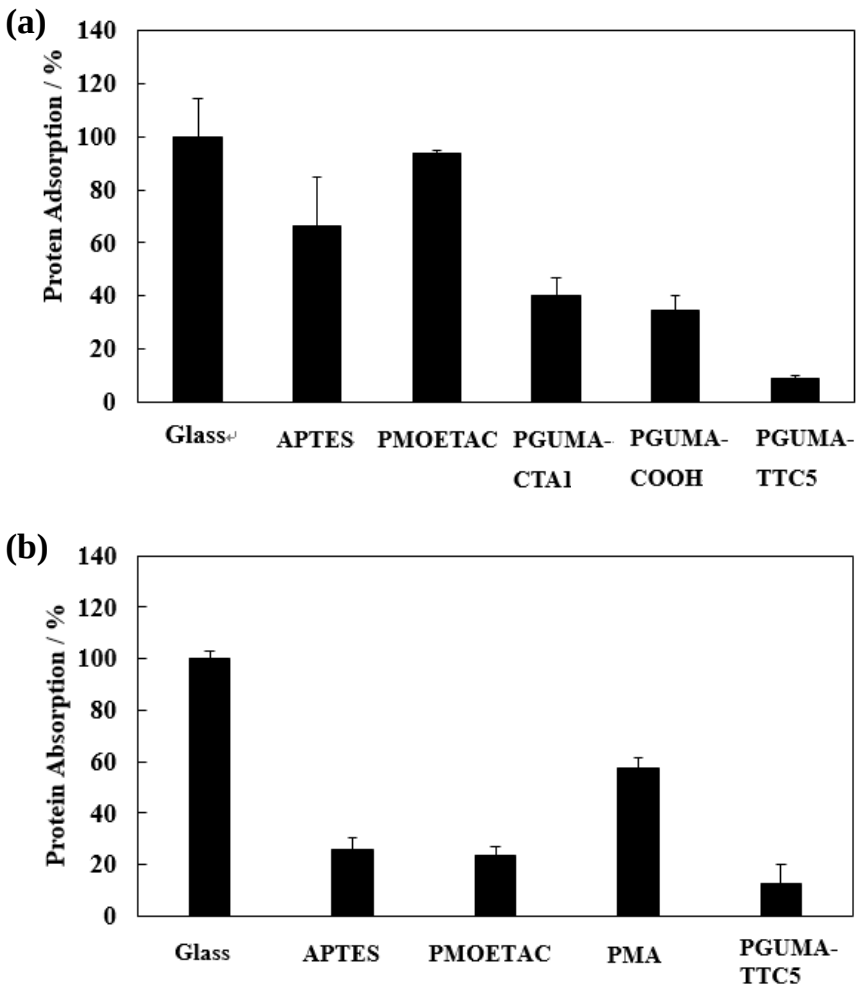

Figure 2-5. Non-specific adsorption of (a) BSA and (b) lysozyme to various polymer brushes at 37 ^{o}C. The y-axis expresses the amount of adsorbed proteins when the relative quantity of proteins adsorbed to bare glass was 100%. ([proteins] = 4.5 mg/mL phosphate buffer).

The ζ-potential for PGUMA-TTC5 brush was a very small negative value (-2.6 mV), whereas that of PGUMA-COOH was more largely negative (-8.3 mV) (**Figure 2-4**). Since the ζ value for the former brush (0.27 chains/nm^2) was larger than that of the latter one (0.10 chains/nm^2), the opposite tendency of ζ-potentials for these brushes having carboxyl end groups could not be clearly explained at this moment. The glass substrate, which has a largely negative ζ-potential (≈ -60 mV) itself, at the bottom of the brush might significantly affect the ζ-potential of the brush with a small surface density (PGUMA-COOH) in comparison with that with a large surface density (PGUMA-TTC5).

2.3.3 Ion-beam irradiation of the polymer brush surface

Finally, the author examined ion-beam irradiation to the surface of PolyGUMA brush (PGUMA-TTC5) (**Scheme 2-7**). The irradiated area was designed to be heart-shaped. Upon incubation of the PolyGUMA-modified glass substrate with HEK293 cells and subsequent rinse with PBS, the micrograph of the glass substrate indicated that the irradiated area was covered with HEK293 cells, while no cells attached to other area, definitely indicating anti-biofouling properties of the PolyGUMA brush (**Figure 6 (a)**). The same tendency was observed for HepG2 cells, too (**Figure 6 (b)**).

As indicated in the figure, the proteins did not adsorb to the surface of the PolyGUMA brush significantly. The introduction of hollow area by the ablation of the brush using ion-beam irradiation might allow the adsorption of proteins and subsequent cell adhesion, confirming the role of PolyGUMA brush in the suppression of cell adhesion. The image printing on the surface of anti-biofouling PolyGUMA brush by ion-beam irradiation may be highly useful for biomedical applications.

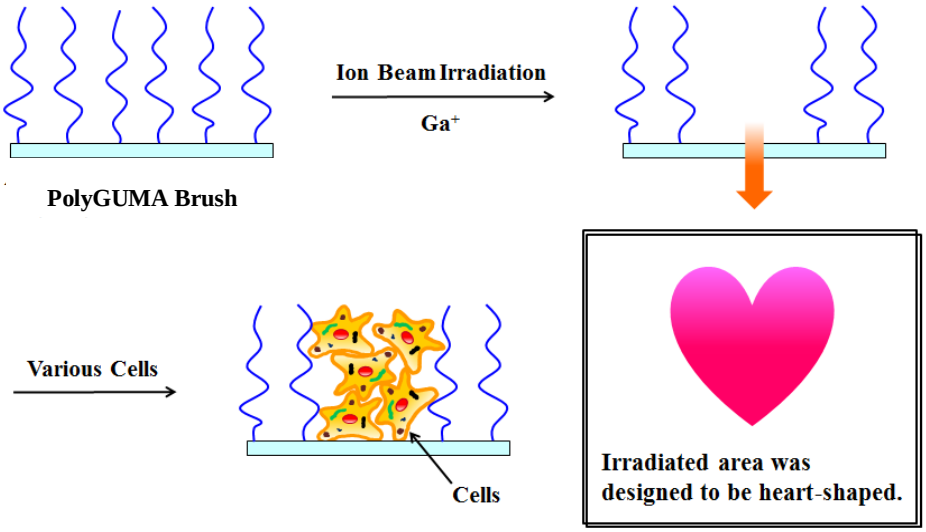

Scheme 2-7. Schematic of adhesion of cells to a hollow space in the PolyGUMA brush. The length of the PolyGUMA brush was largely magnified.

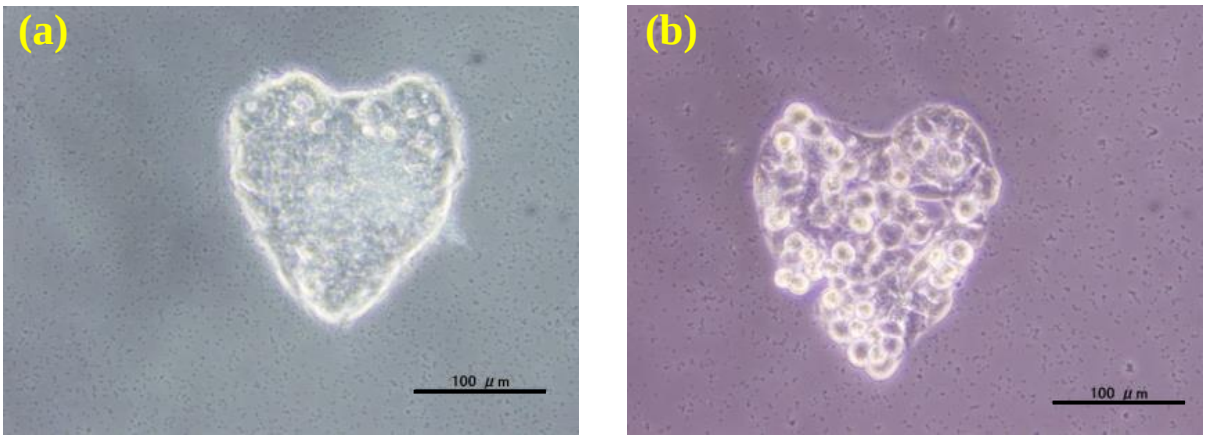

Figure 2-6. Micrographs of (a) HEK293 and (b) HepG2 cells adhered to the heart-shaped area to which ion beam had been irradiated. Substrate, PGUMA-TTC5 brushes on a glass plate. The length of bar is 100 μm.

2-4. Conclusions

PolyGUMA brush could easily be prepared using the surface-confined radical initiator in the presence of a free RAFT agent (CTA-1) and a free radical initiator. The surface density of PolyGUMA brush was not so high probably due to both the bulky side chain of GUMA and the bulkiness of the chain transfer agent. The GUMA polymer brush showed a resistance against non-specific adsorption of proteins, and the degree of resistance was increased by the cleavage of dithiobenzoate group, and subsequent introduction of carboxyl group at the end of the brush. The usage of trithiocarbonate chain transfer agent having carboxylate end groups (TTC5) further increased the anti-biofouling effect of the PolyGUMA brush probably due to the compact size of TTC5. The grafting-from procedures using a surface-confined radical initiator and a free RAFT agent are very convenient to prepare polymer brushes of various compositions for the functionalization of glass, silicon and many kinds of metallic oxide surfaces.

2.5 References

[1] Nuzzo, R. G.; Allara, D. L. *J. Am. Chem. Soc.* **1983**, *105*, 4481.

[2] Porter, M. D.; Bright, T. B.; Allara, D. L.; Chidsey, C. E. D. *J. Am. Chem. Soc.* **1987,** *109*, 3559.

[3] Bain, C. D.; Troughton, E. B.; Tao, Y-T.; Evall, J.; Whitesides, G. M.; Nuzzo, R. G. *J. Am. Chem. Soc.* **1989**, *111*, 321.

[4] Hill, W.; Wehling, B. J. *J. Phys. Chem.* **1993**, 97, 9451

[5] Lopez, G. P.; Albers, M. W.; Schreiber, S. L.; Carroll, R.; Peralta, E. *J. Am. Chem. Soc.* **1993**, *115*, 5877.

[6] Kitano, H.; Saito, T.; Kanayama, N. *J. Colloid. Interface. Sci.* **2002**, *250*, 134.

[7] Spinke, J.; Lileym, M.; Gunder, H-J.; Angermaier, L.; Knoll, W. *Langmuir* **1993**, *9*, 1821.

[8] Schierbaum, K-D.; Weiss, T.; van Velzen, T. E. U. T.; Engbersen, J. F. J.; Reinhoudt, D. N.; Gopel, W. *Science* **1994**, *265*, 1413.

[9] Flink, S.; Boukamp, B. A.; van den Berg, A.; van Veggel, F. C. J. M.; Reinhoudt, D. N. *J. Am. Chem. Soc.* **1998**, *120*, 4652.

[10] Veregin, R. P. N.; Georges, M. K.; Kazmaier, P. M.; Hamer, G. K. *Macromolecules* **1993**, *26*, 5316.

[11] Hawker, C. J.; Elce, E.; Dao, J.; Volksen, W.; Russel, T. P.; Barclay, G. G. *Macromolecules* **1996**, *29*, 2686.

[12] Fukuda, T.; Terauchi, T.; Goto, A.; Tsujii, Y.; Miyamoto, T. *Macromolecules* **1996**, *29*, 3050.

[13] Tsujii, Y.; Ohno, K.; Yamamoto, S.; Goto, A.; Fukuda, T. *Adv. Polym. Sci.* **2006**, *197*, 1.

[14] Baethge, H.; Butz, S.; Schmidt-Naake, G. *Macromol. Rapid. Commun.* **1997**, *18*, 911.

[15] Kato, M.; Kamigaito, M.; Sawamoto, M.; Higashimura, T. *Macromolecules* **1995**, *28*, 1721.

[16] Wang, J-S.; Matyjaszewski, K. J. *J. Am. Chem. Soc.* **1995**, *117*, 5614.

[17] Matsuura, K.; Ohno, K.; Kagaya, S.; Kitano, H. *Macromol. Chem. Phys.* **2007**, *208*, 862.

[18] Patton, D. L.; Mullings, M.; Fulghum, T. et al. *Macromolecules* **2005**, *38*, 8597.

[19] Mitsukami, Y.; Donovan, M. S.; Lowe, A. C.; McCormick, C. L. *Macromolecules* **2001**, *34*, 2248.

[20] McCormick, C. L.; Lowe, A. B. *Acc. Chem. Res.* **2004**, *37*, 312.

[21] Barner-Kowollik, C. editor. *Handbook of RAFT Polymerization*; Wiley-VCH: Weinheim, 2008.

[22] Wang, R.; McCormick, C. L.; Lowe, A. B. *Macromolecules* **2005**, *38*, 9518.

[23] Tsuruta, T.; Hayashi, T.; Kataoka, K.; Kimura, Y.; Ishihara, K.; editors. *Biomedical Application of Polymeric Materials*; CRC Press: Boca Raton, 1993.

[24] Ishihara, K.; Aragaki, R.; Ueda, T.; Watanabe, A.; Nakabayashi, N. *J. Biomed. Mater. Res.* **1990**, *24*, 1069.

[25] Yuan, Y. L.; Ai, F.; Zhang, J.; Zang, X.; Shen, B. J.; Lin, S. C. *J. Biomater. Sci. Polym. Ed.* **2002**, *13*, 1081.

[26] Jun, Z.; Youling, Y.; Kehua, W.; Jian, S.; Sicong, L. *Colloids. Surf. B.* **2003**, *28*, 1.

[27] Yuan, Y.; Zang, X.; Ai, F.; Zhou, J.; Shen, J.; Lin, S. *Polym. Int.* **2004**, *53*, 121.

[28] Kitano, H.; Kawasaki, A.; Kawasaki, H.; Morokoshi, S. *J. Colloid. Interface. Sci.* **2005**, *282*, 340.

[29] Kitano, H.; Tada, S.; Mori, T.; Takaha, K.; Gemmei-Ide, M.; Tanaka, M. et al. *Langmuir* **2005**, *21*, 11932.

[30] Fujishita, S.; Inaba, C.; Tada, S.; Gemmei-Ide, M.; Kitano, H.; Saruwatari, Y. *Biol. Pharm. Bull.* **2008**, *31*, 2309.

[31] Ishihara, K.; Nomura, H.; Mihara, T.; Kurita, K.; Iwasaki, Y.; Nakabayashi, N. et al. *Mater. Res.* **1998**, *39*, 323.

[32] Kitano, H.; Sudo, K.; Ichikawa, K.; Ide, M.; Ishihara, *K. J. Phys. Chem. B.* **2000**, *104*, 11425.

[33] Tanaka, M.; Motomura, T.; Kawada, M.; Anzai, T.; Kasori, Y.; Shiroya, T. et al. *Biomaterials* **2000,** *21*, 1471.

[34] Tanaka, M.; Mochizuki, A.; Ishii, N.; Motomura, T.; Hatakeyama, T. *Biomacromolecules* **2002**, *3*, 36.

[35] Jonsson, B.; Lindman, B.; Holmberg, K.; Kronberg, B.; John Wiley & Sons: Chichester; 1998.

[36] Kitano, H.; Ohhori, K. *Langmuir* **2001**, *17*, 1878.

[37] Morokoshi, S.; Ohhori, K.; Mizukami, K.; Kitano, H. Langmuir **2004**, 2*0*, 8897.

[38] Kitano, H.; Gemmmei-Ide, M.; Anraku, Y.; Saruwatari, Y. *Colloids. Surf. B.* **2007**, *56*, 188.

[39] Kitano, H.; Hayashi, A.; Takakura, H.; Suzuki, H.; Kanayama, N.; Saruwatari, Y. *Langmuir* **200**9, *25*, 9361.

[40] Baum, M.; Brittain, W. J. *Macromolecules* 2002, *35*, 610.

[41] Kitano, H.; Suzuki, H.; Matsuura, K.; Ohno, K. *Langmuir* **2009**, *26*, 6767.

[42] Kitano, H.; Suzuki, H.; Kondo, T.; Sasaki, K.; Iwanaga, S.; Nakamura, M. et al. *Macromol. Biosci.* **2011**, *11*, 557.

[43] Saruwatari, Y. *Compound with glycosyl moiety*; Japanese Patent 2004-018460.

[44] Saruwatari, Y.; Mukaiyama, T. *Composition of moisturizing agent*; Japanese Patent 2005-104879.

[45] Kitano, H.; Kondo, T.; Kamada, T.; Iwanaga, S.; Nakamura, M.; Ohno, K. *Colloids. Surf. B.* **2011**, *88*, 455.

[46] Tsujii, Y.; Ejaz, M.; Sato, K.; Goto, A.; Fukuda, T. *Macromolecules* **2001**, *34*, 8872.

[47] Yu, K.; Kizhakkedathu, J. N. *Biomacromolecules* **2010**, *11*, 3073.

[48] Yamakawa, T.; Imahori, K. editors. *Biochemistry Data Book Vol*. Tokyo Kagaku-Dojin: I; Tokyo; 1979.

[49] Voet, D.; Voet, J. G. *Biochemistry. Third Edition*; John Wiley &Sons: New York; 2004.

[50] Arima, Y.; Iwata, H. *J. Mater. Chem.* **2007**, *17*, 4079

Chapter 3

UV-Patterning of Anti-Biofouling Zwitterionic Copolymer Layer with an Aromatic Anchor Group

3.1 Introduction

Modification of solid surfaces with a functional moiety enhances the functionality of the solid materials. Silane coupling reagents, R-Si-(R')$_3$ where R' can be OMe, OEt, Cl etc., can be used for binding to a glass substrate and silicon wafer via Si-O-Si bonds to form a "self-assembled monolayer" (SAM).[1-3] Organosulfur compounds such as alkyl and aromatic thiols and disulfides can also form an SAM on metal and semiconductor surfaces via chemisorptive bonds (e.g., Au-S or Ag-S bonds).[4-7]

The surface modification of solid materials using polymer chains can be categorized into two classes. The first one employs a "polymer brush" method, in which one end of the polymer chain is physically or chemically attached to the solid substrate (**Scheme 3-1 (a)**). Two strategies for constructing polymer brushes on the surface of solid materials are mainly employed, namely, the grafting of preformed polymers on the surface of solid materials via physical adsorption or covalent bonding, called the "*grafting-to*" method[8-10] and the surface-initiated polymerization, called the "*grafting-from*" method.[11-14]

The second class of surface modification using polymers is by forming a "polymer layer", in which a polymer chain is fixed to the solid substrate at multiple points (**Scheme 3-1 (b)**) via both covalent bonding and chemical and physical adsorption of polymer chains. The implementation of this modification method is significantly easier than that of the "*grafting-*

from" method, which has been widely used in the fabrication of polymer brushes. Furthermore, a copolymer possessing silane-coupling groups at the side chain can be covalently bound to substrates such as glass and silicon wafer. Since such the copolymers cannot be removed (detached) from the surface as easily as physically adsorbed polymers can be, they are highly useful for surface modification.[15-17]

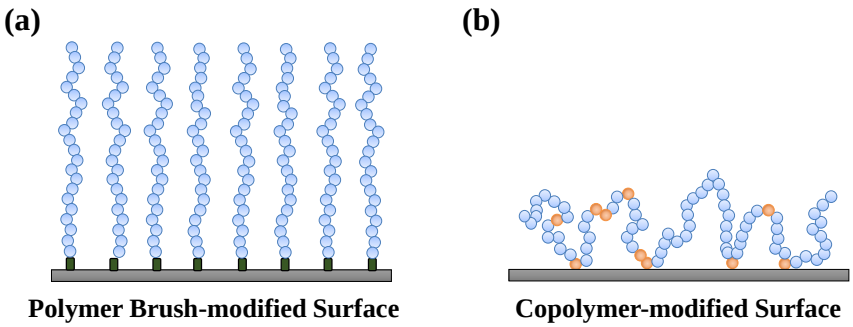

Scheme 3-1. Schematic of (a) zwitterionic polymer brush and (b) copolymer layer.

Non-specific binding of biomolecules to solid surfaces is a serious problem in biomedical applications of materials. Polymer films composed of a zwitterionic monomer such as 1-carboxy-*N*,*N*-dimethyl-*N*-(2-methacryloyloxyethyl)methanaminium hydroxide inner salt (CMB), 2-methacryloyloxyethyl phosphorylcholine (MPC), and 3-sulfo-*N*,*N*-dimethyl-*N*-(3-methacrylamidopropyl)propanaminium hydroxide inner salt (SPB), and a water-insoluble monomer such as *n*-butyl methacrylate (BMA) were found to be highly biocompatible in nature.[18-22] The author previously reported that fewer platelets adhered to a film of a random copolymer of CMB and BMA than to a film of polyBMA.[23-25]

Electrochemical (cyclic voltammetry) and localized surface plasmon resonance spectroscopic measurements indicated that zwitterionic polymer brushes (polyCMB, polyMPC and polySPB) constructed on a gold surface via Au-S bonds exhibit resistance towards the non-specific adsorption of proteins.[26,27] Further, recently, significant resistance against protein adsorption and cell adhesion was reported with a carboxybetaine polymer brush covalently

bound to a glass substrate.[28-30]

Moreover, the unique properties of zwitterionic polymers in solution, which are in contrast to those of typical polyelectrolytes, have received significant attention.[31-33] It was found that the hydrogen-bonded network structure of water in the vicinity of zwitterionic polymers was largely undisturbed by performing vibrational spectroscopic measurements.[23,34-36] Hence, the author hypothesize that the inertness of zwitterionic polymers to water at polymer-water interfaces should be one of the main reasons for their excellent biocompatibility.

However, the existing surface modification methods cannot contribute effectively to the development of novel biological materials, and the materials and methods for achieving surface modification, which provide excellent functionalities and abilities to the modified materials, should be intensively investigated.[37-39] Moreover, optical micro-fabrication techniques involving irradiation with UV light and ion beams have been combined with surface modification techniques using polymers to obtain functional surfaces. In a previous study, a polymer brush possessing an aromatic ring in the base was used for fabricating a micro-pattern (~5 μm) at an excimer laser (ArF, 193 nm) exposure lower than that required for a polymer brush without an aromatic ring in the base.[39] By the introduction of aromatic ring into the anchoring group, the energy of UV is intensively and selectively absorbed to the aromatic ring. Therefore, the bonds between vinyl group or silanol group and aromatic group could be broken. However, for performing surface modification by UV irradiation, several challenges remain such as realizing required resolution and accuracy of modification and achieving easy fabrication of complicated patterns. Moreover, surface modification methods involving a lower exposure time and UV light strength and easy techniques must be developed for fabricating biomedical devices and materials possessing a functional surface.

In this chapter, a carboxymethylbetaine copolymer layer-modified glass substrate has been prepared by a simple silane coupling reaction of a random copolymer of CMB and *p*-trimethoxysilylstyrene (STMS) on a glass substrate and a silicon wafer (**Scheme 3-1 (b)**). An

optimum molar ratio of 9:1 in the formation of copolymers of CMB and 3-methacryloxypropyltrimethoxysilane (MPTMS) was reported for ensuring efficient suppression of the non-specific adsorption and adhesion of proteins and cells.[16,40] Hence, we prepared a copolymer of CMB and STMS using a molar ratio of 9:1, and the resistance to the non-specific adsorption of protein on the copolymer layer surface was compared with that on the poly(CMB-*r*-MPTMS) (9:1) surface. Via UV irradiation, patterning with a fluorescent protein in a resolution range from 1.5 μm to 10 μm could be clearly achieved. Moreover, the layer of poly(CMB-*r*-STMS) could be easily decomposed at a lower irradiation dose than that of poly(CMB-*r*-MPTMS), because of the preferential scission of covalent bond in and/or around the aromatic ring in the anchoring group, resulting in the cleavage of oligomeric CMB domains (**Figure 3-1**). Such a technique would be very useful for the simple modification of solid surfaces and for fabricating patterned surfaces that could be suitable for employing as cell arrays for the screening of novel drugs and the evaluation of cell migration and chemotaxis.

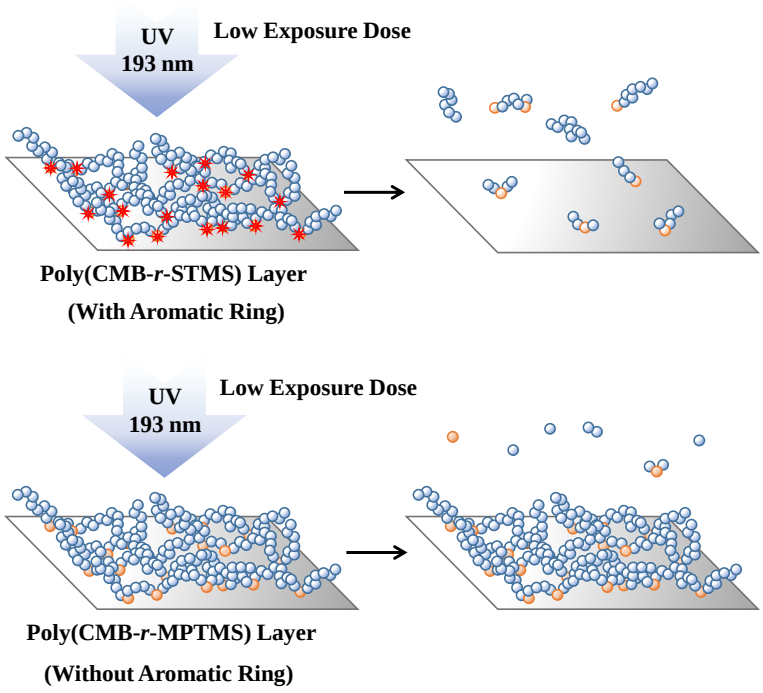

Figure 3-1. Schematic illustration of copolymer layer possessing aromatic ring at the side chain decomposed by 193 nm-UV light (ArF-excimer laser) at a low exposure dose.

3.2 Experimental Section

3.2.1 Materials

CMB (commercial name, GLBT®) and STMS (commercial name KBM1403®) were donated by Osaka Organic Chemical Industry, Osaka, Japan, and ShinEtsu Chemicals, Tokyo, Japan, respectively. MPTMS was purchased from ShinEtsu Chemicals. Bovine serum albumin (BSA) was obtained from Sigma-Aldrich. Other reagents used are commercially available. All aqueous solutions were prepared with ultrapure water (< 18 MΩ.cm, Millipore System).

3.2.2 Preparation of poly(CMB-r-STMS) and poly(CMB-r-MPTMS)

CMB (1.64 g, 7.04 mmol) and STMS (175 mg, 0.78 mmol) were dissolved in ethanol (20.6 mL) at a molar ratio of 9:1 in a glass round bottomed flask (100 mL), which had been pre-coated with propyl trimethoxysilane for the prevention of reaction of STMS with the flask, and N_2 was passed for 30 min. 2,2'-Azobisisobutyronitrile (AIBN; 0.091 g, 0.55 mmol) was then added at 65 °C, and the reaction mixture was incubated at 70 °C under N_2 atmosphere. After 4 h, AIBN (0.018 g, 0.11 mmol) was added again and the mixture was incubated at 70 °C for 4 h (**Scheme 3-2 (a)**). Due to the high reactivity of the trimethoxysilyl group in STMS, the obtained solution was directly used for modifying the glass substrate and the silicon wafer without purifying. NMR measurements indicated the disappearance of most of the vinyl protons corresponding to unreacted vinyl monomers. A similar procedure was employed for the preparation of the copolymer of CMB and MPTMS (9:1) (**Scheme 3-2 (b)**).

The molecular weight of the copolymers was evaluated by viscometry using Fikentscher's formula by measuring the relative viscosity with an Ubbelohde capillary viscometer at 25

°C.[41,42] The Fikentscher's value of viscosity characteristics, *K*-value, represents a viscosity index related to the molecular weight.

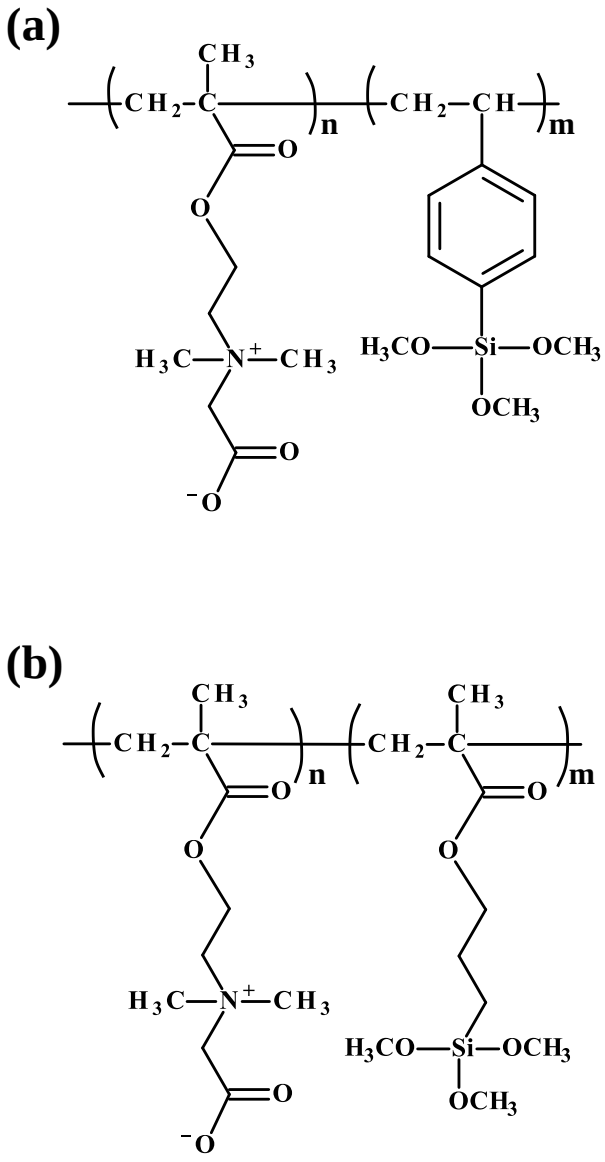

Scheme 3-2. Chemical structures of (a) poly(CMB-*r*-STMS) and (b) poly(CMB-*r*-MPTMS)

3.2.3 Preparation of a Copolymer Layer on a Solid Substrate (Scheme 3-3)

Pristine glass substrate and silicon wafer were treated with a piranha solution (sulfuric acid:25% aqueous hydrogen peroxide solution = 7:3) for 1 h. The substrate was then washed with deionized water more than ten times, rinsed with acetone, and dried under N_2 flow. The pristine substrate was incubated in an ethanolic solution of poly(CMB-*r*-STMS) or poly(CMB-*r*-MPTMS) (1 (w/v)%) for 18 h at 60 ºC. After the reaction, the glass substrate and the silicon wafer were washed repeatedly with methanol and dried under N_2 flow.

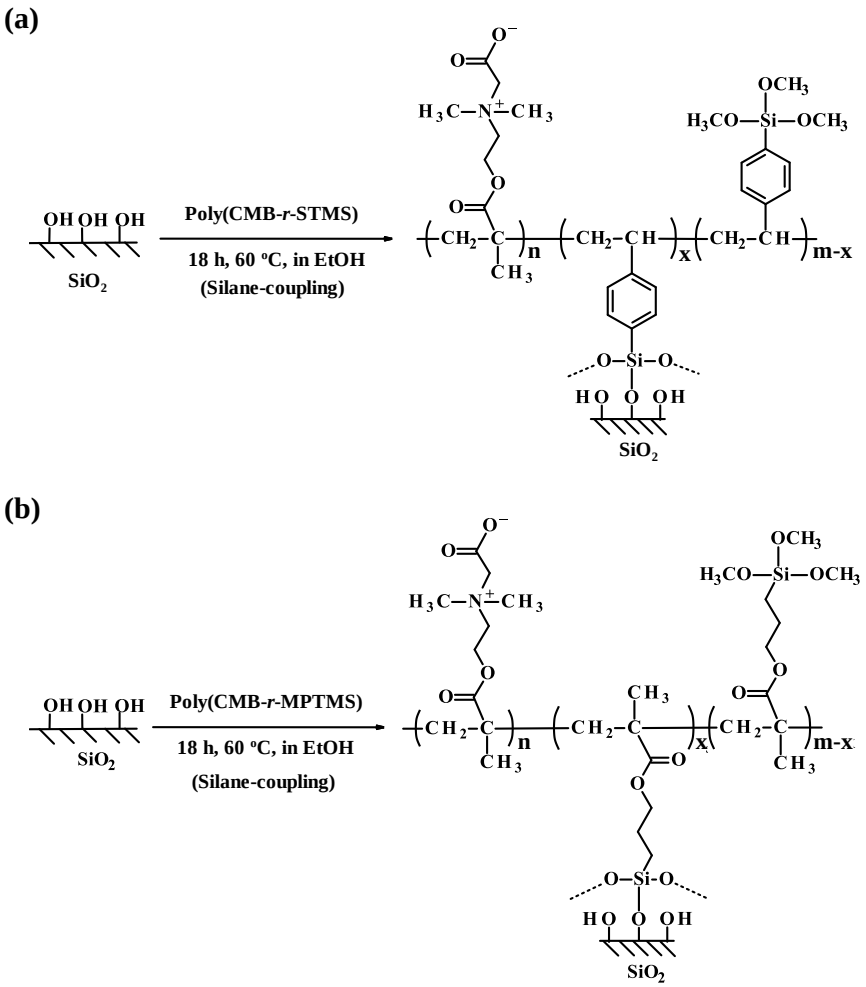

Scheme 3-3. Schematic illustration of the preparation of (a) poly(CMB-*r*-STMS) layer and (b) poly(CMB-*r*-MPTMS) layer.

3.2.4 UV Irradiation of Copolymer Layer

The zwitterionic copolymer layer-modified silicon wafer was irradiated with UV light (ArF excimer laser, 193 nm) by using an NSR-S307E system (Nikon Co., Tokyo, Japan; resolution < 80 nm; numerical a*perture:* 0.85; light source: ArF excimer laser (wavelength, 193 nm); degree of reduction: 1:4; area of irradiation: 26 × 33 mm; total accuracy of alignment < 12 nm). For the patterning experiment, the sample was irradiated through a photomask to adjust the dimensions of the pattern to 1.5 × 1.5 μm - 10 × 10 μm (including 10, 9, 8, 7, 6, 5, 4.5, 4, 3.5, 3, 2.5, 2, and 1.5 μm types) (**Scheme 3-4**).

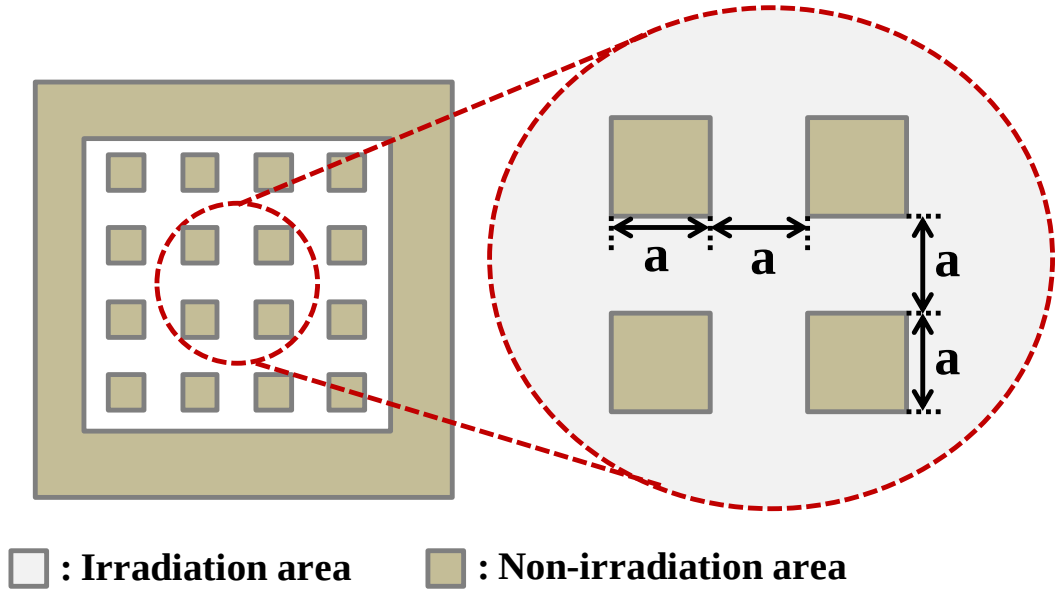

Scheme 3-4. Schematic diagram of a mask used with UV irradiation. (a = 10, 9, 8, 7, 6, 5, 4.5, 4, 3.5, 3, 2.5, 2 and 1.5 μm)

3.2.5 Measurement of Contact Angles

The contact angle of a water droplet on the sample surface was measured for evaluating the surface wettability by using a Drop Master DMs-401 (Kyowa Surface Science, Tokyo, Japan). Static contact angles, θ, of a sessile drop of water (1 μL) on the surface of the copolymer layer on the glass substrates 30 s after placing the water drop on the surface were measured. The measurements were repeated 3-5 times on a sample to obtain a reliable average value (sessile drop method), and the average values of the contact angle were estimated for 3-4 samples.

3.2.6 Measurements of the Thickness of Copolymer Layer

Thickness of the copolymer layer (dry state) was determined by optical ellipsometry (M-2000U, J. A. Woollam Co., Inc., USA) at an incident angle of 70°. The measurements were performed with a wavelength range of 242-999 nm, and the refractive index of the sample layer was assumed to be 1.49 (refractive index of poly(methyl methacrylate)).[43,44]

3.2.7 ζ-Potential of the Glass Plate

The ζ-potential of various samples (33 mm × 15 mm) was determined with a 10 mM NaCl solution using ELSZ-2 (Otsuka Electronics, Hirakata, Japan; semiconductor laser, 660 nm, 30 mW).

3.2.8 X-ray Photoelectron Spectroscopy (XPS) Measurements

XPS (ESCALAB 250Xi, Thermo Fisher Scientific, Inc., Waltham, Massachusetts, USA) was used for evaluating the elements on the substrate surface. A detection angle of 90°, X-ray source

of monochromated/micro-focused AlKα, and an X-ray size of 650 μm were used for the measurements. Analysis of the peak was carried out using the Avantage software (Ver. 4.84) from Thermo Fisher Scientific Corporation.

3.2.9 Atomic Force Microscope (AFM) Measurements

AFM (Dimension Icon, Bruker AXS K. K., Yokohama, Japan, Probe: Si single crystal, spring constant: 3 N/m, resonant frequency: 70 kHz) was used to examine the patterns on the copolymer layer-modified surface after ArF irradiation.

3.2.10 Adsorption of BSA on the Copolymer Layer Surface

The non-specific adsorption of BSA on the copolymer layer on the glass substrate and the silicon wafer was evaluated using the bicinchoninic acid (BCA) method reported elsewhere.[40]

3.3 Results and Discussion

3.3.1 Preparation of Copolymer Layer on a Substrate

By ^{1}H NMR measurement, the composition of poly(CMB-*r*-STMS) determined from peak strength of protons derived from methylene group between methacrylate and quaternary ammonium base groups in CMB (δ 4.40) and aromatic group in STMS (δ 7.22-7.53), resulting that the ratio of CMB:STMS was approximately 9:1. On the other hands, that of poly(CMB-*r*-MPTMS) could not be determined from the result of ^{1}H NMR because of overlap of peaks derived from CMB and MPTMS. However, the complete disappearance of proton peaks derived from methacrylate (δ 5.6 and δ 6.3) was observed by ^{1}H NMR. From its results, the author determined that the copolymerization ratio is the same as the feeding ratio of monomers.

An ethanolic solution of the copolymer was incubated with a pristine glass substrate or a silicon wafer. The contact angle of the plate measured by the sessile drop method changed both after incubation of the substrate with the copolymers and subsequent immersion of the sample in water for 1 h (**Table 3-1**). The copolymer-modified surfaces are hydrophilic in nature, enhancing its hydrophilicity after immersing in water, which is indicated by a small decrease in the contact angle. The initial change in the contact angle after immersion indicates the chemical modification of the glass substrate by the polymer layer. Subsequent changes in the contact angle on immersion of the copolymer layer-modified substrate in water could be attributed to a sol-gel reaction of unreacted methoxysilyl group (Si-OCH_3) in the copolymer, involving the hydrolysis of the methoxy group into the hydroxyl group (Si-OH) and subsequent intra- and inter-molecular condensation of Si-OH groups to form Si-O-Si bonds. However, the presence or absence of 10% trimethoxysilyl group does not seem to affect the wettability of the copolymer-modified surface significantly. With the sol-gel reaction, the hydrophilic CMB residues might be relatively more exposed to the solution phase, which would mainly lead to

an increase in hydrophilicity of the surface.[16,40]

Table 3-1. Characteristics of various polymer layers.

Sample	Contact angle / Degree[a]		ζ-Potential / mV[b]
Bare glass	3.8 (±0.3)	-	-60.17 (±0.32)
Poly(CMB-*r*-STMS)	11.8 (±1.0)	4.0 (±0.6)[c]	-1.47 (±0.13)[c]
Poly(CMB-*r*-MPTMS)	12.8 (±1.7)	3.3 (±0.3)[c]	-4.13 (±0.21)[c]

a, Sessile drop method.

b, In a 10 mM NaCl. c, After immersion in water for 1 h.

The molecular weights of poly(CMB-*r*-STMS) and poly(CMB-*r*-MPTMS) were determined to be 1.0×10^4 and 2.0×10^4, respectively, using viscometry measurements. The thickness of the copolymer layer on the silicon wafer was measured to be about 2 nm using ellipsometry, which is in agreement with the previously reported values.[16] This suggests that significant inter-molecular coupling of the Si-OH groups, which could result in the formation of a gel layer on the solid substrate, does not occur.

The nitrogen peak observed in the XPS spectra (N_{1s}, ca. 402 eV) is derived from the CMB unit on the poly(CMB-*r*-STMS)-modified surface. The carbon peak intensity (C_{1s}, ca. 286 eV) increased when the bare silicon wafer was modified with the copolymer (**Figure 3-2 (a)** and **(b)**). Similar results were observed with the poly(CMB-*r*-MPTMS)-modified surface (**Figure 3-2 (c)**). These results confirm the coating of the surfaces with the copolymers.

The ζ-potentials of poly(CMB-*r*-STMS) and poly(CMB-*r*-MPTMS)-modified surfaces were slightly negative (-1.47 (±0.13) mV and -4.13 (±0.21) mV, respectively), in contrast with the highly negative value of the bare glass (*ca*. -60 mV) (**Table 3-1**). The ζ-potentials of the glass plates modified with a brush of poly(methacrylic acid) (polyMA) and poly[2-(dimethylamino)ethyl methacrylate] (polyDMAEMA) were -30.2 mV and 35.3 mV, respectively, whereas those for glass plates modified with a brush of poly(MA-*r*-

DMAEMA)(MA : DMAEMA = 1 : 1) and polyCMB were -6.8 mV and -4.9 mV, respectively.[30] These results indicate the electrically neutral nature of the copolymer surface examined in the present chapter.

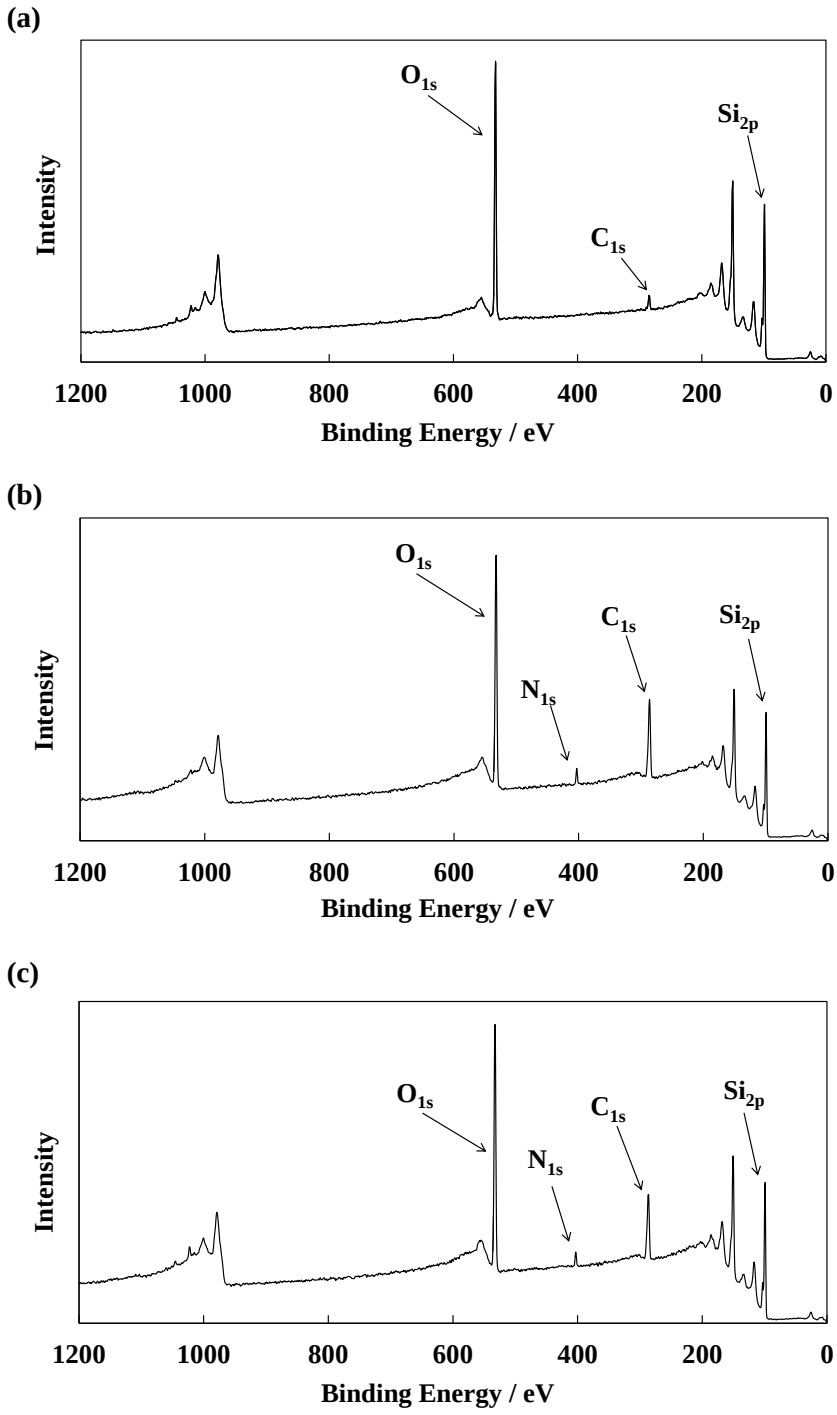

Figure 3-2. XPS data for (a) bare silicon wafer, (b) poly(CMB-*r*-STMS) layer-modified surface and (c) poly(CMB-*r*-MPTMS) layer-modified surface.

3.3.2 Decomposition of the Copolymer Layer on Substrate by UV Irradiation

The thickness of the copolymer layer decreased with an increase in the irradiation dose, and most copolymers were decomposed at 1000-2000 mJ/cm^2 (**Figure 3-3 (a)**). Moreover, the composition ratio of carbon and nitrogen elements derived from the copolymer was reduced with an increase in the irradiation dose, whereas that of the silicon elements derived from the silicon wafer was increased. The changes in the composition of each element reached plateau at about 1000-2000 mJ/cm^2 (**Figure 3-3 (b)** and **(c)**).

Correspondingly, the contact angle of the copolymer-modified surface increased with an increase in the irradiation dose (**Figure 3-4**). However, at the initial stage of irradiation (0-500 mJ/cm^2), the poly(CMB-*r*-STMS) surface quickly changed to be less hydrophophilic as compared with the poly(CMB-*r*-MPTMS) surface (**Figure 3-4 (a)**). In particular, the contact angle on the poly(CMB-*r*-STMS) surface was 15^o higher than that on the poly(CMB-*r*-MPTMS) surface at an irradiation dose of 250 mJ/cm^2 (**Figure 3-4 (b)**). This result suggests that poly(CMB-*r*-STMS) was decomposed at a low irradiation dose, which does not affect the surface modified with poly(CMB-*r*-MPTMS). This is in good agreement with the previous result obtained for a polymer brush having an aromatic ring at its base: the covalent binding between the polymer brush and the substrate could be more easily cleaved with the introduction of an aromatic ring.[39]

Furthermore, when the difference in the composition ratio of N_{1s} between poly(CMB-*r*-STMS) and poly(CMB-*r*-MPTMS), ΔN (= $N_{Poly(CMB\text{-}r\text{-}MPTMS)} - N_{Poly(CMB\text{-}r\text{-}STMS)}$), was plotted against the UV irradiation dose, a prominent peak was observed at the low irradiation dose (**Figure 3-5**). This suggests that poly(CMB-*r*-STMS) with an aromatic ring between the SiO_2 layer and the copolymer layer was decomposed faster than poly(CMB-*r*-MPTMS) without an aromatic ring.

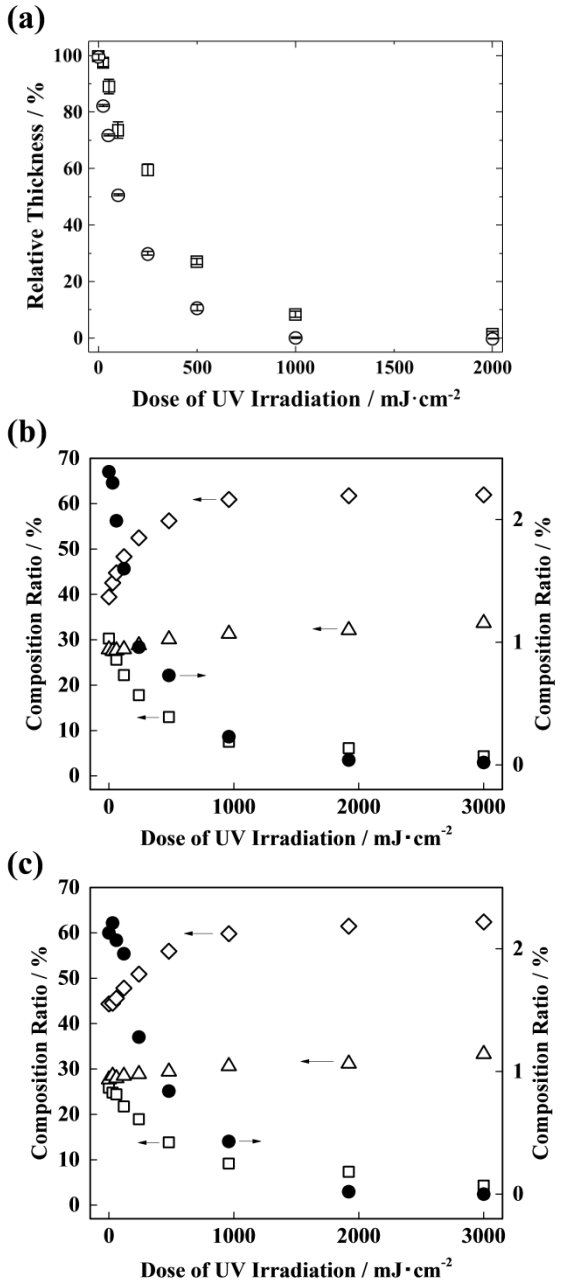

Figure 3-3. (a) The relative thickness of (○) poly(CMB-*r*-STMS) layer and (□) poly(CMB-*r*-MPTMS) layer with increasing irradiation dose. The thickness was determined with the average of three independent samples, and the data are expressed as the mean ± standard deviation. The composition ratio of each element (◊, Si; □, C; △, O; ●, N) on (b) poly(CMB-*r*-STMS) layer and (c) poly(CMB-*r*-MPTMS) layer with increasing irradiation dose. The composition ratio was shown by one experimental result for the avoidance of complication. The XPS measurement was carried out twice for independent samples, and the similar data were obtained by all measurements (error of data: Si = ± 1.22%, C = ± 1.35%, O = ± 0.83%, N = ±0.08%).

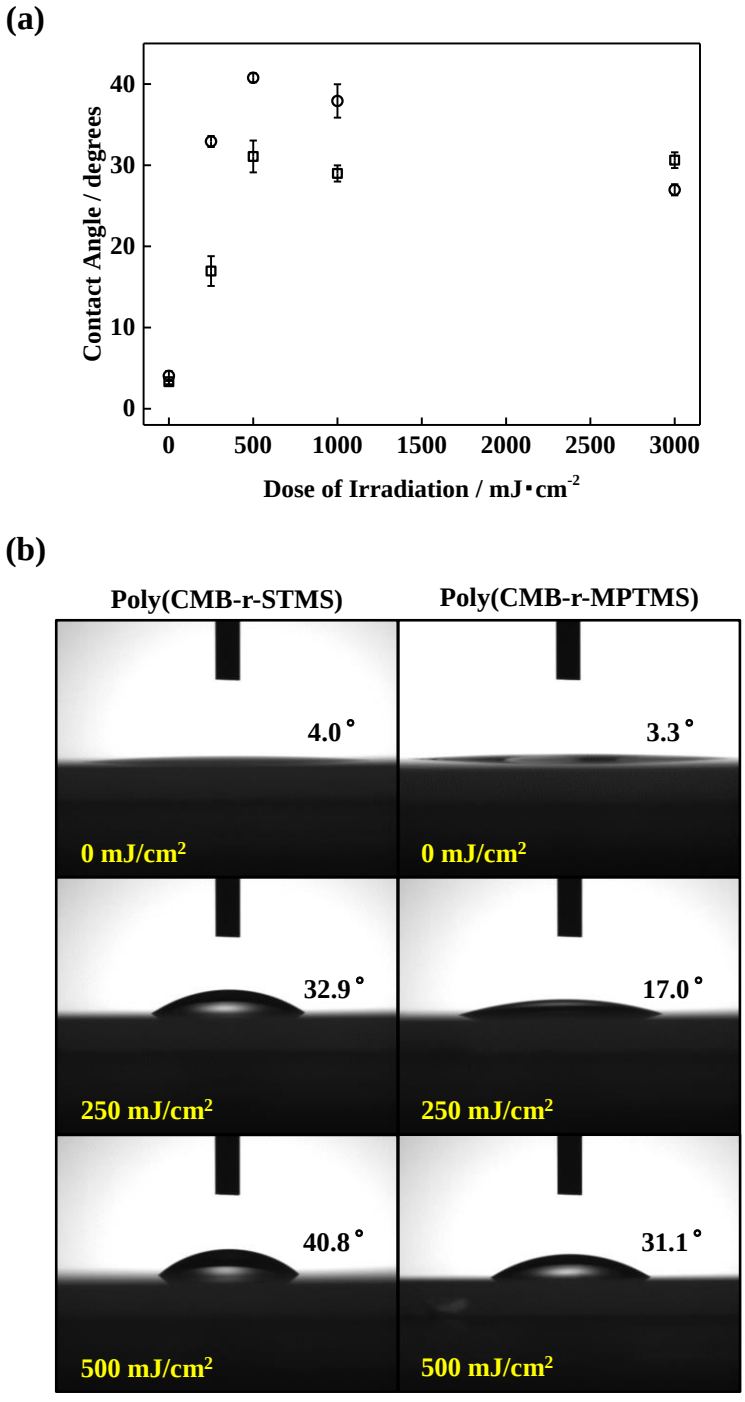

Figure 3-4. (a) Contact angle of copolymer layers after UV irradiation at various doses. (○) poly(CMB-*r*-STMS), and (□) poly(CMB-*r*-MPTMS). The data are shown as mean value ± standard deviation for three or four independent samples. (b) Photo images of water droplet on each copolymer surface.

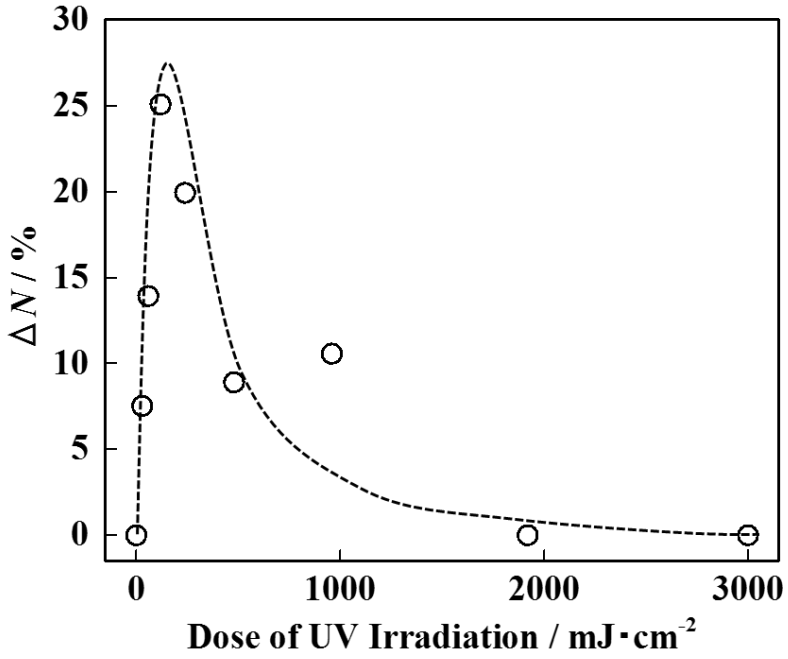

Figure 3-5. The difference in the composition ratio of the N_{1s} between poly(CMB-*r*-STMS) and poly(CMB-*r*-MPTMS), ΔN (= $N_{poly(CMB\text{-}r\text{-}MPTMS)} - N_{poly(CMB\text{-}r\text{-}STMS)}$), with an increase in the irradiation dose. The dashed line is drawn for easy understanding.

The non-specific adsorption of the protein (BSA) on the surface of the copolymer layers, poly(CMB-*r*-MPTMS) and poly(CMB-*r*-STMS), was examined using the BCA method. The polymer layer exhibited a slight non-specific adsorption upon mixing with BSA (pI 4.5–5.0) solution, in contrast with the significant adsorption of the protein on the UV-irradiated copolymer-modified surfaces (**Figure 3-6**). Among the copolymers composed of various ratios of CMB and MPTMS, the copolymer prepared with 90 mol% CMB was reported to exhibit the highest resistance to protein adsorption.[16,40]

BSA was extremely adsorptive to the UV-irradiated copolymer-modified glass (**Figure 3-6**), which could be attributed to the hydrophobic interaction between the protein and the substrates. According to previous studies,[16,41] the adsorption of both a positively charged protein

(lysozyme pI 11.0) and a negatively charged protein (BSA pI 4.5-5.0) was not significant on the poly(CMB-*r*-MPTMS) layer, indicating the crucial role of zwitterionic side groups in suppressing the protein adsorption. A similar tendency could be expected in the case of poly(CMB-*r*-STMS). The proteins attached to the zwitterionic copolymer layer could be easily detached; thereby, retaining their native structures.[18,19]

Similar differences as in the contact angle of the copolymer-modified surfaces could be observed with the amount of protein adsorbed (**Figure 3-6**). The protein adsorption to each surface saturated at about 1000 mJ/cm^2. In particular, in the irradiation range of 0-1000 mJ/cm^2, the amount of protein adsorbed on the poly(CMB-*r*-MPTMS) surface slowly increased with an increase in the irradiation dose, whereas protein adsorption on poly(CMB-*r*-STMS) drastically increased at lower irradiation dose. These results suggest that a clear pattern of fluorescent proteins would be obtained on the poly(CMB-*r*-STMS) surface with a low UV exposure dose (**Figure 3-1**).

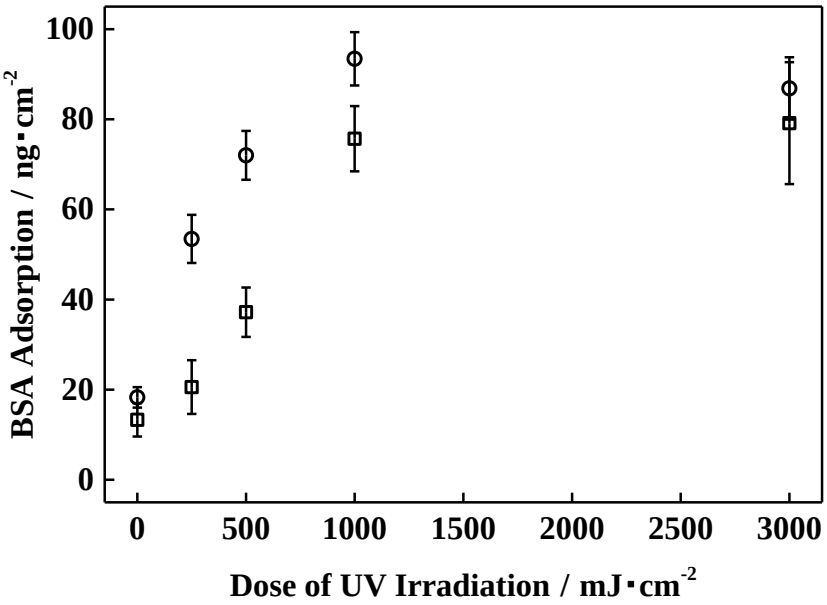

Figure 3-6. BSA adsorption on copolymer layers after UV irradiation at various doses. (○) poly(CMB-*r*-STMS), and (□) poly(CMB-*r*-MPTMS). The data are shown as mean value ± standard deviation for three independent samples.

3.3.3 Patterning of Copolymer Layer-Modified Surface by ArF Irradiation

The significant BSA adsorption on the UV-irradiated copolymer surface indicates that irradiation causes the polymer layer to lose its capability to suppress protein adsorption. Hence, the surface can be selectively patterned by utilizing the difference in the protein adsorption behavior on the irradiated and non-irradiated regions of the copolymer layer. To confirm this, the surface of a silicon wafer modified with the zwitterionic copolymer layer was examined before and after performing ArF irradiation at various doses. Fluorophore-labeled immunoglobulin G (A488-IgG) was incubated with the wafer, and the protein adsorbed on the wafer surface was examined using a fluorescence microscope.

Furthermore, the fluorescence intensity of the adsorbed protein in the patterned region, normalized with that obtained with the non-irradiated protein-adsorbed region, increased with an increase in the irradiation dose (**Figure 3-7**). Thus, a large amount of A488-IgG was adsorbed in the UV-irradiated region, resulting in a clear fluorescence pattern.

However, the fluorescence intensities corresponding to the stripe patterns formed on the poly(CMB-*r*-STMS) and poly(CMB-*r*-MPTMS) surfaces were very different when the irradiation dose of 250-500 mJ/cm^2 was employed. On the former surface, a stripe pattern was first observed at 250 mJ/cm^2 and it became clearer at 500 mJ/cm^2. However, a stripe pattern could be observed on the latter surface at 500 mJ/cm^2, but not at 250 mJ/cm^2 (**Figure 3-7**). This result is consistent with the results obtained for protein adsorption (**Figure 3-6**). Therefore, a clear pattern can be constructed on the surface of poly(CMB-*r*-STMS) at a relatively lower irradiation dose than on the surface of poly(CMB-*r*-MPTMS).

Only larger patterns (square patterns with > 6 μm lengths) were clearly observed on the poly(CMB-*r*-MPTMS) surface that was subjected to UV light irradiation with > 1000 mJ/cm^2. Interestingly, the square shapes with < 10 μm lengths collapsed on the surface of poly(CMB-*r*-MPTMS) layer after irradiation at around 3000 mJ/cm^2 (**Figure 3-8**), though large square

patterns with around 50 μm lengths could be clearly observed.

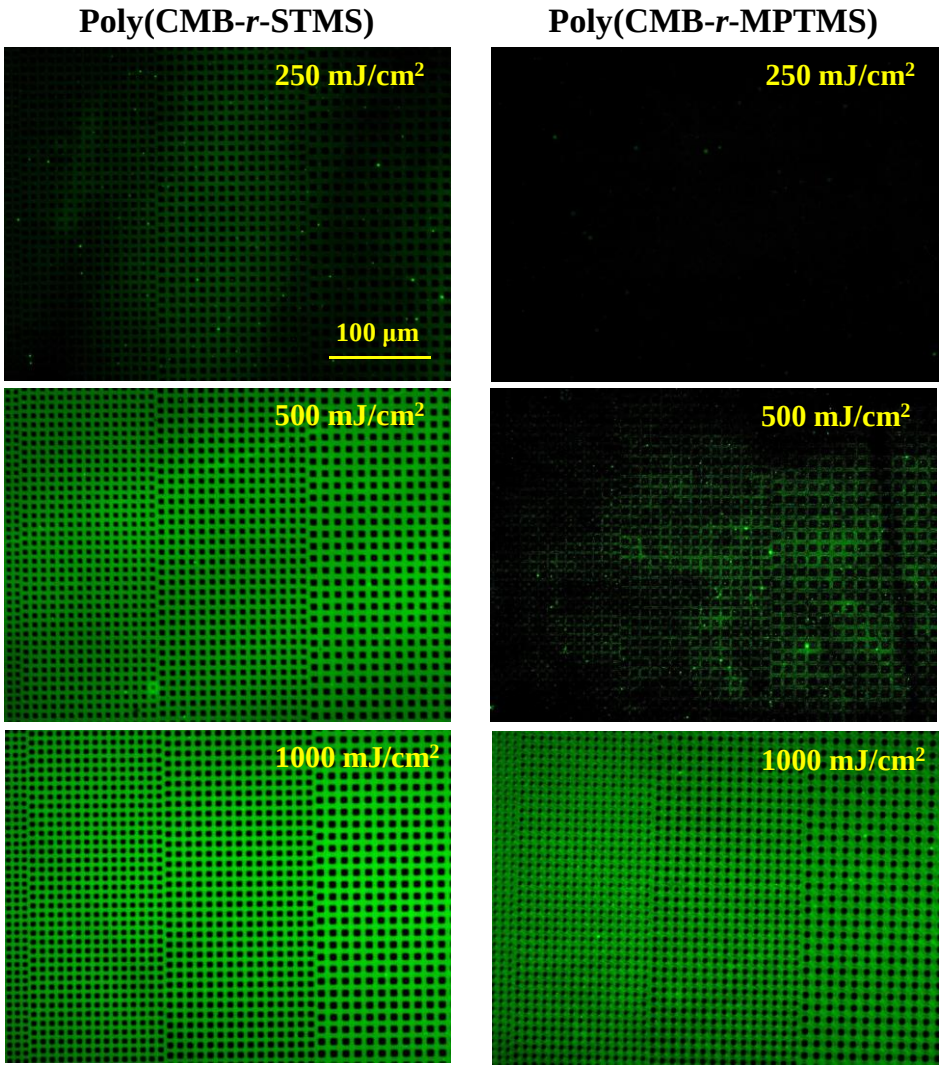

Figure 3-7. Fluorescence images of A488-IgG adsorbed onto poly(CMB-*r*-STMS) surface and poly(CMB-*r*-MPTMS) surface after UV irradiation (at 250, 500 and 1000 mJ/cm^2; Mask size: 4, 4.5, and 5 μm).

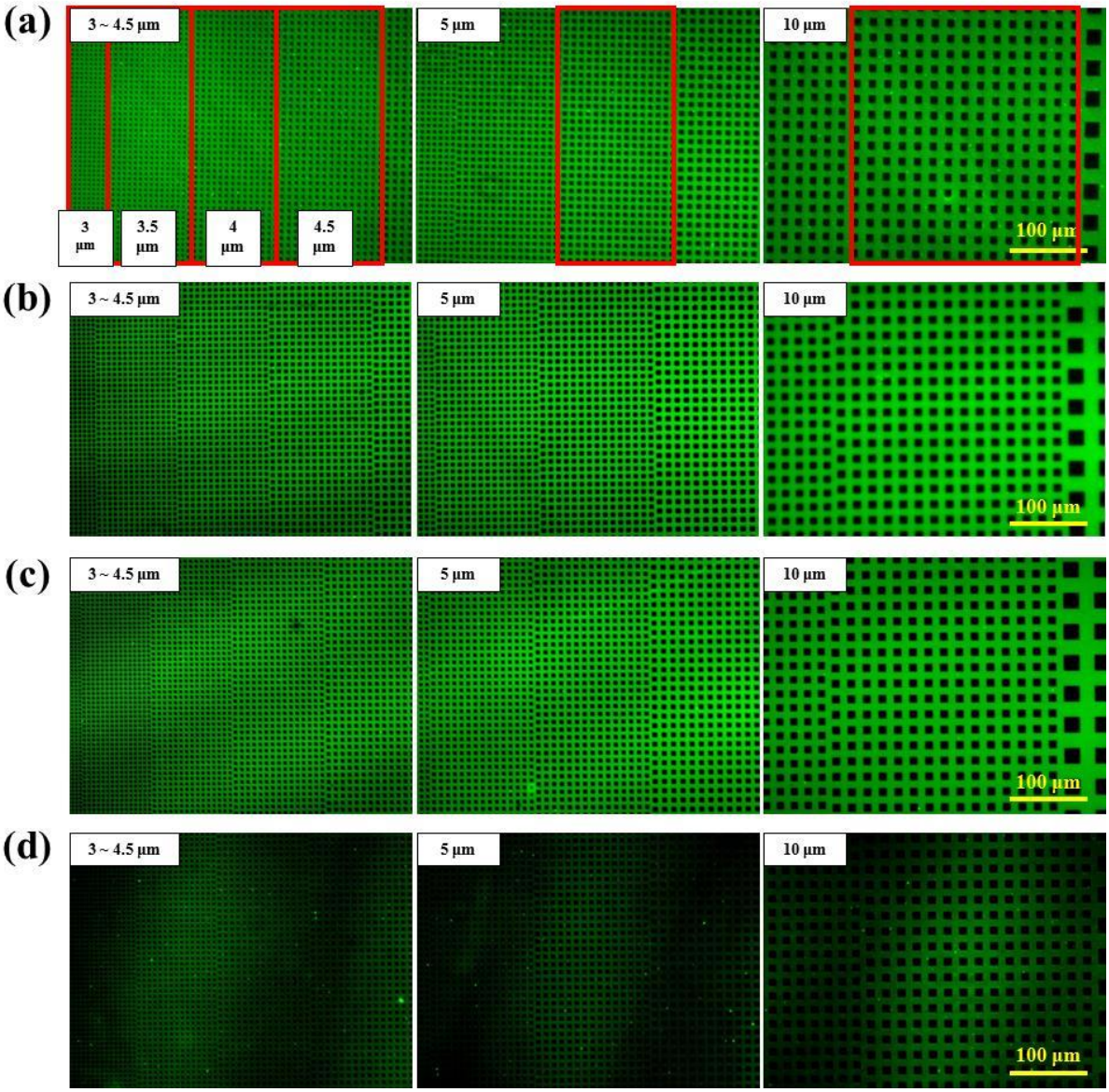

Figure 3-8. Fluorescence images of A488-IgG adsorbed on the poly(CMB-*r*-STMS) surface after UV irradiation at (a) 3000, (b) 1000, (c) 500, and (d) 250 mJ/cm^2.

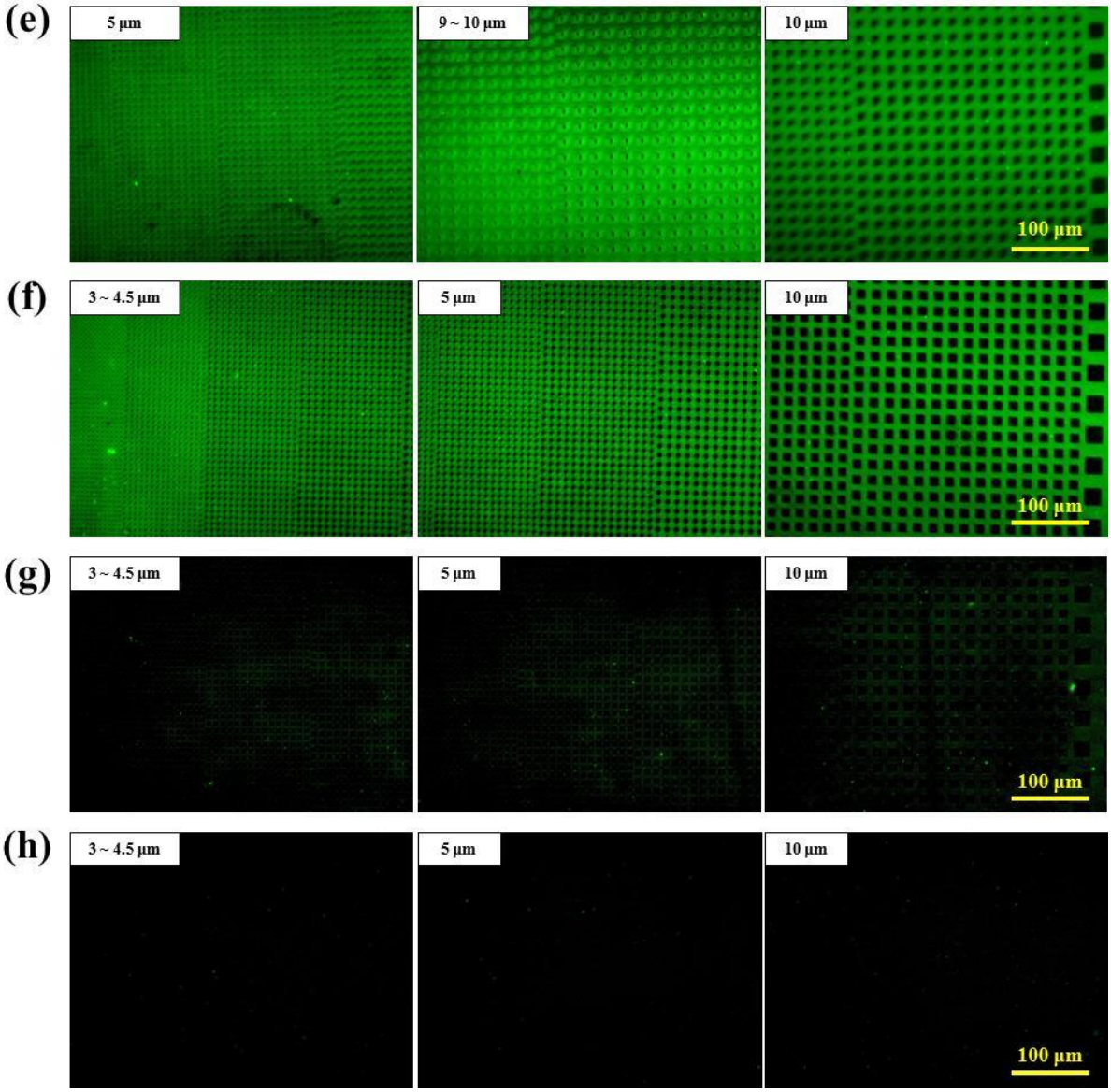

Figure 3-8. Fluorescence images of A488-IgG adsorbed on the poly(CMB-*r*-MPTMS) surface after UV-irradiation at (e) 3000, (f) 1000, (g) 500 and (h) 250 mJ/cm^2.

Additionally, the UV-irradiated pattern of poly(CMB-*r*-STMS) and poly(CMB-*r*-MPTMS) surfaces were evaluated by AFM measurement (**Figure 3-9**). On the surface of poly(CMB-*r*-STMS), clearly ablated area by the UV-irradiation with 1000 mJ/cm^2 was observed, and the height difference between the non-irradiated area and the UV-irradiated area was 1~ nm. In contrast, the ablated area of the surface of poly(CMB-*r*-MPTMS) by the irradiation with 3000 mJ/cm^2 was unclear (depth of ablated area: ~0.5 nm). From these results, the copolymer having the aromatic ring in the anchoring group is more easily ablated with low irradiation dose, and the clearer patterns can be constructed on the surface.

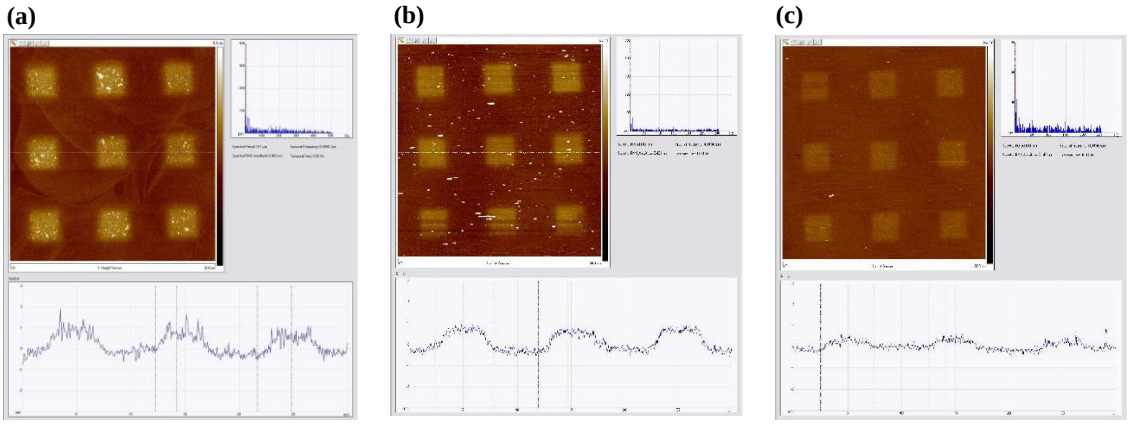

Figure 3-9. AFM images of copolymer layer surfaces obtained after UV irradiation at various doses: (a) poly(CMB-*r*-STMS) (1000 mJ/cm^2; depth and width of ablated area are 1 nm and 6.3 μm, respectively), (b) poly(CMB-*r*-STMS) (3000 mJ/cm^2; depth and width of ablated area are 1.3 nm and 5.6 μm, respectively), and (c) poly(CMB-*r*-MPTMS) (3000 mJ/cm^2; depth and width of ablated area are 0.5 nm and 5.0 μm, respectively).

Previously, it was reported that a polymer brush with an aromatic ring base could be decomposed more easily than a polymer brush without an aromatic ring base when irradiated with an ArF excimer laser (193 nm).[39] However, a pattern with lengths below 5 μm constructed with the polymer brush layer could not be clearly observed. This is probably because protein adsorption was not effectively suppressed with the spread of polymer brushes located at border of the non-irradiated area into the hollow area where the brush had been cleaved.[39]

In contrast to the polymer brush system, the copolymer layer exhibited a thickness of around 2 nm,[16,40] which enabled the complete removal of the copolymer layer with the UV irradiation. In particular, a pattern in an area of 1.5 × 1.5 μm could be clearly observed upon irradiation at 500 mJ/cm^2 on the poly(CMB-*r*-STMP) layer-modified wafer surface (**Figure 3-10**), exhibiting a higher contrast than that observed with the poly(CMB-*r*-MPTMS) layer. No pattern was observed at doses less than 3000 mJ/m^2 for the copolymer layer without an aromatic anchor group.

The microcontact printing method, which has been widely studied, exhibits high spatial resolution (100 nm) since physically stable polymer materials such as polydimethylsiloxane (PDMS) are commonly used in this method.[45] In contrast, due to the soft nature of the copolymer layer examined in this chapter, the edge of the patterned block would spread to the neighboring hollow space. Therefore, the spatial resolution obtained using the copolymer layer system cannot be as high as that obtained using microcontact printing.

However, the number of steps involved in microcontact printing is usually large.[45] In a typical procedure, a master is prepared by employing traditional photolithography techniques. For that purpose, a photoresist applied to the substrate surface is patterned by a photomask and UV light. The master is baked, developed, and cleaned. Then, a fabricated PDMS stamp is inked and applied to the substrate.

In contrast, the patterning procedure adopted in this chapter is very simple. It involves a silane coupling of CMB-*p*-trimethoxysilylstyrene copolymer to the solid substrates and ArF

irradiation through a photomask followed by rinsing.

Despite the disadvantages of using photomasks, this method has advantages such as the simple preparation techniques employed and the improved anti-biofouling properties achieved. Therefore, the advantages and the shortcomings, such as the relatively small spatial resolution should be taken into account before adopting the method.

Thus, significant protein adsorption was not realized on the surface of the poly(CMB-*r*-STMS) layer, while the introduction of a small amount of styryl groups to the layer enabled more distinct patterning in comparison with that obtained without the aromatic ring. The poly(CMB-*r*-STMS) layer-modified glass that does not exhibit bio-fouling would be highly useful in biomedical applications.

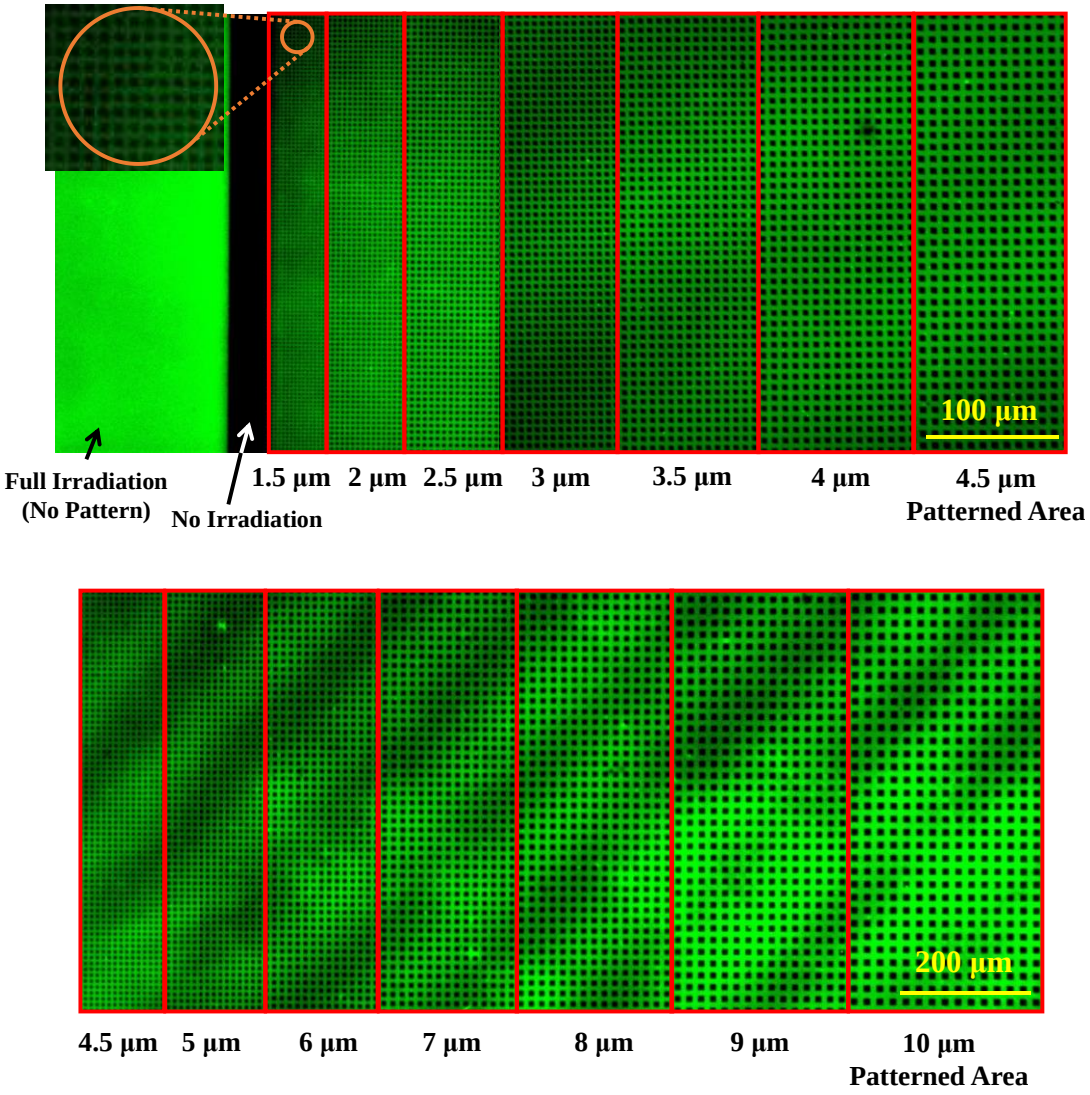

Figure 3-10. Fluorescence images of A488-IgG adsorbed on poly(CMB-r-STMS)-modified surfaces after UV irradiation (500 mJ/cm^2).

3.4 Conclusion

The poly(CMB-*r*-STMS) layer, with an aromatic ring in the anchoring group, on a glass plate exhibited excellent hydrophilicity and resistance to non-specific adsorption of protein (BSA) on the surface, which is consistent with the previous results concerning blood- and bio-compatibilities of the PCMB polymers. The efficient cleavage of the layer upon UV-irradiation makes poly(CMB-*r*-STMS) highly useful in diverse biomedical applications.

3.5 References

[1] Ulman, A. *Chem. Rev.* **1996**, *96*, 1533.

[2] Moineau, J.; Granier, M.; Lanneau, G. F. *Langmuir* **2004**, *20*, 3202.

[3] Nomura, K.; Mikuni, S.; Nakaji-Hirabayashi, T.; Gemmei-Ide, M.; Kitano, H.; Noguchi, H.; Uosaki, K. *Colloids Surf. B* **2015**, *135*, 267.

[4] Nuzzo, R. G.; Allara, D. L. *J. Am. Chem. Soc.* **1983**, *105*, 4481.

[5] Porter, M. D.; Bright, T. B.; Allara, D. L.; Chidsey, C. E. D. *J. Am. Chem. Soc.* **1987,** *109*, 3559.

[6] Bain, C. D.; Troughton, E. B.; Tao, Y. T.; Evall, J.; Whitesides, G. M.; Nuzzo, R. G. *J. Am. Chem. Soc.* **1989**, *111*, 321.

[7] Love, J. C.; Estroff, L. A.; Kriebel, J. K.; Nuzzo, R. G.; Whitesides, G. M. *Chem. Rev.* **2005**, *105*, 1103.

[8] Zhou, F.; Liu, W.; Xu, T.; Liu, S.; Chen, M.; Liu, J. *J. Appl. Polym. Sci.* **2004**, *92*, 1695.

[9] Sethi, D.; Kumar, A.; Gupta, K. C.; Kumar, P. *Bioconjugate. Chem.* **2008**, *19*, 2136.

[10] Kitano, H.; Hayashi, A.; Takakura, H.; Suzuki, H.; Kanayama, N.; Saruwatari, Y. *Langmuir* **2009**, *25*, 9361.

[11] Ohno, K.; Koh, K.; Tsujii, Y.; Fukuda, T. *Macromolecules* **2002**, *35*, 8989.

[12] Ohno, K.; Koh, K.; Tsujii, Y.; Fukuda, T. *Angew. Chem. Int. Ed.* **2003**, *42*, 2751.

[13] Mandal, T. K.; Fleming, M. S.; Walt, D. R. *Nano. Lett.* **2002**, *2*, 3.

[14] Jordan, R.; West, N.; Ulman, A.; Chou, Y. M.; Nuyken, O. *Macromolecules* **2001**, *34*, 1606.

[15] Kondo, T.; Nomura, K.; Gemmei-Ide, M.; Kitano, H.; Noguchi, H.; Uosaki, K.; Saruwatari, Y. *Colloids. Surf. B* **2014**, *113*, 361.

[16] Suzuki, H.; Li, L.; Nakaji-Hirabayashi, T.; Kitano, H.; Ohno, K.; Matsuoka, K.; Saruwatari, Y. *Colloids. Surf. B* **2012**, *94*, 107.

[17] Xu, Y.; Takai, M.; Konno, T.; Ishihara, K. *Lab. Chip.* **2007**, *7*,199

[18] Ishihara, K.; Aragaki, R.; Ueda, T.; Watanabe, A.; Nakabayashi, N.; Biomed, J. *Mater. Res.* **1990**, *24*, 1069.

[19] Ishihara, K. *Sci. Technol. Adv. Mater.* **2000**, *1*, 131.

[20] Lewis, A. L. *Colloids. Surf. B* **2000**, *18*, 261.

[21] Kitano, H.; Mori, T.; Tada, S.; Takeuchi, Y.; Gemmei-Ide, M.; Tanaka, M. *Macromol. Biosci.* **2005**, *5*, 314.

[22] Kitano, H. *Polym. J.* **2016**, *48*, 15.

[23] Kitano, H.; Tada, S.; Mori, T.; Takaha, K.; Gemmei-Ide, M.; Tanaka, M.; Fukuda, M.; Yokoyama, Y. *Langmuir* **2005**, *21*, 11932.

[24] Tada, S.; Inaba, C.; Mizukami, K.; Fujishita, S.; Gemmei-Ide, M.; Kitano, H.; Mochizuki, A.; Tanaka, M.; Matsunaga, T. *Macromol. Biosci.* **2009**, *9*, 63.

[25] Fujishita, S.; Inaba, C.; Tada, S.; Gemmei-Ide, M.; Kitano, H.; Saruwatari, Y. *Biol. Pharm. Bull.* **2008**, *31*, 2309.

[26] Kitano, H.; Kawasaki, A.; Kawasaki, H.; Morokoshi, S. *J. Colloid. Interface. Sci.* **2005**, *282*, 340.

[27] Matsuura, K.; Ohno, K.; Kagaya, S.; Kitano, H. *Macromol. Chem. Phys.* **2007**, *208*, 862.

[28] Zhang, Z.; Chao, T.; Chen, S.; Jiang, S. *Langmuir* **2006**, *22*, 10072.

[29] Kitano, H.; Suzuki, H.; Matsuura, K.; Ohno, K. *Langmuir* **2010**, *26*, 6767.

[30] Kitano, H.; Kondo, T.; Kamada, T.; Iwanaga, S.; Nakamura, M.; Ohno, K. *Colloids. Surf. B* **2011**, *88*, 455.

[31] Lowe, A. B.; McCormick, C. L. *Chem. Rev.* **2002**, *102*, 4177.

[32] Laschewsky, A.; Touillaux, R.; Hedlinger, P.; Vierengel, A. *Polymer* **1995**, *36*, 3045.

[33] Kudaibergenov, S.; Jaeger, W.; Laschewsky, A. *Adv. Polym. Sci.* **2006**, *201*, 157.

[34] Kitano, H.; Sudo, K.; Ichikawa, K.; Ide, M.; Ishihara, K. *J. Phys. Chem. B.* **2000**, *104*, 11425.

[35] Kitano, H.; Imai, M.; Sudo, K.; Ide, M. *J. Phys. Chem. B* **2002**, *106*, 11391.

[36] Kitano, H.; Imai, M.; Mori, T.; Gemmei-Ide, M.; Yokoyama, Y.; Ishihara, K. *Langmuir* **2003**, *19*, 10260.

[37] Besson, E.; Gue, A. M.; Sudor, J.; Korri-Youssoufi, H.; Jaffrezic, N.; Tardy, J. *Langmuir* **2006**, *22*, 8346.

[38] Chen, T.; Jordan, A. I. *Chem. Soc. Rev.* **2012**, *41*, 3280.

[39] Kamada, T.; Yamazawa, Y.; Nakaji-Hirabayashi, T.; Kitano, H.; Usui, Y.; Hiroi, Y.; Kishioka, T. *Colloids. Surf. B* **2014**, *123*, 878.

[40] Nishida, M.; Nakaji-Hirabayashi, T.; Kitano, H.; Matsuoka, K.; Saruwatari, Y. *J. Biomed. Mat. Res.* **2016**, *104*, 2029.

[41] Fikentscher, H. *Cellulosechemie* **1932**, *13*, 58.

[42] Fikentscher, H. *Cellulosechemie* **1932**, *13*, 71.

[43] Ohno, K.; Morinaga, T.; Koh, K.; Tsujii, Y.; Fukuda, T. *Macromolecules* **2005**, *38*, 2137.

[44] Brandrup, J.; Immergut, E. H.; Grulke, E. A.; Abe, A.; Bloch, D. R. *Polymer Handbook-4th Edition*, Wiley-Interscience **2003**.

[45] Kumar, A; Whitesides, G. M. *Appl. Phys. Lett.* **1993**, *63*, 2002.

[46] Nomura, K.; Nakaji-Hirabayashi, T.; Gemmei-Ide, M.; Kitano, H.; Noguchi, H.; Uosaki, K. *Colloids. Surf. B* **2014**, *121*, 264.

Chapter 4

Gradation of Proteins and Cells Attached to the Surface of Bio-Inert Zwitterionic Polymer Brush

4.1 Introduction

For the modification of solid surfaces, so-called “polymer brushes” have been widely used. In the construction of polymer brushes, “grafting-from” and “grafting-to” procedures can be used. To obtain condensed polymer brushes, the former method has been preferentially adopted, whereas the latter can be easily pursued.[1-5] For the preparation of polymer brushes by the grafting-from method, controlled radical polymerization methods such as atom transfer radical polymerization (ATRP),[6-9] reversible addition-fragmentation chain transfer polymerization,[10, 11] and nitroxide-mediated polymerization [12,13] have been widely used.

Zwitterionic polymers have been extensively used for the construction of biocompatible surfaces.[14-17] By the vibrational spectroscopic analyses of the hydrogen-bonded network structure of vicinal water, it has been pointed out that charge-neutralized polymers including zwitterionic and amphoteric polymers are inert to vicinal water, which provides biocompatible properties to the polymer surface.[18-21] It has previously been reported that the surface of zwitterionic brushes exhibit interesting properties with respect to friction and lubricity.[22-24]

Recently, the construction of surfaces with additional values, including the modification of solid surfaces with polymeric materials and micro-fabrication technology, is highly sought after.[25-27]

Many research groups, have reported that surfaces modified with zwitterionic polymers can efficiently suppress protein adsorption and cell adhesion.[28-32] Furthermore, patterned surfaces of proteins and cells could be constructed using UV light or high-energy beams such as an ArF-excimer laser and focused ion beams.[33-35] Ahmad et al., for example, reported poly[oligo(ethylene glycol)methacrylate] brushes grown from photo-patterned halogen initiators using a unique technology, the selective decomposition of the C-Br bond of the initiator for ATRP by using UV light at 244 nm.[36]

It is very difficult to understand cellular behaviors in vivo because various events occur simultaneously. In the literature, gradated materials have been quite useful for the construction of surfaces with a concentration gradient of cells and proteins.[37-40] The applicability of gradated materials is quite promising because a wide range of information on the interaction of biological materials can be obtained on the same surface. Until now, various methods have been reported for constructing a gradation surface by using SAMs and polymers.[41-43] Moreover, a method, which adjusts a dose of irradiation to cause decomposition or photo-polymerization while moving the light shutter, has also been adopted to prepare the gradation surfaces.[44-47] In particular, based on the inherent property of a polymer, the wettability and charge of the surface can be controlled by the gradation of the polymer; these properties are attracting significant attention in advanced research fields.[48-52] The length and graft density of the polymer chains could be easily controlled for the concentrated polymer brush constructed via SI-ATRP. Therefore, it can be expected that microfabricated surfaces can be prepared more precisely by this method compared to other methods.[53-54]

In this chapter, a zwitterionic polymer brush was prepared by surface-initiated atom transfer radical polymerization (SI-ATRP) from the self-assembled monolayer (SAM) of the ATRP initiator having a 2-bromoisobutyryl end group. With UV irradiation at 254 nm, the bromine atom essential for the initiation of ATRP could be selectively cleaved and therefore, by varying the irradiation time, the surface density of the polymer brush could be easily controlled. Since

the zwitterionic polymer brush strongly suppressed protein adsorption and cell adhesion, the author expected that he could manipulate the protein adsorption and cell adhesiveness onto the originally bio-inert polymer brush introduced to the surface of glass, silicon wafers, and various metal oxides.

Furthermore, by gradation of the irradiation period along the ATRP initiator-modified SAM, the gradation of the zwitterionic polymer brush can be easily realized (**Figure 4-1**). Such a technique will be highly useful for bio-related applications.

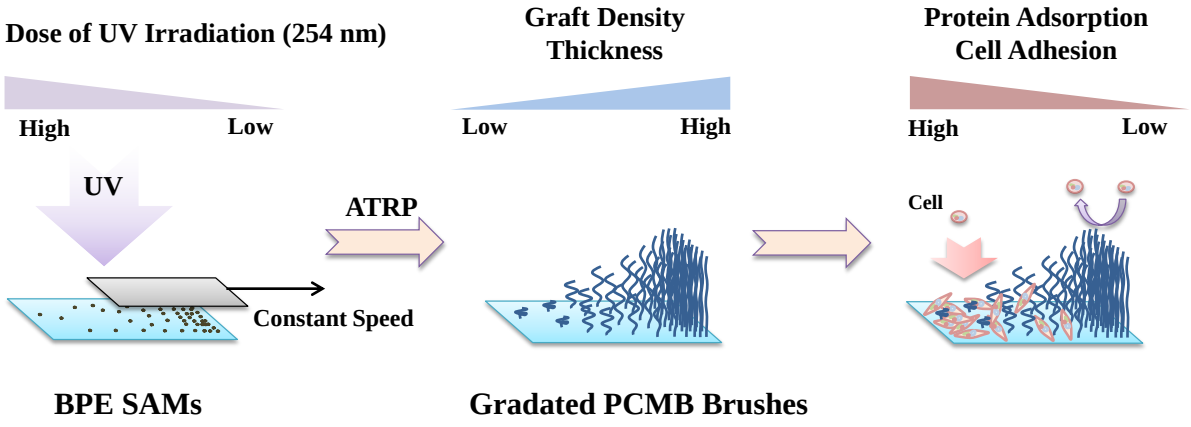

Figure 4-1. Schematic illustration of protein adsorption and cell adhesion to the gradated polymer brushes prepared after UV irradiation of BPE SAMs.

4.2 Experimental section

4.2.1 *Materials*

1-carboxy-*N*,*N*-dimethyl-*N*-(2-methacryloyloxyethyl)methanaminium hydroxide inner salt (CMB, GLBT®) (**Scheme 4-1(a)**) was kindly donated by Osaka Organic Chemical Industries, Osaka, Japan. 3-(2-Bromo-2-isobutyryloxy)propyltriethoxysilane (BPE, **Scheme 4-1(b)**) was prepared as described elsewhere.[55] 2,2′-Bipyridine (Bpy, 99.5%) and copper (I) bromide (Cu(I)Br, 99.999%) were purchased from Wako Pure Chemicals Osaka, Japan. Cu(I)Br was purified by stirring in acetic acid overnight and dried after filtration at low pressure. Ethyl 2-bromoisobutyrate (EBiB, 98%, **Scheme 4-1(c)**) and bovine serum albumin (BSA) were purchased from Nacalai Tesque (Kyoto, Japan) and Sigma-Aldrich (Milwaukee, WI, USA), respectively. Toluene (99.5%, Wako Pure Chemicals) was stirred with concentrated sulfuric acid, followed by washing with saturated aqueous sodium carbonate solution and water. The purified toluene was finally obtained by distillation. Other reagents were commercially available. Milli-Q grade water (< 18 MΩ.cm) was used for preparation of sample solutions.

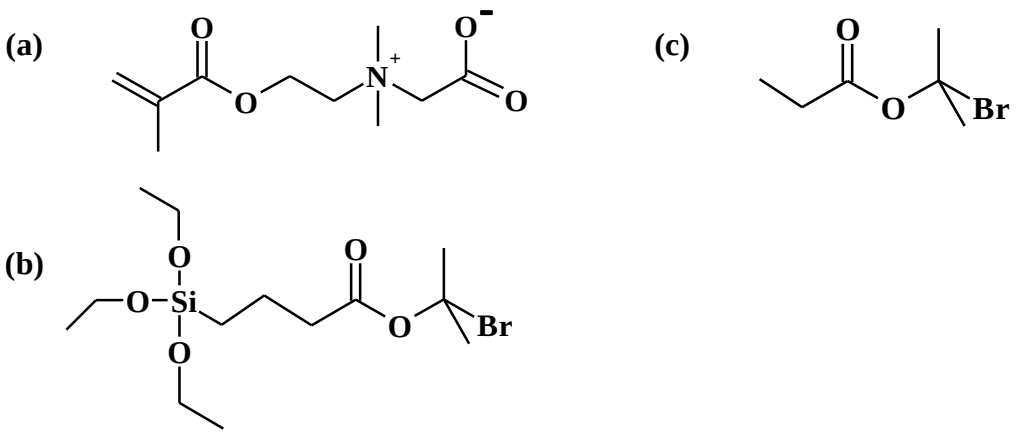

Scheme 4-1. Chemical structures of (a) 1-carboxy-*N*,*N*-dimethyl-*N*-(2-methacryloyloxyethyl)methanaminium hydroxide inner salt (CMB, GLBT®), (b) 3-(2-bromo-2-isobutyryloxy)propyltriethoxysilane (BPE), and (c) Ethyl 2-bromoisobutyrate (EBiB).

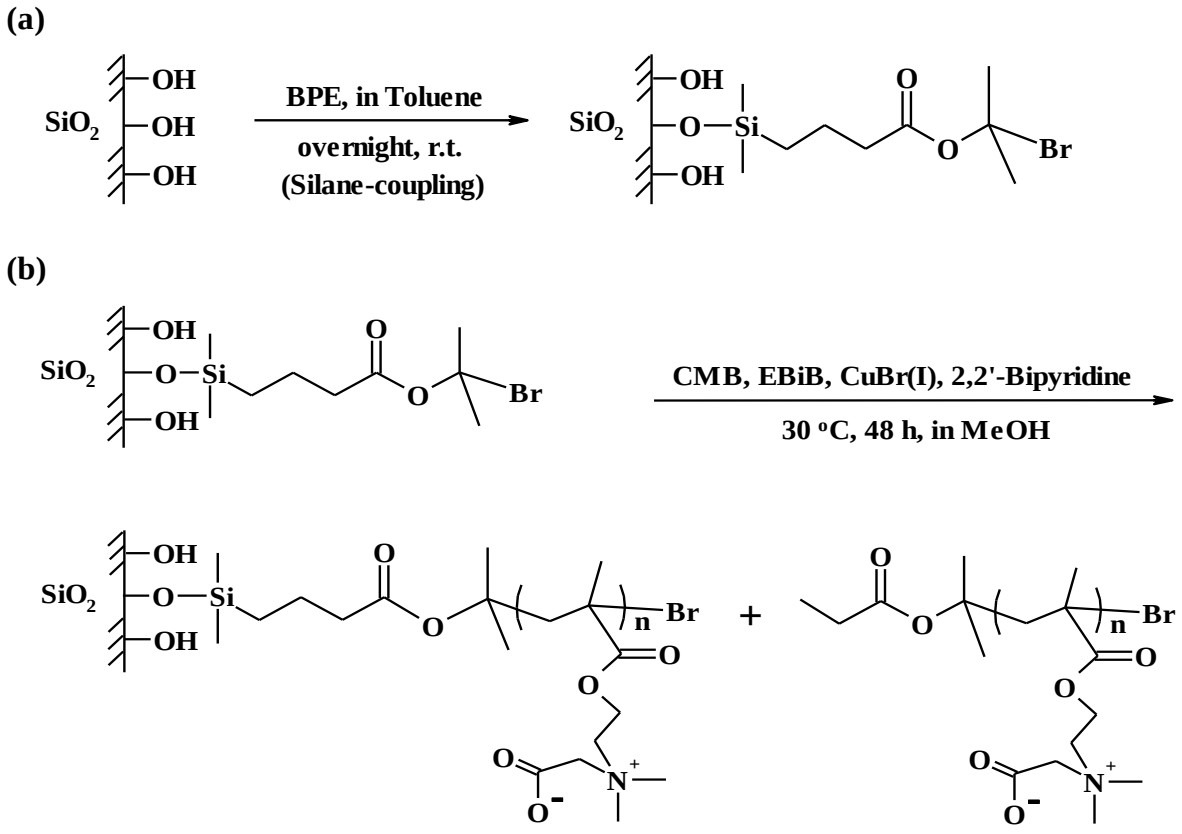

Scheme 4-2. Preparation of (a) BPE SAM by a silane-coupling reaction and (b) PCMB brush-modified substrate via SI-ATRP, and accompanying polymerization of free PCMB.

4.2.1 Construction of polymer brush

4.2.1.1 Introduction of ATRP initiator (BPE) (**Scheme 4-2(a)**)

A glass substrate (20 × 26 mm^2) was washed by ultrasonication in methanol for 10 min and rinsed with water before immersing in a piranha solution (sulfuric acid : hydrogen peroxide solution = 7 : 3) for 1 h. The glass substrate was further washed with deionized water more than ten times, rinsed with acetone, and dried by N_2 gas. The pristine glass substrate was incubated in a toluene solution of BPE (2 mM) overnight in the dark. The BPE-modified substrate was washed with toluene, ultrasonicated in toluene, repeatedly rinsed with methanol and acetone, and finally dried by N_2 gas.

4.2.1.2 Construction of PCMB brush via SI-ATRP (**Scheme 4-2(b)**)

CMB (3.50 g, 15.0 mmol) and ethyl 2-bromoisobutyrate (EBiB, ATRP initiator, 22.2 μL, 0.15 mmol) were dissolved in methanol (30 mL) and vacuum-degassed with argon 10 times. Thereafter, the mixed solution was sent to the reaction vessel containing 2,2′-bipyridyl (Bpy, 46.9 mg, 0.30 mmol), CuBr (21.5 mg, 0.15 mmol), and the BPE SAM-modified glass substrate through a PTFE tube under an argon atmosphere. The molar ratio was configured to [CMB]:[EBiB]:[CuBr]:[Bpy] = 100:1:1:2, and the ATRP reaction was carried out for 48 h at 30°C. After the reaction, the PCMB brush-modified substrate was washed with methanol, ultrasonicated in methanol, repeatedly rinsed with methanol, water, and acetone, and finally dried by a flush of N_2 gas. The solution of PCMB produced in the liquid phase at the same time was recovered and, after passing through a chelate resin column (IRC748 AmBerlite, Organo Ltd., Tokyo, Japan) in water to remove copper salt, condensed by evaporation. The purified solution containing PCMB was dialyzed against methanol for a week. The PCMB solution was condensed by evaporation, dissolved in water, and finally lyophilized (yield: 2.9 g, 83.1%). The number-averaged molecular weight (M_n), weight-averaged molecular weight (M_w), and

distribution of molecular weight (M_w/M_n) of PCMB were determined by gel permeation chromatography (GPC, Wako beads G-50, Wako Pure Chemicals; mobile phase, 0.1 M NaBr aq. soln.).

4.2.2 UV Irradiation of substrates

4.2.2.1 Quantitative irradiation

The PCMB-modified glass plate was UV-irradiated at 254 nm (0.135 mJ・cm^{-2}/s, MODEL UVGL-58, UVP, USA). The glass substrate was washed with methanol and dried by a flush of N_2 gas.

4.2.2.2 Gradation of irradiation

A UV irradiation system was prepared to continuously change the dose of irradiation (**Figure 4-2**). A UV shutter and the BPE-modified substrate were set on an irradiation stage made of a Teflon plate (43 mm × 43 mm, NICHIAS Corporation, Tokyo, Japan). The shutter of the system can be smoothly moved at a set speed using a stepping motor (0.1×10^{-3} mm/s ~ 0.11 mm/s). It was expected that a different range of Br gradation can be formed by moving the UV shutter at different speeds under a certain dose of irradiation. Two modes of sliding-speed were adopted to move the UV shutter for the irradiation (**Table 4-1**)

Table 4-1. The moving conditions of the UV shutter.

	Speed ($mm \cdot s^{-1}$)	Time (min)	Moving distance (mm)
Mode 1	0.542×10^{-3}	370	12.0
Mode 2	0.217×10^{-3}	370	4.81

Wavelength: 254 nm; Strength: 0.135 $mJ \cdot cm^{-2}/s$.

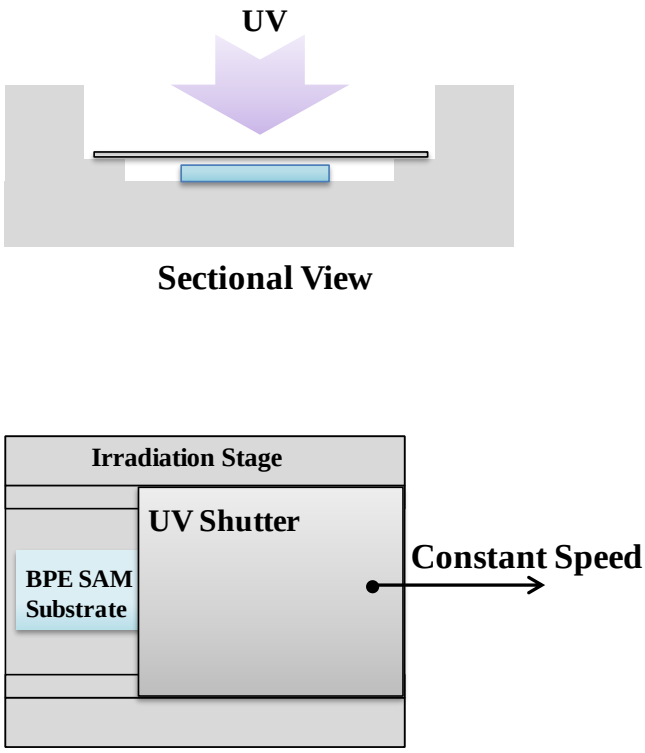

Figure 4-2. Mechanism of UV irradiation for gradation.

4.2.3 Characterization of polymer brush

4.2.3.1. Evaluation of thickness by ellipsometry measurements

The thickness of the polymer brush (dry state) was evaluated by ellipsometry (Lambda Ace RE-3100, DAINIPPON SCREEN MFG. Co., Ltd). The measurements were performed at a wavelength of 640 nm while the refractive index of the sample layer was assumed to be 1.49 (refractive index of poly(methyl methacrylate)).[56,57]

4.2.3.2 Wettability evaluation of substrate

The contact angle of a water droplet was measured to evaluate the wettability of the substrate using CA-D (Kyowa Surface Science, Tokyo, Japan). A droplet of deionized water (3-4 μL) was put in contact with the surface of the dried substrate to determine the contact angle 30 s after the contact. The measurement was performed 5 times for each sample, and an average value was obtained.

4.2.3.3 XPS measurements

X-ray photoelectron spectroscopy (XPS, ESCALAB 250Xi, Thermo Fisher Scientific, Inc., Waltham, Massachusetts, USA) was used for the evaluation of various elements on the substrate surface. Measurement conditions: detection angle, 90°; X-ray source type, monochromated/micro-focused AlK-Alpha; X-ray size, 650 μm. Analysis of the peak was carried out using Avantage (Ver. 4.84) of Thermo Fisher Scientific Corporation.

4.2.4 Protein adsorption

Protein adsorption on the PCMB brush-modified substrate was measured using a BCA method reported in previous studies.[35,58] For the gradated pattern of adsorbed A488-IgG (Alexa Fluor

488 goat anti-rabbit IgG), the adsorption of fluorescence-labeled protein was observed on a substrate modified with the PCMB brush. After mounting the A488-IgG solution (150 μL, 100 μg/mL in PBS) onto the substrate, incubation under a dark box at 25 ℃ for 2 h, and rinsing thoroughly with PBS, fluorescence images were observed by a fluorescence microscope (IX71, Olympus Corporation).

4.2.5 Cell adhesion

Adhesion of NIH3T3 cells was observed on the PCMB brush-modified substrate and the number of cells was counted. Experimental procedures were the same as those reported elsewhere.[35,58]

4.3 Results and discussion

4.3.1. Decomposition of ATRP initiator by UV irradiation

The ATRP initiator, BPE, was easily introduced to a glass surface as indicated by the drastic increase in contact angle (from 3.8° of bare glass to 69.4° after incubation with BPE). By subjecting the BPE-modified silicon wafer to UV irradiation, the XPS signal for bromine (Br_{3d}, ca. 71 eV) was observed to decrease (**Figure 4-3(a)**), indicating the scission of the C-Br bond, whereas the signals for other elements did not change significantly (**Figure 4-3(b)**). Therefore, UV irradiation easily reduced the surface density of BPE on the substrate. Consequently, it can be expected that the density of polymer chains could be simply modulated.

In previous studies, UV light (180-190 nm) was used to decompose a part of SI-ATRP initiator-modified surface for the construction of patterned polymer brushes.[15, 40] Therefore, the author tried to irradiate at 184 nm wavelength in a preset experiment. However, it was shown that not only the C-Br bond but also all bonds such as C-O and C-C were decomposed. This is because the graft density of the polymer brush and the density of adhered cells could not be controlled precisely. Thus, a UV light at 254 nm wavelength (with a comparatively lower energy) was adopted to decompose the C-Br bond selectively.

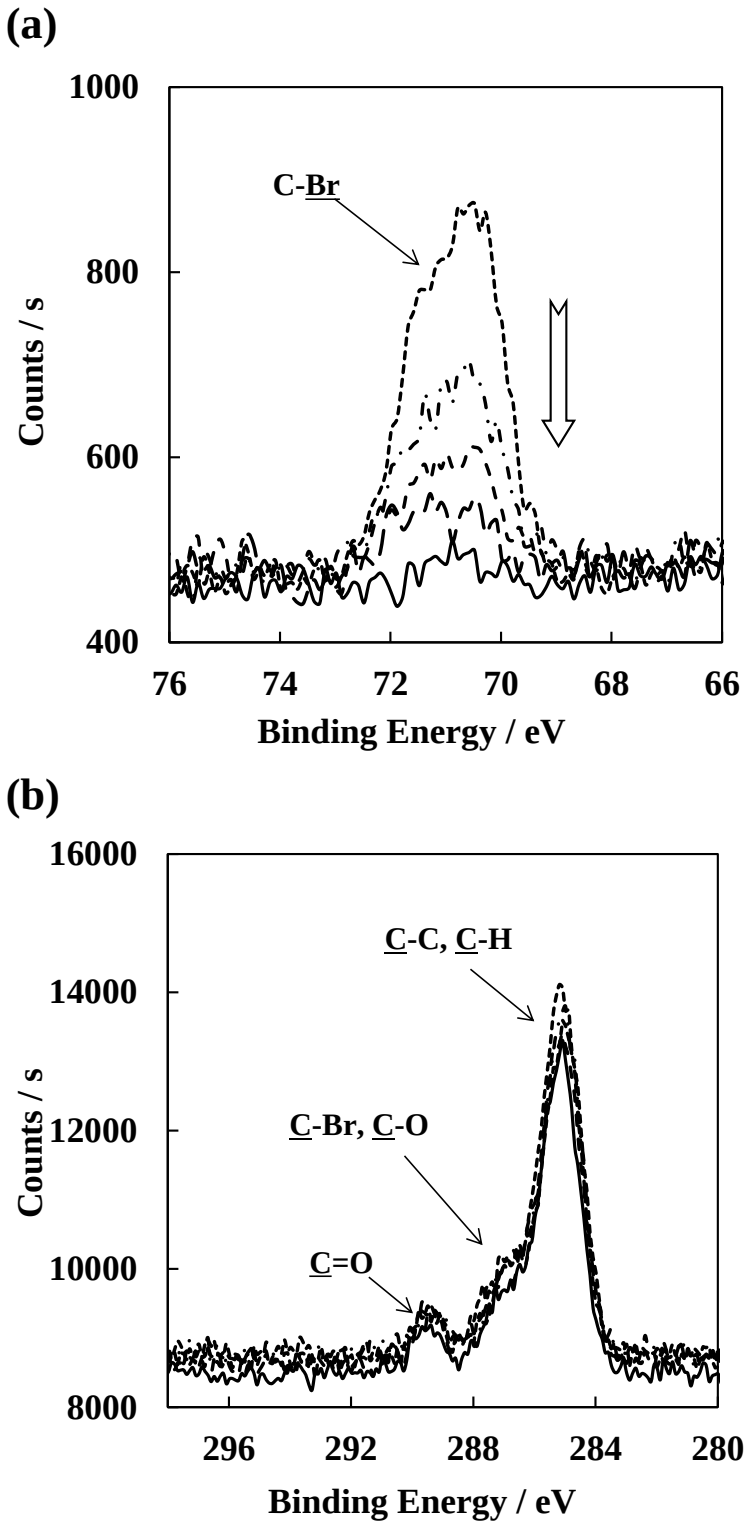

Figure 4-3. (a) Bromine signal and (b) carbon signal of each BPE SAM at various irradiation doses of UV light at 254 nm at 100 mJ/cm^2 (dotted line), 500 mJ/cm^2 (dotted-chain line), 1000 mJ/cm^2 (dashed line), 2000 mJ/cm^2 (long-dashed line), and 3000 mJ/cm^2 (solid line).

4.3.2. Construction of PCMB brush

PCMB brushes could be easily constructed by SI-ATRP on both BPE-modified glass and silicon wafer. With the introduction of the PCMB brush, the contact angle of the glass substrate was drastically decreased from 69.4° (BPE-SAM) to 12.5° (PCMB) (**Figure 4-4**), which is in agreement with previous results.[19]

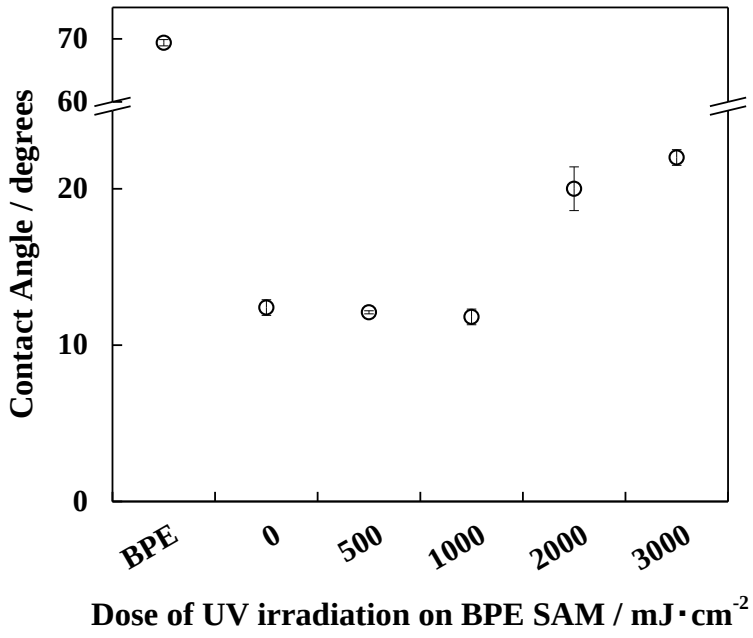

Figure 4-4. Effect of irradiation dose of UV light (254 nm) on the contact angle of PCMB brush surface on BPE SAM. The data are shown as mean value ± standard deviation for three independent samples.

Meanwhile, it was reported that the M_n and M_w/M_n values for the grafted and free polystyrene subjected to ATRP at the same time were nearly equal.[59-60] Assuming the same tendency, i.e. the degree of polymerization of the PCMB brush is the same as that of PCMB produced in the solution phase at the same time, the degree of polymerization of the PCMB brush was estimated

to be 125 (close to the target degree of polymerization, 100) using GPC. The M_n and M_w/M_n values of the PCMB brush were estimated to be 2.9×10^4 and 1.48, respectively, which showed the relatively narrow molecular weight distribution of this polymer.

The thickness of the PCMB brush on the silicon wafer was estimated by ellipsometry and the surface density of the brush (σ) was determined using equation (1).

$$\sigma = \rho\, d\ N_A \times\ 10^{-21}\ /\ M_n \qquad (1)$$

where σ is the graft density (chains/nm^2), ρ is the polymer density (g/cm^3), N_A is Avogadro's number, d is the thickness of the polymer brush (nm), and M_n is the number-averaged molar mass of bulk polymer. The ρ value for poly(methacryloyloxyethyl phosphorylcholine) (1.30 g/cm^3) available in the literature [15] was used to calculate the surface density of the PCMB brush.

When the graft density is higher than 0.1 chains/nm^2, the brush is referred to as a "concentrated polymer brush" [15]. The thickness of the PCMB brush prepared on the BPE SAM in this chapter was estimated to be 8.1 nm, and the graft density without UV irradiation was determined to be 0.21 chains/nm^2, which means that a concentrated PCMB brush was constructed (**Figure 4-5**).

4.3.3. PCMB brush on UV-irradiated BPE SAMs

XPS data indicated that, as a result of the UV irradiation of BPE SAM, the signal intensity of bromine atoms was gradually decreased and at 3000 mJ/cm^2, almost completely diminished (**Figure 4-3(a)**). Therefore, the thickness and surface density of the PCMB brush were observed to decrease by UV irradiation, as expected (**Figure 4-5**). Correspondingly, the water contact angle on the PCMB brush surface was largely increased with exposure time up to about 2000 mJ/cm^2 (**Figure 4-4**). In the case of a concentrated zwitterionic brush, the large hydrophilicity of the brush-modified surface has been reported,[19,28] which means that the initiator layer did not affect the surface properties of the brush when the thickness of the brush was larger than

2.5–5 nm.[60] The thickness of the PCMB brush was estimated to be 3.0 and 1.9 nm at 1000 mJ/cm^2 and 2000 mJ/cm^2 of UV irradiation, respectively, on the BPE SAM.

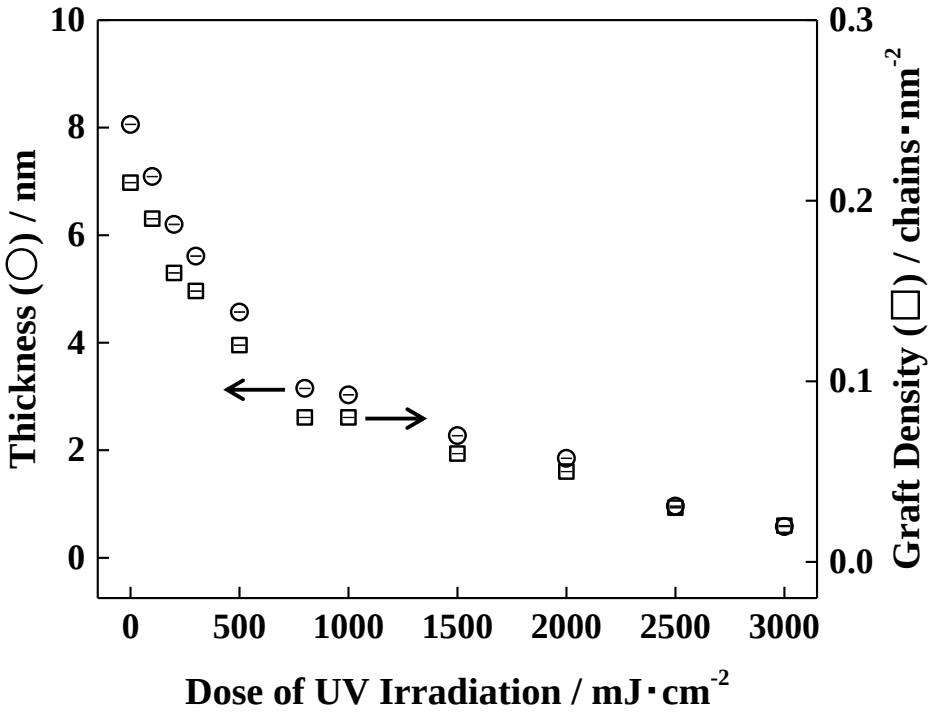

Figure 4-5. Thickness (○) and graft density (□) of various PCMB brush surfaces at various irradiation doses of UV light (254 nm) on BPE SAM. The data are shown as mean value ± standard deviation for three independent samples.

In addition, the author tried to construct a gradated PCMB brush using a stepping motor-driven UV shutter smoothly moving above the stage of both the BPE-modified glass and silicon wafer at a constant speed (**Table 4-1**). The XPS data along the direction of the movement of the UV shutter indicated that the signal intensity of bromine elements (Br_{3d}, ca. 71 eV) at the end of the ATRP initiator linearly decreased, indicating the gradation of the surface density of Br along the substrate (**Figure 4-6(a)**). Changes were hardly observed in the other elements (Si_{2p}, ca. 100 eV; C_{1s}, ca. 286 eV) after UV irradiation (**Figure 4-6(b)**).

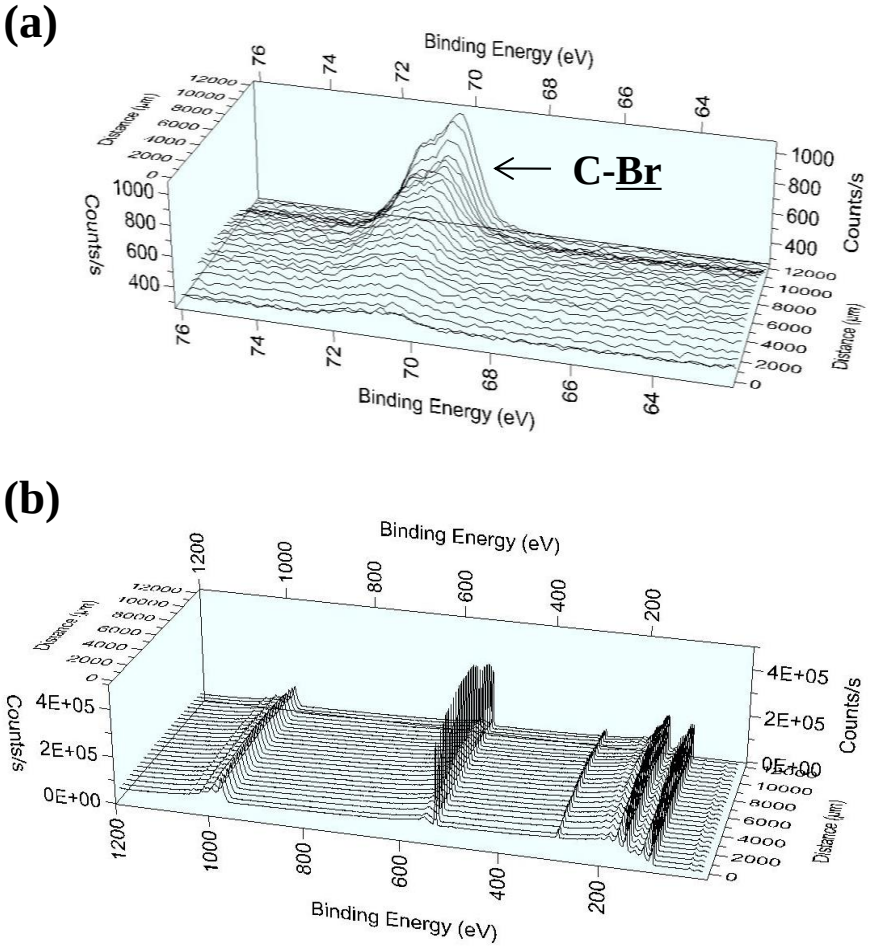

Figure 4-6. XPS line scans of (a) Br_{3d} area and (b) total area of "Mode 1" plates of BPE SAMs.

Furthermore, an increase in the peak of nitrogen elements (N_{1s}, ca. 402 eV) ascribable to the CMB unit was observed along the moving direction of the UV shutter on the PCMB brush surface constructed above the BPE SAM-modified substrate surface that had been subjected to continuous irradiation. Moreover, **Figures 4-7(a) and (b)** showed that it was possible to prepare a gradated PCMB brush corresponding to the setting range of 12.0 mm (Mode 1) and 4.81 mm (Mode 2) (**Table 4-1**). In addition, the variations of the peak (Si_{2p}, C_{1s}) in the total spectra except N_{1s} corresponded to the setting range of gradation (**Figure 4-8(a) and (b)**).

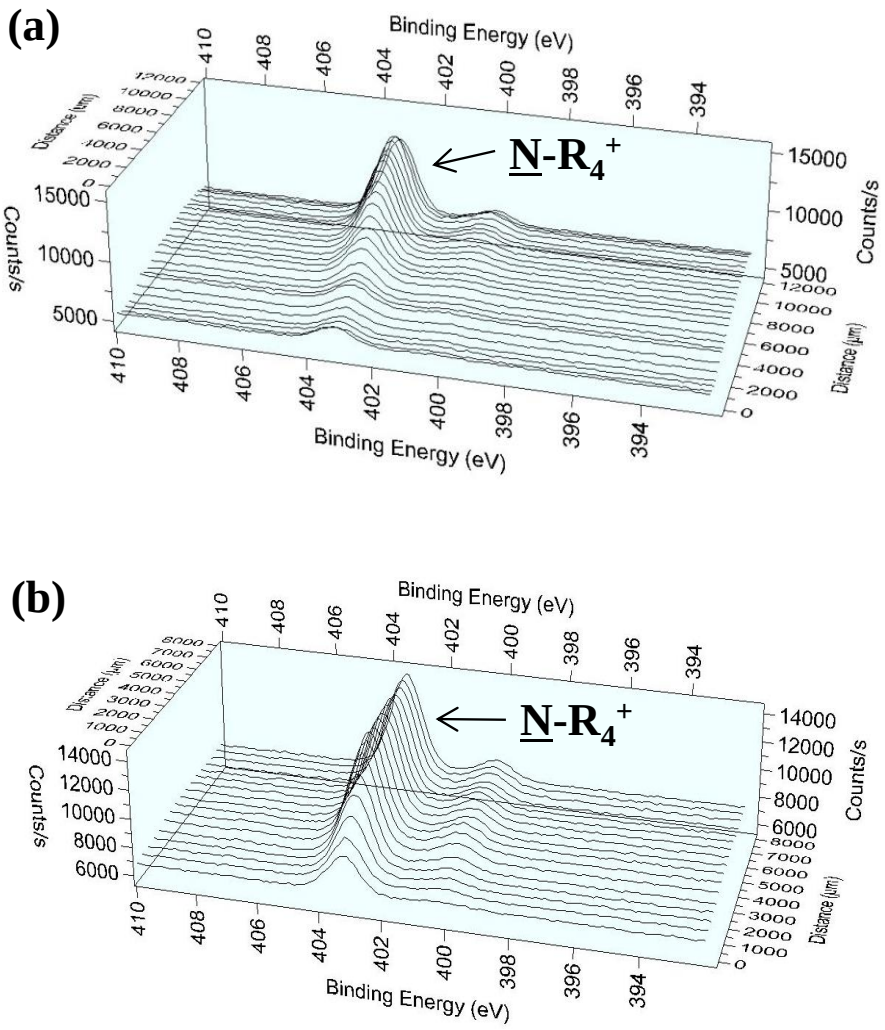

Figure 4-7. XPS line scans of N_{1s} area of (a) "Mode 1" and (b) "Mode 2" plates of PCMB brushes.

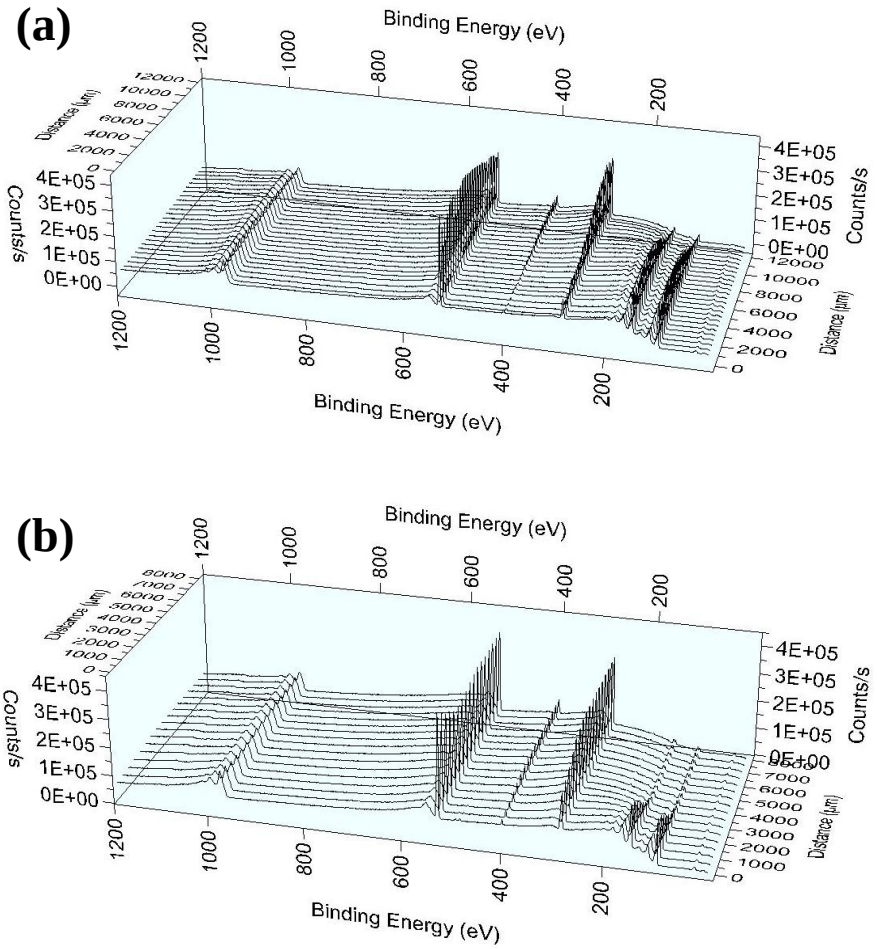

Figure 4-8. XPS line scans of total area of (a) "Mode 1" plates of PCMB brushes, and (b) "Mode 2" plates of PCMB brushes.

4.3.4. Gradation in protein adsorption and cell adhesion to the PCMB brush

The XPS data suggest that the surface density of protein adsorption and cell adhesion to the surface of the PCMB brush can be varied with irradiation time. Actually, the amount of proteins adsorbed was increased with an increase in the dose of UV irradiation from a region between 500-1000 mJ/cm^2. In the same region, the graft density of the PCMB brush was 0.12-0.08 chains/nm^2 (**Figure 4-9(a)**). Thus, it was speculated that BSA molecules were hardly adsorbed to a concentrated PCMB brush-modified surface when the graft density was above 0.1 chains/nm^2, whereas adsorption occurred below 0.1 chains/nm^2. For concentrated polymer brushes, various unique properties such as high elasticity, ultra-low friction, and size exclusion effects have been reported.[61-64]

In a similar manner, the number of NIH3T3 cells adhered to the substrate was increased with an increase in the dose of UV irradiation above 1500 mJ/cm^2 (**Figure 4-9(b)**). It has often been pointed out that cells tend to adhere via the anchor proteins adsorbed to the solid substrate.[65] At a UV irradiation of 1500 mJ/cm^2, the amount of BSA adsorbed was approximately 40 ng/cm^2. Therefore, it could be expected that protein adsorption needs to exceed approximately 40 ng/cm^2 for cells to adhere to the PCMB brush-modified surface.

The scaffold proteins might adsorb to the area where the surface density of the PCMB brush was much smaller than that in the non-irradiated area, which would result in the preferential adhesion of NIH3T3 cells (**Figure 4-10**).

The author further examined the possibility of gradation in the amount of adsorbed proteins and number of adhered cells controlled by the irradiation period of UV light. The XPS data along the direction of the movement of the UV shutter indicated that the intensity of Br atoms at the end of the ATRP initiator linearly increased. In other words, the gradation of Br along the substrate was observed (**Figure 4-6(a)**). Consequently, the gradation of the surface polymer brush density could be realized, which resulted in the gradation of the densities of adsorbed

proteins and adhered cells.

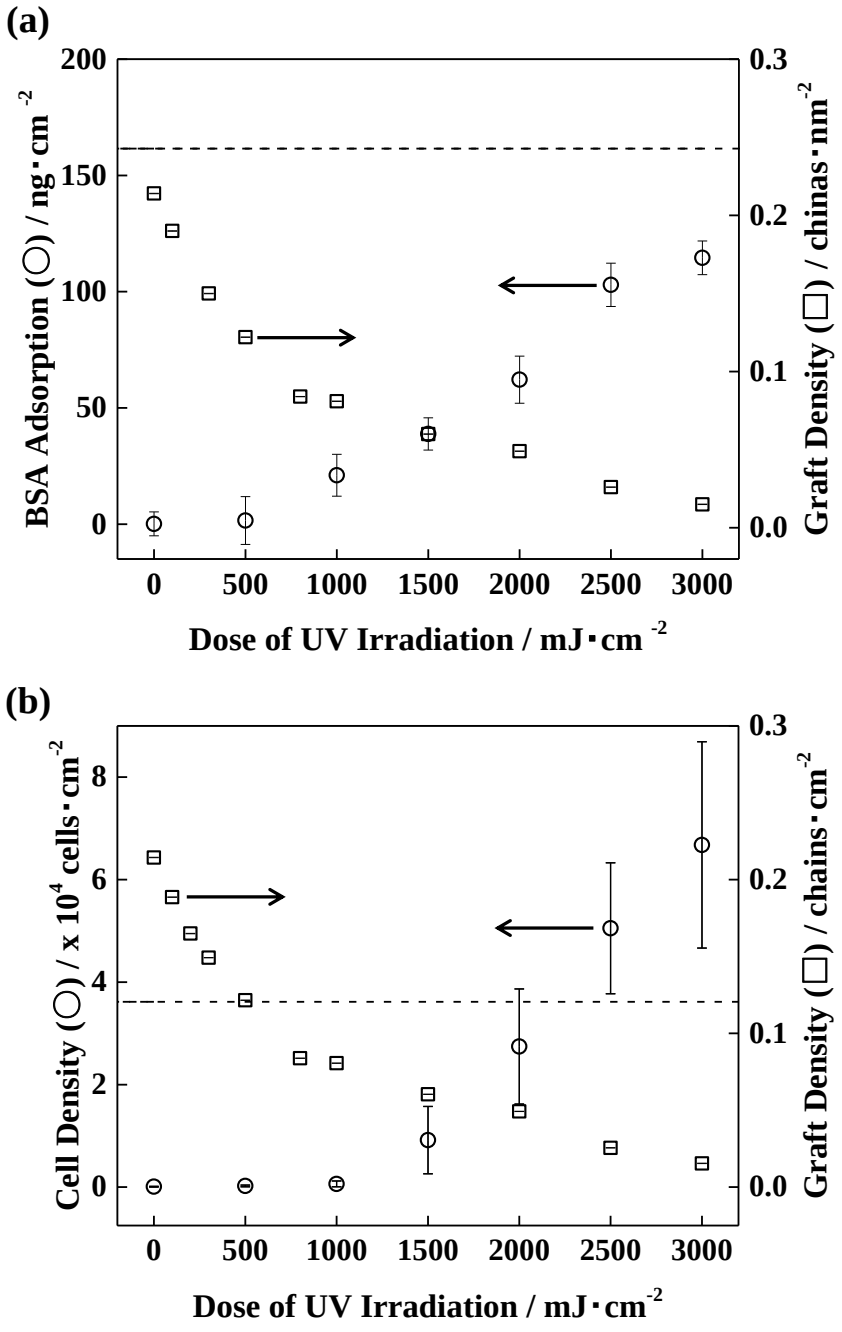

Figure 4-9. (a) Correlation between amount of adsorbed BSA (○) and graft density (□) of the PCMB brush surfaces upon irradiation of various doses at 254 nm on BPE SAM. (Dashed line: BSA adsorption to BPE SAM); (b) Correlation between cell density (○) and graft density (□) of the PCMB brush on BPE SAM with doses of UV irradiation (254 nm). (Dashed line: Cell density of BPE). The data are shown as mean value ± standard deviation for three independent samples.

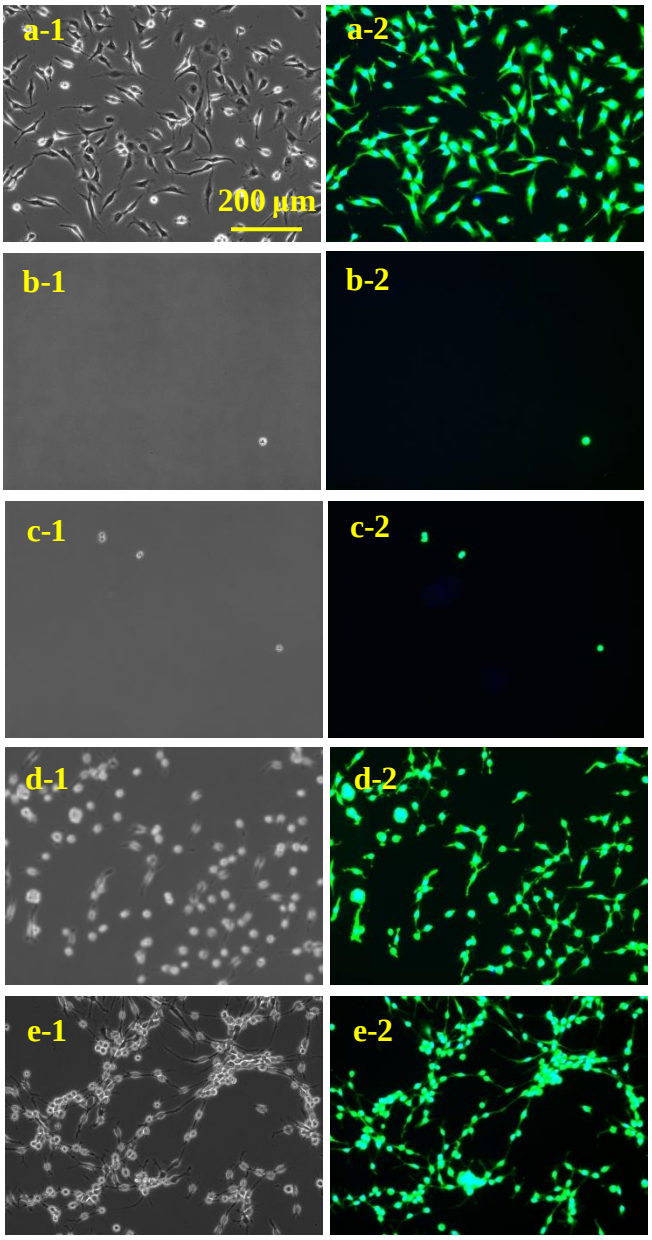

Figure 4-10. Phase-contrast (x-1) and fluorescence microscopic images (x-2, green: Calcein-AM; blue: Hoechst 33342) of NIH3T3 cells cultured for 24 h on (a) BPE substrates and various PCMB brush surfaces at various doses of UV irradiation (254 nm) on BPE SAM. PCMB brushes (b) 0 mJ/cm^2, (c) 1000 mJ/cm^2, (d) 2000 mJ/cm^2, and (e) 3000 mJ/cm^2.

In fact, it was found that the adsorption of fluorescent proteins decreased gradually from the starting point (0 mm) of irradiation on the gradated PCMB brush surface that was prepared under the conditions of Mode 1 (12.0 mm) (**Figure 4-11(a)**). The adhesion of NIH3T3 cells showed a similar tendency (**Figure 4-11(b)**). The number of adherent cells observed showed that adhesion no longer appeared at the region at around 7.4 mm (**Figure 4-12**). On the other hand, changes in cell adhesion on the gradated PCMB brush surface that had been prepared under the conditions of Mode 2 (4.81 mm) showed that adhesion no longer appeared at around 3.0 mm (**Figure 4-13**).

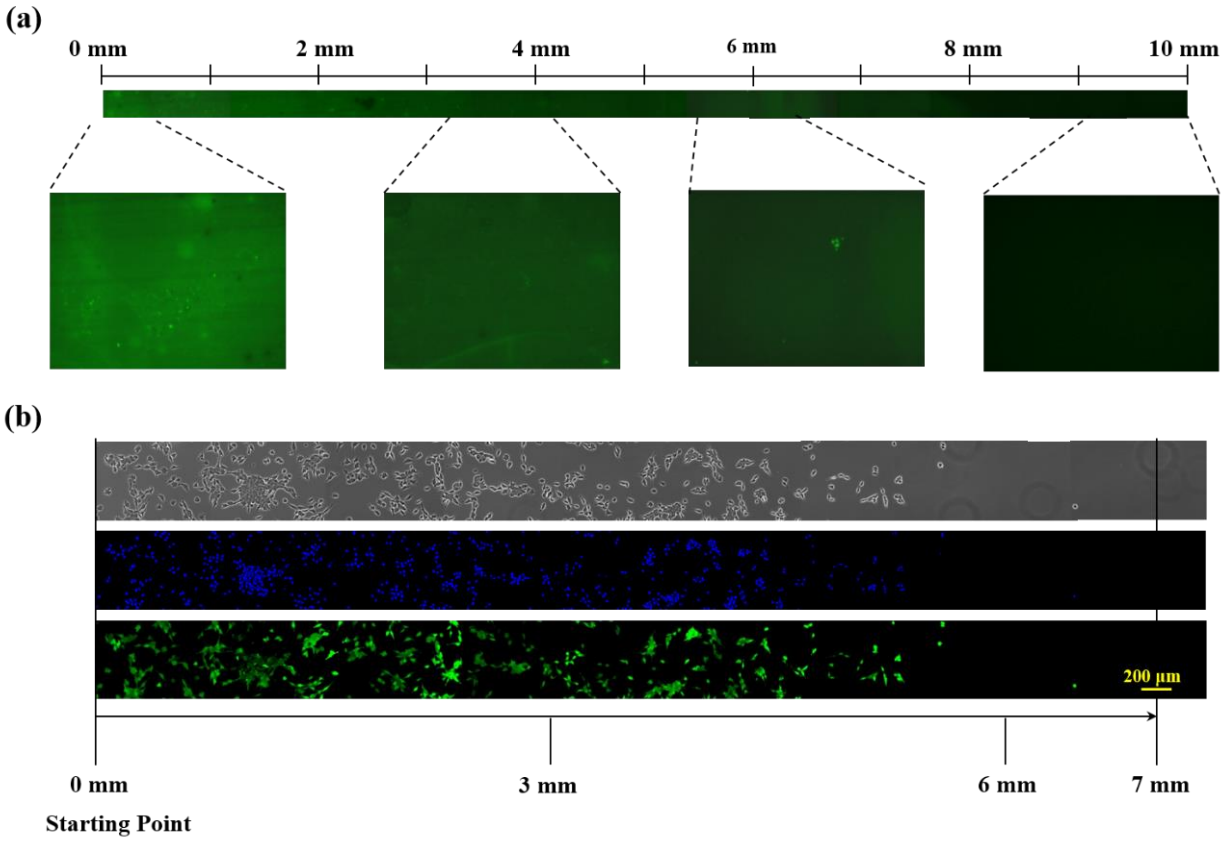

Figure 11. (a) Fluorescence images of A488-IgG adsorbed onto the gradated PCMB brushes; (b) Phase-contrast and fluorescence microscopic images (green: Calcein-AM; blue: Hoechst 33342) of NIH3T3 cells cultured for 24 h onto gradated PCMB brushes.

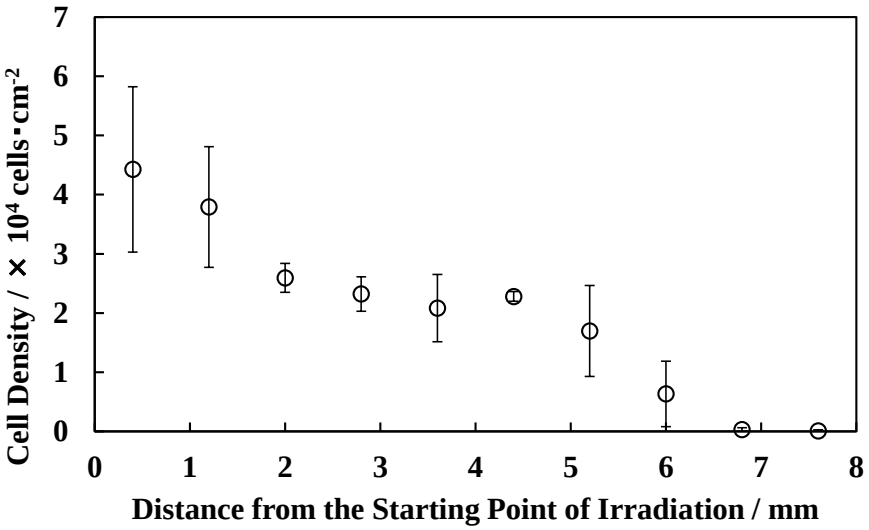

Figure 12. The density of 3T3 cells adhered onto the gradated PCMB brushes at various distances from the starting point of irradiation. The data are shown as mean value ± standard deviation for three independent samples.

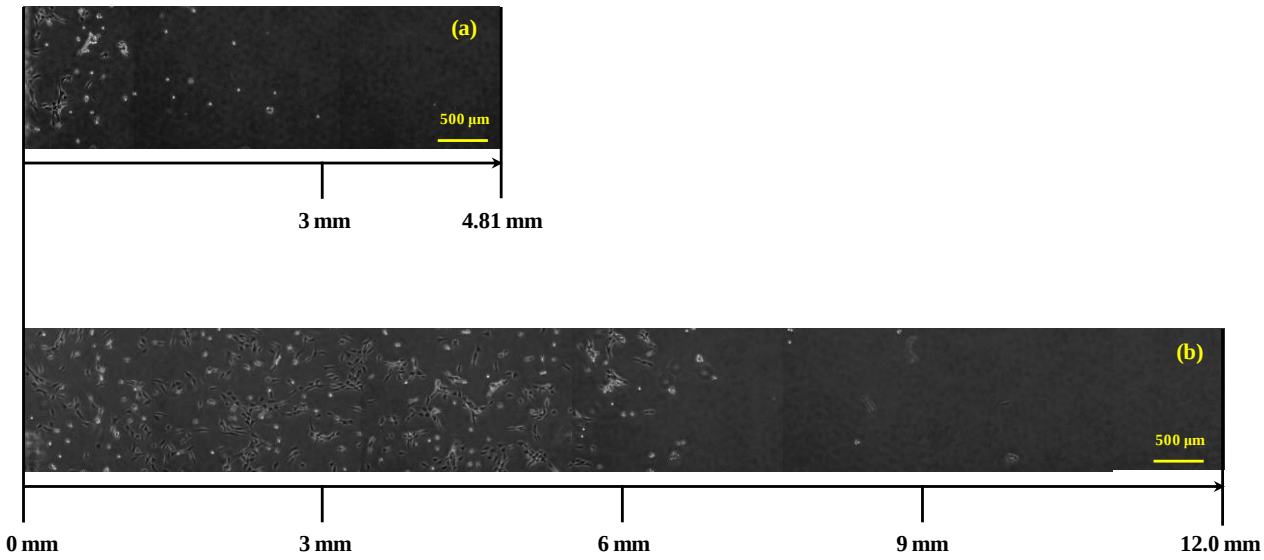

Figure 4-13. Micrographs of NIH3T3 cells cultured for 24 h on the gradated PCMB brushes. (a) Mode 2 and (b) Mode 1.

In addition, when the UV irradiation dose (Q) was calculated using equation (2) and irradiation conditions (**Table 4-1**) at a position (*d*) (Mode 1: 7.4 mm and Mode 2: 3.0 mm) where cell adhesion no longer appeared, quite similar results of irradiation dose (1145 mJ/cm^2 and 1128 mJ/cm^2, respectively) were obtained.

$$Q = (d_0 - d)\ w\ /\ v \qquad (2)$$

where d_0 is the moving distance of the UV shutter (mm), w is the strength of UV irradiation (mJ・cm^{-2}/s), and v is the speed of sliding the UV shutter (mm・s^{-1}). Therefore, using this method, the range could provide variously gradated materials, and high reproducibility and controllability were verified.

Thus, by controlling the changing rate of the dose of UV (254 nm) irradiation along the surface of the initiator SAM-modified substrate, the construction of gradated polymer brushes could be realized. There was no need for complicated procedures and sophisticated devices in the polymerization. Moreover, the author do not need to worry about the disadvantageous effect of UV on the polymer brush because the process of UV irradiation was only administered to the initiator-modified substrate and selectively decomposed the active site of SI-ATRP. The proposed simple method to precisely control the surface density of bio-inert polymer brushes is anticipated not only in scientific research but also in industrial applications.

4.4 Conclusion

By UV irradiation, a bromine atom at the end of an ATRP initiator SAM introduced to the surface of glass and silicon wafer could be easily removed, and the surface density of PCMB brushes constructed from the radical produced by the dissociation of the C-Br bond could be controlled by the regulation of irradiation time. The author was able to correlate graft density of polymer brushes with protein adsorption or cell adhesion using this technique. Furthermore, because the irradiation using 254 nm hardly affected other bonds, it can be applied to not only solid materials such as glass and metal but also polymer/plastic-based materials that can be easily deteriorated by intense UV light (<200 nm). Using a motor-driven UV shutter, the surface density of cells adhered to the brush could be easily gradated along the direction of the shutter movement, suggesting the gradation of the amount of adsorbed proteins to which cells adhered.

4.5 References

[1] Edmondson, S.; Osborne, V. L.; Huck, W. T. S. *Chem. Soc. Rev.* **2004**, *33*, 14.

[2] Zhou, F.; Liu, W.; Xu, T.; Liu, S.; Chen, M.; Liu, J. J. *Appl. Polym. Sci.* **2004**, *92*, 1695.

[3] Sethi, D.; Kumar, A.; Gupta, K. C.; Kumar, P. *Bioconjugate. Chem.* **2008**, *19*, 2136.

[4] Kitano, H.; Hayashi, A.; Takakura, H.; Suzuki, H.; Kanayama, N.; Saruwatari, Y. *Langmuir* **2009**, *25*, 9361.

[5] Suzuki, H.; Li, L.; Nakaji-Hirabayashi, T.; Kitano, H.; Ohno, K.; Matsuoka, K.; Saruwatari, Y. *Colloids Surf. B* **2012**, *94*, 107.

[6] Wang, J. S.; Matyjaszewski, K. *J. Am. Chem. Soc.* **1995**, *117*, 5614.

[7] Matyjaszewski, K.; Xia, *J. Chem. Rev.* **2001**, *101*, 2921.

[8] Kato, M.; Kamigaito, M.; Sawamoto, M.; Higashimura, T. *Macromolecules* **1995**, *28*, 1721.

[9] Kamigaito, M.; Ando, T.; Sawamoto, M. *Chem. Rev.* **2001**, *101*, 3689.

[10] Mitsukami, Y.; Donovan, M. S.; Lowe, A. B.; McCormick, C. L. *Macromolecules* **2001**, *34*, 2248.

[11] McCormick, C. L.; Lowe, A. B. *Acc. Chem. Res.* **2004**, *37*, 312.

[12] Husseman, M.; Malmstrom, E. E.; McNamara, M.; Mate, M.; Mecerreyes, D.; Benoit, D. G.; Hedrick, J. L.; Mansky, P.; Huang, E.; Russell, T. P.; Hawker, C. J. *Macromolecules* **1999**, *32*, 1424.

[13] Hawker, C. J.; Bosman, A. W.; Harth, E. *Chem. Rev.* **2001**, *101*, 3661.

[14] Feng, W.; Brash, J. L.; Zhu, S. *Biomaterials* **2006**, *27*, 847.

[15] Iwata, R.; Suk-In, P.; Hoven, V. P.; Takahara, A.; Akiyoshi, K.; Iwasaki, Y. *Biomacromolecules* **2004**, *5*, 2308.

[16] Feng, W.; Zhu, S.; Ishihara, K.; Brash, J. L. *Langmuir* **2005**, *21*, 5980.

[17] Lewis, A. L. *Colloids. Surf. B* **2000**, *18*, 261.

[18] Kondo, T.; Gemmei-Ide, M.; Kitano, H.; Ohno, K.; Noguchi, H.; Uosaki, K. *Colloids. Surf.*

B **2012**, *91*, 215.

[19] Kondo, T.; Nomura, K.; Murou, M.; Gemmei-Ide, M.; Kitano, H.; Noguchi, H.; Uosaki, K.; Ohno, K.; Saruwatari, Y. *Colloids. Surf. B* **2012**, *100*, 126.

[20] Kondo, T.; Nomura, K.; Gemmei-Ide, M.; Kitano, H.; Noguchi, H.; Uosaki, K.; Saruwatari, Y. *Colloids. Surf. B* **2014**, *113*, 361.

[21] Kitano, H. *Polymer Journal* **2016**, *48*, 15.

[22] Zhang, Z.; Morse, A. J.; Armes, S. P.; Lewis, A. L.; Geoghegan, M.; Leggett, G. J. *Langmuir* **2013**, *29*, 10684.

[23] Zhang, Z.; Morse, A. J.; Armes, S. P.; Lewis, A. L.; Geoghegan, M.; Leggett, G. J. *Langmuir* **2011**, *27*, 2514

[24] Morse, A. J.; Edmondson, S.; Dupin, D.; Armes, S. P.; Zhang, Z.; Leggett, G. J.; Thompson, R. L.; Lewis, A. L. *Soft Matter* **2010**, *6*, 1571.

[25] Kitano, H.; Mori, T.; Tada, S.; Takeuchi, Y.; Gemmei-Ide, M.; Tanaka, M. *Macromol. Biosci.* **2005**, *5*, 314.

[26] Kitano, H.; Tada, S.; Mori, T.; Takaha, K.; Gemmei-Ide, M.; Tanaka, M.; Fukuda, M.; Yokoyama, Y. *Langmuir* **2005**, *21*, 11932.

[27] Ishihara, K. *Technol. Adv. Mater.* **2000**, *1*, 131.

[28] Kitano, H.; Suzuki, H.; Matsuura, K.; Ohno, K. *Langmuir* **2010**, *26*, 6767.

[29] Kitano, H.; Tokuwa, K.; Ueno, H.; Li, L.; Saruwatari, Y. *Colloid. Polym. Sci.* **2015**, *293*, 2931

[30] Suzuki, H.; Murou, M.; Kitano, H.; Ohno, K.; Saruwatari, Y. *Colloids. Surf. B* **2011**, *84*, 111.

[31] Murou, M.; Kitano, H.; Fujita, M.; Maeda, M.; Saruwatari, Y. *J. Colloid Interface Sci.* **2013**, *390*, 47.

[32] Matsuura, K.; Ohno, K.; Kagaya, S.; Kitano, H. *Macromol. Chem. Phys.* **2007**, *208*, 862.

[33] Kitano, H.; Suzuki, H.; Kondo, T.; Sasaki, K.; Iwanaga, S.; Nakamura, M.; Ohno, K.;

Saruwatari, Y. *Macromol. Biosci.* **2011**, *11*, 557.

[34] Kitano, H.; Kondo, T.; Kamada, T.; Iwanaga, S.; Nakamura, M.; Ohno, K. *Colloids. Surf. B* **2011**, *88*, 455.

[35] Kamada, T.; Yamazawa, Y.; Nakaji-Hirabayashi, T.; Kitano, H.; Usui, Y.; Hiroi, Y.; Kishioka, T. *Colloids. Surf. B* **2014**, *123*, 878.

[36] Ahmad, S. A.; Legett, G. J.; Hucknall, A.; Chilkoti, A. *Biointerphases* **2011**, *6*, 8.

[37] Wu, J.; Mao, Z.; Tan, H.; Han, L.; Ren, T.; Gao, C. *Interface Focus* **2012**, *2*, 337.

[38] Kim, S. E.; Harker, E. C.; Leon, A. C. D.; Advincula, R. C.; Pokorski, J. K. *Biomacromolecules* **2015**, *16*, 860.

[39] Plummer, S. T.; Wang, Q.; Bohn, P. W.; Stockton, R.; Schwartz, M. A. *Langmuir* **2003**, *19*, 7528.

[40] Kennedy, S. B.; Washburn, N. R.; Simon, C. G.; Amis, E. J. *Biomaterials* **2006**, *27*, 3817.

[41] Elwing, H.; Welin, S.; Askendal, A.; Nilsson, U.; Lundström, I. *J. Colloid Interface Sci.* **1987**, *119*, 203.

[42] Morgenthaler, S.; Zink, C.; Spencer, N. D. *Soft Matter* **2008**, *4*, 419.

[43] Chaudhury, M. K.; Whitesides, G. M. *Science* **1992**, *256*, 1539.

[44] Ito, Y.; Heydari, M.; Hashimoto, A.; Konno, T.; Hirasawa, A.; Hori, S.; Kurita, K.; Nakajima, A. *Langmuir* **2007**, *23*, 1845.

[45] Larsson, A.; Liedberg, B. *Langmuir* **2007**, *23*, 11319.

[46] Harris, B. P.; Metters, A. T. *Macromolecules* **2006**, *39*, 2764.

[47] Ekblad, T.; Andersson, O.; Tai, F. I.; Ederth, T.; Liedberg, B. *Langmuir* **2009**, *25*, 3755.

[48] Iwasaki, Y.; Ishihara, K.; Nakabayashi, N.; Khang, G.; Jeon, J. H.; Lee, J. W.; Lee, H. B. *J. Biomater. Sci, Polym. Edn.* **1998**, *9*, 801.

[49] Iwasaki, Y.; Sawada, S.; Nakabayashi, N.; Khang, G.; Lee, H. B.; Ishihara, K. *Biomaterials* **1999**, *20*, 2185.

[50] Ionov, L.; Houbenov, N.; Sidorenko, A.; Stamm, M.; Luzinov, I.; Minko, S. *Langmuir* **2004**, *20*, 9916.

[51] Ionov, L.; Stamm, M.; Diez, S. *Nano Letters* **2005**, *5*, 1910.

[52] Gallant, N. D.; Lavery, K. A.; Amis, E. J.; Becker, M. L. *Adv. Mater.* **2007**, *19*, 965

[53] Gosecka, M.; Pietrasik, J.; Decorse, P.; Glebocki, B.; Chehimi, M. M.; Slomkowski, S.; Basinska, T. *Langmuir* **2015**, *31*, 4853.

[54] Shida, N.; Koizumi, Y.; Nishiyama, H.; Tomita, I.; Inagi, S. *Angew. Chem. Int. Ed.* **2015**, *54*, 3922.

[55] Ohno, K.; Akashi, T.; Huang, Y.; Tsujii, Y. *Macromolecules* **2010**, *43*, 8805.

[56] Ohno, K.; Morinaga, T.; Koh, K.; Tsujii, Y.; Fukuda, T. *Macromolecules* **2005**, *38*, 2137.

[57] Brandrup, J.; Immergut, E. H.; Grulke, E. A.; Abe, A.; Bloch, D. R. *Polymer Handbook-4th Edition*; Wiley-Interscience, 2003.

[58] Nomura, K.; Mikuni, S.; Nakaji-Hirabayashi, T.; Gemmei-Ide, M.; Kitano, H.; Noguchi, H.; Uosaki, K. *Colloids. Surf. B* **2015**, *135*, 267.

[59] Ohno, K.; Koh, K.; Tsujii, Y.; Fukuda, T. *Macromolecules* **2002**, *35*, 8989.

[60] Inoue, Y.; Ishihara, K. *Colloids. Surf. B* **2010**, *81*, 350.

[61] Tsujii, Y.; Ejaz, M.; Sato, K.; Goto, A.; Fukuda, T. *Macromolecules* **2001**, *34*, 8872.

[62] Xue, C.; Yonet-Tanyeri, N.; Brouette, N.; Sferrazza, M.; Braun, P. V.; Leckband, D. E. *Langmuir* **2011**, *27*, 8810.

[63] Zou, Y.; Rossi, N. A. A.; Kizhakkedathu, J. N.; Brooks, D. E. *Macromolecules* **2009**, *42*, 4817.

[64] Rossi, G.; Elliott, I. G.; Ala-Nissila, T.; Faller, R. *Macromolecules* **2012**, *45*, 563.

[65] Yoshikawa, C.; Goto, A.; Tsujii, Y.; Fukuda, T.; Kimura, T.; Yamamoto, K.; Kishida, A.; *Macromolecules* **2006**, *39*, 2284.

Chapter 5

A Novel Approach for Patterning with Binary Polymer Brushes

5. 1 Introduction

Construction of biocompatible surfaces has been extensively examined using zwitterionic polymers such as polyphosphobetaine, polycarboxybetanine and polysulfobetaine.[1-5] The vibrational spectroscopic analyses such as Raman, infra-red and sum frequency generation (SFG) spectroscopies have clarified that charge-neutralized polymers including zwitterionic polymers and amphoteric polymers having comparable contents of oppositely charged monomer residues are inert to the vicinal water, which provides biocompatible (anti-biofouling) properties to the polymer surface.[6-11]

Meanwhile, attention has been focusing on a so-called "polymer brush" for the modification of solid surfaces. At the construction of polymer brush, "grafting-from" and "grafting-to" procedures can be used. To obtain a condensed polymer brush, the former method has preferentially been adopted, while the latter can be very easily pursued, though the surface density of polymer brush prepared by the latter cannot be sufficiently large.[12] At the preparation of polymer brushes by the "grafting-from" method, controlled radical polymerization such as atom transfer radical polymerization (ATRP),[13-15] reversible addition-fragmentation chain transfer (RAFT) polymerization,[16-18] and nitroxide-mediated radical polymerization (NMRP)[19,20] have been widely used.

In this chapter, the author tried to construct a patterned surface with binary polymer brushes (**Figure 5-1**). For that purpose, solid substrates (glass plate and silicon wafer) were modified

with a mixed self-assembled monolayer (SAM) of an initiator having a 2-bromoisobutyryl end group for ATRP and an agent for RAFT polymerization. At first, the UV-irradiation at 254 nm through a photomask to the mixed SAM surface was carried out, and the bromine atom essential for the initiation of ATRP could be selectively cloven.

Subsequently, a polymer brush of hydrophobic monomer, 2-ethylhexyl methacrylate (EHMA), was prepared by the surface-initiated (SI)-ATRP from the SAM of the ATRP initiator, while a polymer brush of zwitterionic monomer, carboxymethyl betaine (CMB), was prepared by the SI-RAFT polymerization. CMB was chosen in this work mostly because of its anti-biofouling property.[22-26] and partly because of its thermal stability endurable of incubation even above 80 ^{o}C. This is a good contrast to the thermal instability of carboxyethylbetaine methacrylate which tends to decompose during ordinary radical polymerization at 80 ^{o}C probably due to the Hofmann degradation.[27]

Thus, the shape and size of both PEHMA brush domain and PCMB brush domain could be easily controlled. Since the zwitterionic polymers strongly suppress the adsorption and adhesion of proteins and cells, respectively,[22-26] we could expect the control of absorptivity and adhesiveness of proteins and cells, respectively, to the surface domain of glass, silicon wafer, and various metal oxides.

In recent years, binary polymer brush has been examined by many researchers.[28-33] For example, a binary polymer brush of polystyrene (PSt) and poly(2-vinyl pyridine) (PVP) was constructed by the sequential grafting-to method.[28] α-Fe_2O_3 was modified with the copolymer, PSt-$SiCl_2$-PVP, prepared by anionic polymerization to provide binary polymer brush-conjugated microparticles dispersible in both aqueous medium and organic solvent.[29] A Y-shaped initiator was fixed onto a silicon wafer and PSt and poly(*t*-butyl acrylate) chains were grafted on the wafer.[30] Furthermore, a binary polymer brush of poly(*n*-butyl acrylate) and poly(acrylic acid) was prepared by the two-step reverse ATRP method.[33]

Meanwhile, patterning of solid substrate modified with a polymer material has been

attracting our attention.[34-39] For example, Ga ion beam,[34-36] ArF excimer laser (193 nm)[37] (**Chapter 3**) and UV light (254 nm) (**Chapter 4**) were adopted for decomposition of polymer brush,[34,35,37] polymer layer[36] (**Chapter 3**) and initiation site (**Chapter 4**) on the substrate. However, as far as we know, the patterning with domains of different polymer brushes has not been examined yet. Such a technique will be highly useful for the application of functionalized solid substrates mentioned above to bio-related fields.

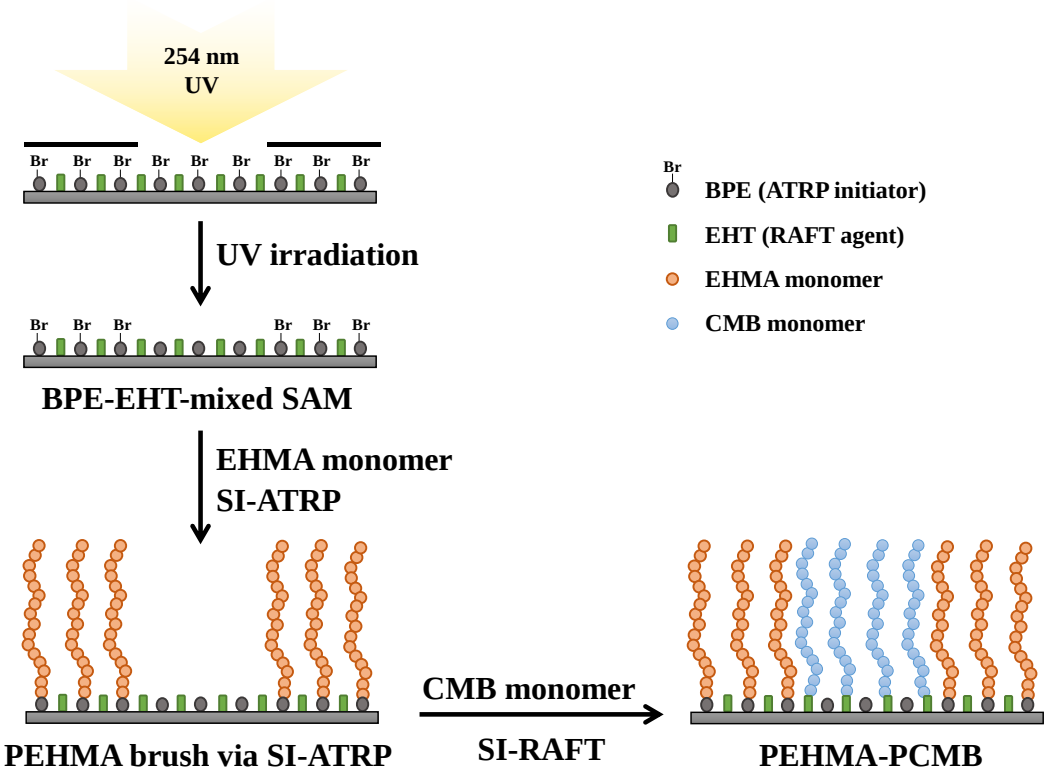

Figure 5-1. Schematic procedures to construct binary polymer brush.

5.2 Experimental section

5.2.1 Materials

Carboxymethyl betaine, (1-carboxy-*N*,*N*-dimethyl-*N*-(2-methacryloyloxyethyl) methanaminium hydroxide inner salt (CMB, commercial name GLBT®),[38,39] and 2-ethylhexyl methacrylate (EHMA) were kindly donated from Osaka Organic Chemical Industries, Osaka, Japan. EHMA was distilled under reduced pressure before use. 3-(2-Bromo-2-isobutyryloxy)propyl triethoxysilane (BPE) was prepared as described elsewhere.[40] A RAFT agent, 6-(triethoxysilyl)hexyl 2-(((methylthio)carbonothioyl)thio)-2-phenylacetate (EHT), was prepared as described before.[41] Cu(I)Br from Wako Pure Chemicals, Osaka, Japan, was purified by stirring in acetic acid overnight and, after filtration, dried at low pressure. 4-Cyanopentanoic acid dithiobenzoate (CTA-1, 97%)[17] was purchased from Sigma-Aldrich (Milwaukee, WI, USA). Toluene (99.5%, Wako Pure Chemicals) was stirred with concentrated sulfuric acid, followed by washing with saturated aqueous sodium carbonate solution and water. The purified toluene was finally obtained by distillation. Tetrahydrofuran (THF, 99.5 %, Wako Pure Chemicals) was dried with molecular sieve (4A) prior to use. Other reagents were commercially available. A Milli-Q grade water (< 18 MΩ.cm) was used for preparation of sample solutions.

5.2.2 Construction of polymer brush (Scheme 5-1)

5.2.2.1 Introduction of ATRP initiator (BPE) and RAFT agent (EHT) to substrate surface

The substrate (20 × 20 mm^2, glass plate or silicon wafer) was rinsed with methanol, ultrasonified in methanol for 10 min, rinsed with water before immersed in a piranha solution (sulfuric acid:hydrogen peroxide solution = 7:3) at 80 ^oC for 1 h, and rinsed with a large amount of water more than ten times. The substrate was rinsed with acetone and dried by a flush of N_2 gas. The pristine glass substrate was incubated in a mixture of BPE and EHT at a molar ratio of 1:1 (total concentration: 4 mM) in toluene solution at 60 ^oC overnight in dark. The substrate was repeatedly washed with toluene and methanol, and dried by a flush of N_2 gas.

5.2.2.2 Construction of PEHMA Brush

A tetrahydrofuran (THF) solution (30 mL) containing EHMA (5.6 mL, 25.0 mmol) and ethyl 2-bromoisobutyrate (EBiB, free ATRP initiator) (18.5 μL, 0.125 mmol) was vacuum-degassed with argon 10 times. Then, the mixed solution was sent to a reaction vessel containing 4,4'-dinonylbipyridyl (DNBpy, 204 mg, 0.5 mmol) and Cu(I)Br (35.9 mg, 0.25 mmol) ([EHMA]:[EBiB]:[Cu(I)Br]:[DNBpy] = 200:1:1:2) and the BPE-EHT mixed SAM-modified substrate through a PTFE tube while N_2 gas was passed through the reaction vessel for 30 min. The SAM-modified substrate was incubated at 30 ^oC for 24 h. The PEHMA brush-modified substrate was rinsed with THF, ultrasonicated in THF, repeatedly rinsed with chloroform and acetone, and finally dried by a flush of N_2 gas.

The solution of PEHMA produced in the liquid phase at the same time was recovered and, after passing through an alumina column to remove copper salt, condensed by evaporation, precipitated in MeOH and dried *in vacuo*. The number-averaged molecular weight (M_n) and distribution of molecular weight (M_w/M_n) of PEHMA were determined by GPC (Shodex

K801, Showa Denko; mobile phase, chloroform).

5.2.2.3 Construction of PCMB Brush

The polymer brush of CMB on the surface of BPE-EHT-mixed SAM-modified substrate was constructed and characterized in a similar manner to that of PEHMA brush. CMB was dissolved in EtOH (30 mL) and vacuum-degassed with argon 10 times. Then, the CMB solution was sent to the reaction vessel containing CTA-1 (41.9 mg, 0.15 mmol), 2,2'-azobisisobutyronitrile (AIBN, 4.9 mg, 0.03 mmol) and BPE-EHT SAM-modified substrate or PEHMA-carrying mixed SAM (PEHMA@BPE-EHT SAM)-modified substrate through a PTFE tube under a nitrogen atmosphere. The molar ratio was configured to [CMB]:[CTA-1]:[AIBN] = 100:1:0.2, and RAFT polymerization was carried out for 24 h at 70 ^{o}C. After the reaction, the PCMB brush-modified substrate was washed with EtOH, ultrasonified in EtOH, repeatedly rinsed with MeOH, water and acetone, and finally dried with a flush of N_2 gas. The solution of PCMB produced in liquid phase at the same time was recovered and dialyzed in MeOH for a week. The PCMB solution was condensed by evaporation, dissolved in water, and finally lyophilized. The M_n and M_w/M_n values of obtained PCMB were determined by GPC (Wako beads G-50, Wako Pure Chemicals; mobile phase, 0.1 M NaBr aq. soln.).

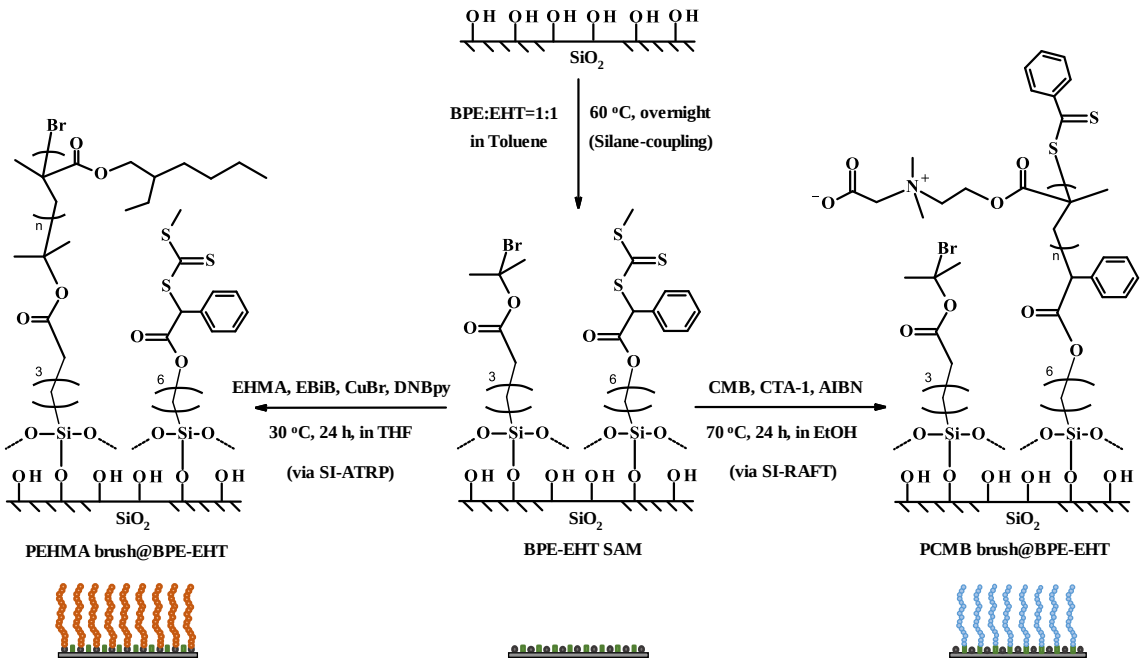

Scheme 5-1. ATRP and RAFT polymerization of EHMA and CMB, respectively.

5.2.3 UV Irradiation of substrate

The BPE-EHT mixed SAM-modified glass plate or silicon wafer was UV-irradiated at 254 nm (0.135 $mJ.cm^{-2}/s$, MODEL UVGL-58, UVP, USA). Afterwards the glass substrate or silicon wafer was washed with methanol and dried by a flush of N_2 gas.

5.2.4 Characterization of polymer brush

5.2.4.1 Wettability of substrate

Contact angle of the water droplet on the sample surface was measured for evaluating the surface wettability using a Drop Master DMs-401 (Kyowa Surface Science, Tokyo, Japan). Static contact angle, θ, of a sessile drop of water (1 µL) on the surface of polymer brush 30 s after placing the water drop on the surface was measured. The measurements were repeated 3 - 5 times on a sample to obtain a reliable average value (sessile drop method), and the average value of sessile drop was estimated for 3-4 samples.

5.2.4.2 XPS Measurements

X-ray photoelectron spectroscopy (XPS, ESCALAB 250Xi, Thermo Fisher Scientific, Inc., Waltham, Massachusetts, USA) was used for evaluating the elements on the substrate surface. A detection angle of 90^{o}, X-ray source of monochromated/micro-focused Al K-Alpha, and an X-ray size of 650 µm were used in the measurements. Analysis of the peak was carried out using the Avantage software (Ver. 4.84) from Thermo Fisher Scientific Corporation.

5.2.4.3 Adhesion of cells

Adhesion of NIH3T3 cells was observed on the polymer brush-modified substrate. Experimental procedures were the same as those reported elsewhere.[35,36]

5.3 Results and discussion

5.3.1 Preparation of PEHMA and PCMB in liquid phase

Two kinds of polymers, PEHMA and PCMB, were prepared by ATRP and RAFT polymerization, respectively, in liquid phase. At the ATRP of EHMA in THF, polymerization was carried out at various ratios of EHMA, EBiB, Cu(I)Br and DNBpy, and by the GPC measurements, the M_n and M_w/M_n values for the produced polymers were evaluated (**Table 5-1**). The table showed that the *DP* value was increased with an increase in the feeding ratio of EHMA. The M_w/M_n value for the produced polymers was sufficiently small, indicating that the controlled polymerization could be pursued.

Table 5-1. Preparation of PEHMA in liquid phase (solvent, THF)

[M] : [I] : [CuBr] : [L][a]	M_n **(×10^3)**	M_w **/** M_n[b]	***DP***
30 : 1 : 2 : 4	6.3	1.35	31.0
50 : 1 : 2 : 4	7.5	1.36	36.7
100 : 1 : 2 : 4	11.7	1.33	58.3
200 : 1 : 2 : 4	18.0	1.31	89.8
300 : 1 : 2 : 4	24.7	1.29	123.5
400 : 1 : 2 : 4	30.5	1.22	152.7

[a] M: EHMA, I: EBiB , L: DNBpy. [EHMA] = 1.0 M

[b] M_w / M_n was determined with GPC in chloroform.

At the RAFT polymerization of CMB in EtOH, furthermore, the polymerization was carried out in a similar manner to the ATRP of EHMA. The M_n and M_w/M_n values indicated that the polymerization was well controlled (**Table 5-2**). There were no significant changes in the molecular weight when the concentration of CMB was changed from 1.0 M to 0.5 M.

Based on the results in **Tables 5-1** and **5-2**, the polymerization of EHMA was pursued under the conditions [EHMA]:[EBiB]:[Cu(I)Br]:[DNBpy] = 200:1:1:2 ([EHMA] = 1.0 M), and that of CMB was [CMB]:[CTA-1]:[AIBN]= 100:1:0.2 ([CMB] = 0.5 M) hereafter.

Table 5-2. Preparation of PCMB in liquid phase (solvent, ETOH).

[M] : [I] : [R][a]	M_n **(×10^3)**	M_w **/** M_n [d]	***DP***
50 : 0.2 : 1 [b]	12.3	1.32	51.4
100 : 0.2 : 1 [b]	20.9	1.42	88.6
150 : 0.2 : 1 [b]	28.3	1.48	120.4
100 : 0.2 : 1 [c]	20.4	1.33	86.4

[a] M: CMB, I: AIBN, R: CTA-1. [b] [CMB] = 1 M. [c] [CMB] = 0.5 M.

[d] M_w / M_n was determined with GPC in 0.1 M NaBr aq.

5.3.2 Decomposition of surface-bound ATRP initiator by UV-irradiation

The ATRP initiator, BPE, could be easily introduced to a surface of the glass and silicon wafer as indicated by the drastic increase in contact angle (from 3.8 ^{o} (bare glass) to 69.4 ^{o} (after incubation with BPE)) as described in **Chapter 4**. Similarly, the contact angle of the RAFT

agent (EHT)-modified substrate was 62.8 °. Furthermore, the contact angle of the mixed SAM-modified substrate was between those for BPE and EHT (67.6 °), which is reasonable for the mixed SAM surface.

By the UV-irradiation of BPE-modified silicon wafer at 254 nm, XPS signal for bromine was observed to decrease, whereas the signals for other elements were not changed noticeably as reported before, indicating the selective scission of Br-C bond (**Chapter 4**). By the irradiation of 4000-5000 mJ/cm^2, the signal of Br atom was observed to be completely diminished. Furthermore, the XPS data for Si, C, O and S did not largely change with the irradiation, indicating that the EHT was hardly damaged with the irradiation. Therefore, it can be said that UV-irradiation can easily and selectively reduce the surface density of BPE on the mixed SAM-modified substrate (**Figure 5-2**).

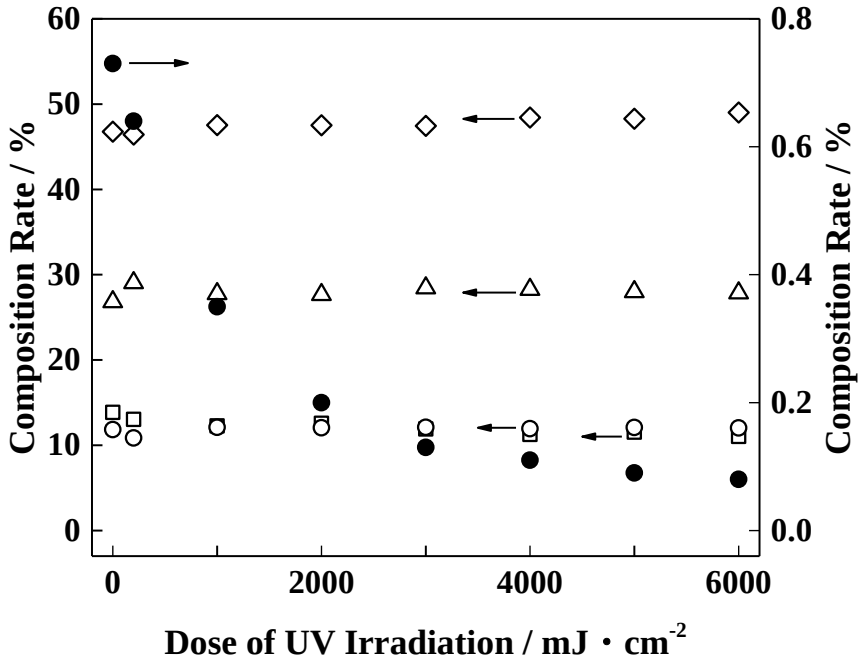

Figure 5-2. Effect of 254 nm-UV irradiation on the composition of elements at the surface of BPE-EHT-mixed SAM. ◊, Si; □, C; Δ, O; ○, S; ●, Br.

5.3.3 Construction of PEHMA and PCMB brushes

PEHMA brush could be easily constructed by the SI-ATRP at the BPE-modified glass and silicon wafer. By the introduction of PEHMA brush, the contact angle of the glass substrate drastically increased from 69.4 ^{o} (BPE-SAM) to 94.9 ^{o}, which is in agreement with the contact angle of PEHMA brush (*DP* = 36.7) constructed using (2-bromo-2-methyl)propionyloxyhexyltriethoxysilane (BHE) as SI-ATRP initiator (100.1 ± 1.0 ^{o}) (unpublished result). In contrast, PCMB brush constructed on BPE-EHT mixed SAM by RAFT method indicated a large hydrophilicity (θ = 8.8 ^{o}) (**Figure 5-3**). Thus, it was suggested that the PHEMA and PCMB brushes could be constructed on the BPE-EHT mixed SAM-modified surface.

XPS measurements indicated that, in the region of C_{1s}, the peak intensity of C-C (285 eV) for PEHMA was twice of that for PCMB. In addition, in the regions of C-O (287 eV) and C=O (289 eV) bonds, the peak intensity for PCMB was relatively larger than those for PEHMA. These results definitely indicated that, on the BPE-EHT mixed SAM surface, the PEHMA brush by ATRP and PCMB brush by RAFT polymerization method could be constructed (**Figure 5-4**).

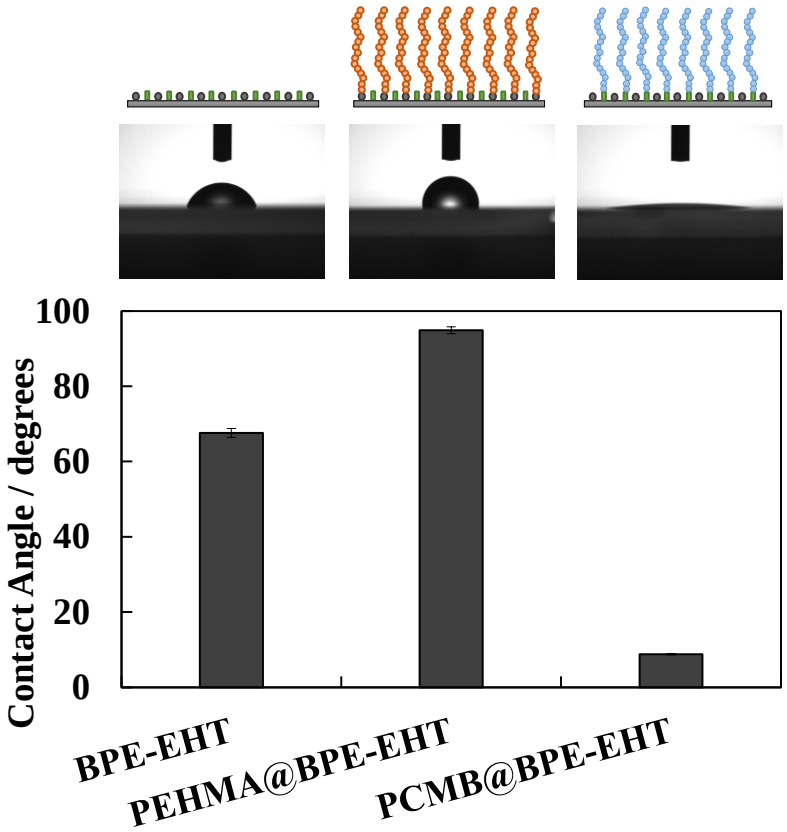

Figure 5-3. Wettability of polymer brush-modified surfaces.

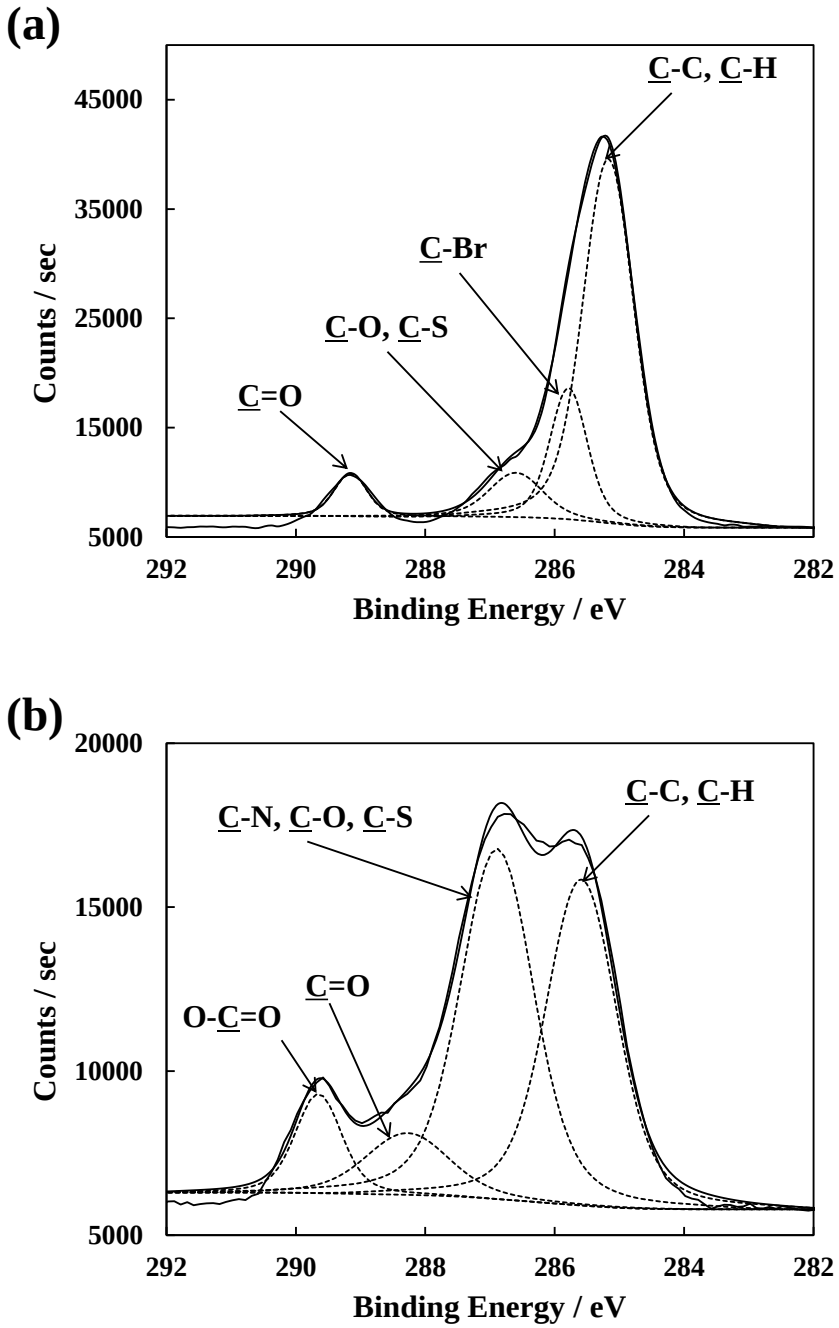

Figure 5-4. Carbon signal of (a) PEHMA brush and (b) PCMB brush on BPE-EHT-mixed SAM modified surface, respectively.

Previously, it was reported that the M_n and the M_w/M_n values for grafted and free polystyrene subjected to ATRP were nearly equal.[42] Assuming the same tendency is valid in the present work, i.e. the degree of polymerization of PEHMA brush is the same as that of

PEHMA produced in the solution phase at the same time, the degree of polymerization of PEHMA brush was estimated to be 89.8 using GPC. The M_n and M_w/M_n values of the PEHMA brush were estimated to be 1.8×10^4 and 1.31, respectively, which showed the relatively narrow molecular weight distribution of this polymer (**Table 5-1**).

The RAFT polymerization of CMB from the BPE-EHT SAM-modified substrate was pursued in a similar manner. Previously it was reported that the M_n and the M_w/M_n values for grafted and free polystyrene subjected to RAFT were nearly equal.[43] Therefore, assuming the same tendency is valid in the present work, the *DP*, M_n and M_w/M_n values of the PCMB brush were estimated to be 86.4, 2.0×10^4 and 1.33, respectively (**Table 5-2**).

The thickness of PEHMA brush and PCMB brush on the silicon wafer was determined to be 4.66 nm and 2.92 nm, respectively, by ellipsometry. The graft densities (σ) of the brushes were estimated to be 0.20 chains/nm^2 and 0.11 chains/nm^2, respectively, using equation (1).[42,43]

$$\sigma = \rho d \ N_A \times 10^{-21} / \ M_n \qquad (1)$$

where σ is the graft density (chains/nm^2), ρ is the polymer density (g/cm^3), N_A is Avogadro number, d is the thickness of polymer brush (nm), and M_n is the number-averaged molar mass of bulk polymer. The ρ value for PMMA (1.318 g/cm^3)[44] in the literature was used for calculating the surface density of the PEHMA brush. The ρ value for PMPC (1.30 g/cm^3)[45] available in the literature was used for calculating the surface density of the PCMB brush.

Based on the results described above, the construction of PEHMA brush via ATRP method and the construction of PCMB via RAFT method were confirmed. Further, both polymer brushes showed the high graft density (concentrated polymer brush) and narrow molecular weight distribution (the length of the brush chain was well controlled).

The PCMB brush was also easily constructed via SI-ATRP method as previously reported

(**Chapter 4**), but it was extremely difficult to introduce the PEHMA brush into BPE-EHT-mixed SAM or EHT SAM-modified surface via RAFT polymerization.

5.3.4 UV irradiation of polymer brushes

For a construction of binary polymer brush, SI-ATRP of EHMA was carried out at first and, subsequently, a SI-RAFT polymerization of CMB was pursued (**Figure 5-1**).

XPS data indicated that, at the first step (construction of PEHMA), the signal for C in the irradiated region was 13.9 % and much smaller than that for C_{1s} in the non-irradiated region (60.2 %). This is because the irradiation at 254 nm induced the selective cleavage of C-Br bond, and the ATRP of EHMA was largely inhibited. In contrast, the ATRP of EHMA could be easily pursued in the non-irradiated region (**Table 5-3**).

Furthermore, at the second step (RAFT polymerization of CMB), the signal of N_{1s} was 21 % in the irradiated region, and that in the non-irradiated region was nearly 0. This indicates that, in the PEHMA brush constructed at the first step, PCMB graft chain could not be grown, whereas, in the irradiated region, a very few PEHMA graft chains allowed the growth of PCMB graft chains (**Table 5-3**).

Table 5-3. Composition of elements at the surface of various polymer brushes.

	Domain	Si	C	O	S	Br	N
Step I	PEHMA@BPE-EHT_Non UV	17.0	60.2	17.7	4.9	0.3	0
	PEHMA@BPE-EHT_UV	46.3	13.9	28.2	11.6	0	0.1
Step II	PEHMA-PCMB@BPE-EHT_Non UV	16.0	61.2	17.4	4.8	0.2	0.3
	PEHMA-PCMB@BPE-EHT_UV	33.0	30.7	26.1	8.1	0	2.1

The XPS data of the two-step polymerization of PEHMA and PCMB chains at various irradiation doses was examined (**Figures 5-5 (a)** and **(b)**). By the increase in irradiation dose, the signal intensities of Br_{3d} and C_{1s} were decreased and that for Si_{2p} was increased. This is because, due to the decomposition of C-Br bond, the amount of PEHMA chain first produced on the substrate was decreased, and resultingly, the influence of the signal for Si_{2p} corresponding to the substrate itself was increased. In the second step, at the small irradiation dose, the growth of PCMB brush in the region of PEHMA brush was not so significant, giving a small N_{1s} intensity. With an increase in irradiation dose, on the contrary, the signal of C_{1s} for PEHMA was decreased, and the contents of N_{1s} corresponding to the PCMB brush was increased.

Previously, it was reported that the control of UV irradiation of BPE SAM enabled the modulation of the surface density of PCMB brush produced by the SI-ATRP.[38] Therefore, an increase in the density of PEHMA brush inhibited the penetration of PCMB brush, and a decrease in the density of PEHMA brush allowed the growth of PCMB brush. These results indicated that, by the control of irradiation dose, the composition of binary brush could be regulated.

To confirm the effect of UV irradiation on the RAFT agent (EHT), polymerization of CMB was carried out on the BPE-EHT-mixed SAM surface. With an increase in irradiation dose, there were no significant changes in N_{1s} for PCMB chains (**Figure 5-5 (c)**). In addition, there was no effect of irradiation dose on the contact angle of PCMB brush constructed via RAFT polymerization, either (**Figure 5-6**).

Ellipsometric measurements indicated that the ATRP of EHMA induced an increase in thickness from 0.60 nm to 4.66 nm. In the UV-irradiated region, the thickness of the layer was 0.63 nm, and there was no significant difference in thickness from that for the initiator SAM, indicating the absence of growth of PEHMA brush. As for the secondary construction of PCMB brush, the thickness in the non-irradiated region, in other words, the PEHMA brush

region, was 4.82 nm, indicating no significant changes. However, the thickness in the irradiated region was 1.96 nm, indicating the construction of PCMB brush.

Using equation (1) and the data of thickness shown in **Table 5-4**, the graft density of polymer brush was evaluated. Similar to the tendency of the thickness, the construction of PEHMA brush and that of the PCMB brush were confirmed in the irradiated region and in the non-irradiated region, respectively. However, the density of PCMB brush (0.08 chains/nm^2) was much smaller than that of PEHMA brush (0.21 chains/nm^2), indicating the possibility that, though the feeding ratio of BPE and EHT was 1:1, the actual composition of BPE-EHT SAM was not 1:1 but around 2:1. This is due to the bulkiness of aromatic ring corresponding to the EHT molecule, which results in the less dense SAM of EHT than that of BPE. A similar tendency was observed in **Chapter 2**. The graft density of PolyGUMA brush having the RAFT agent with an aromatic ring at the end of brush was lower than the case without aromatic group.

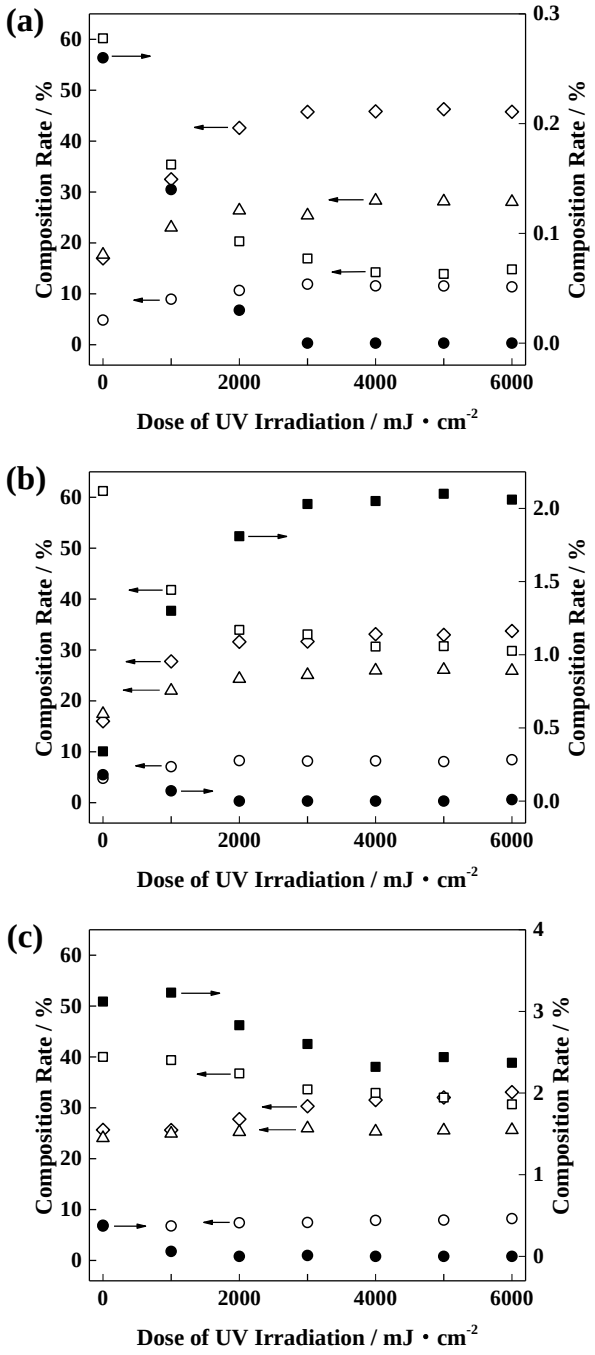

Figure 5-5. Effect of UV irradiation on the composition of elements at the surface of polymer brushes. ◊, Si; □, C; Δ, O; ○, S; ●, Br; ■, N. (a) PEHMA brush constructed by SI-ATRP on the BPE-EHT mixed SAM which had been UV-irradiated at various doses. (b) Binary brush (PEHMA-PCMB@BPE-EHT) which was prepared by sequential polymerization of EHT (SI-ATRP) and CMB (SI-RAFT) on the BPE-EHT mixed SAM which had been UV-irradiated at various doses. (c) PCMB brush constructed by SI-RAFT on the BPE-EHT mixed SAM which had been UV-irradiated at various doses.

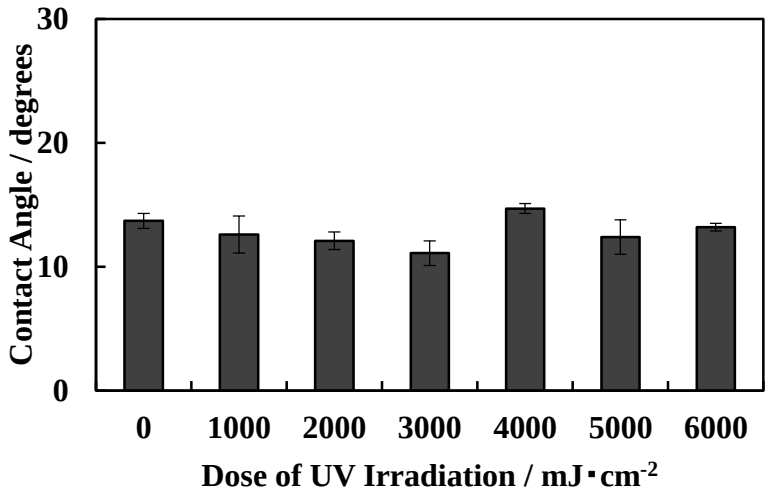

Figure 5-6. Effect of irradiation dose on the contact angle of PCMB brush constructed on the BPE-EHT mixed SAM.

Table 5-4. Characterization of various polymer brushes.

Samples		Thickness (nm)	Graft density (chains·nm^{-2})
BPE-EHT-mixed SAM		0.60 ± 0.03	n.d.
Step I [a]	PEHMA@BPE-EHT_Non UV	4.66 ± 0.23	0.20 ± 0.01
	PEHMA@BPE-EHT_UV	0.63 ± 0.02	0.03 ± 0.001
Step II [b]	PEHMA-PCMB@BPE-EHT_Non UV	4.82 ± 0.18	0.21 ± 0.01
	PEHMA-PCMB@BPE-EHT_UV	1.96 ± 0.05	0.08 ± 0.002

[a] PEHMA brush constructed on BPE-EHT-mixed SAM with non-irradiated domain and irradiated domain.

[b] PCMB brush constructed on PEHMA@BPE-EHT surface (included non-irradiated domain and irradiated domain) that had been prepared at Step I.

5.3.5 Patterning with PEHMA and PCMB brushes

When the two-step (sequential) polymerization was carried out using a photomask, the contact angle in the non-irradiated region was not changed (*ca*. 95 °), whereas that in the irradiated region was largely decreased to *ca*. 30 °, which means that, by the irradiation at 254 nm, both hydrophobic and hydrophilic regions can be modulated on the same substrate (**Figure 5-7(a)**). In addition, an increase in irradiation dose gradually changed the wettability of the substrate from hydrophobic to hydrophilic (**Figure 5-7 (b)**). This is consistent with the composition of elements determined by XPS data (**Figure 5-5 (b)**). Therefore, the regulation of mixing ratio of binary polymer brush (PEHMA-PCMB) is possible. Furthermore, there was no significant effect of irradiation on the wettability of the PCMB brush.

The PCMB brush could easily be constructed in both UV-irradiated and non-irradiated regions, which indicated that the SAM of RAFT agent (EHT) was not noticeably damaged by the UV-irradiation at 254 nm. The decrease in contact angle for the PEHMA brush after UV-irradiation of BPE-EHT mixed SAM and subsequent SI-ATRP was due to the decomposition of the ATRP initiator (BPE) giving the less condensed PEHMA brush. The decrease in contact angle for the mixed polymer brush after UV-irradiation could also be attributed to the same reason.

When a water droplet was put on the patterned mixed polymer brush, water was definitely localized above the PCMB-modified domain (**Figure 5-8**). Therefore, it is suggested that the hydrophilic/hydrophobic patterning with on/off of the UV irradiation can be readily pursued. Furthermore, micrograph of the mixed polymer brushes indicated patterning of cells adhered to the PEHMA brush domains (**Figure 5-9**).

Such technique will be quite useful for application of both bio-inert polymer brush and adhesive polymer brush to biomedical fields.

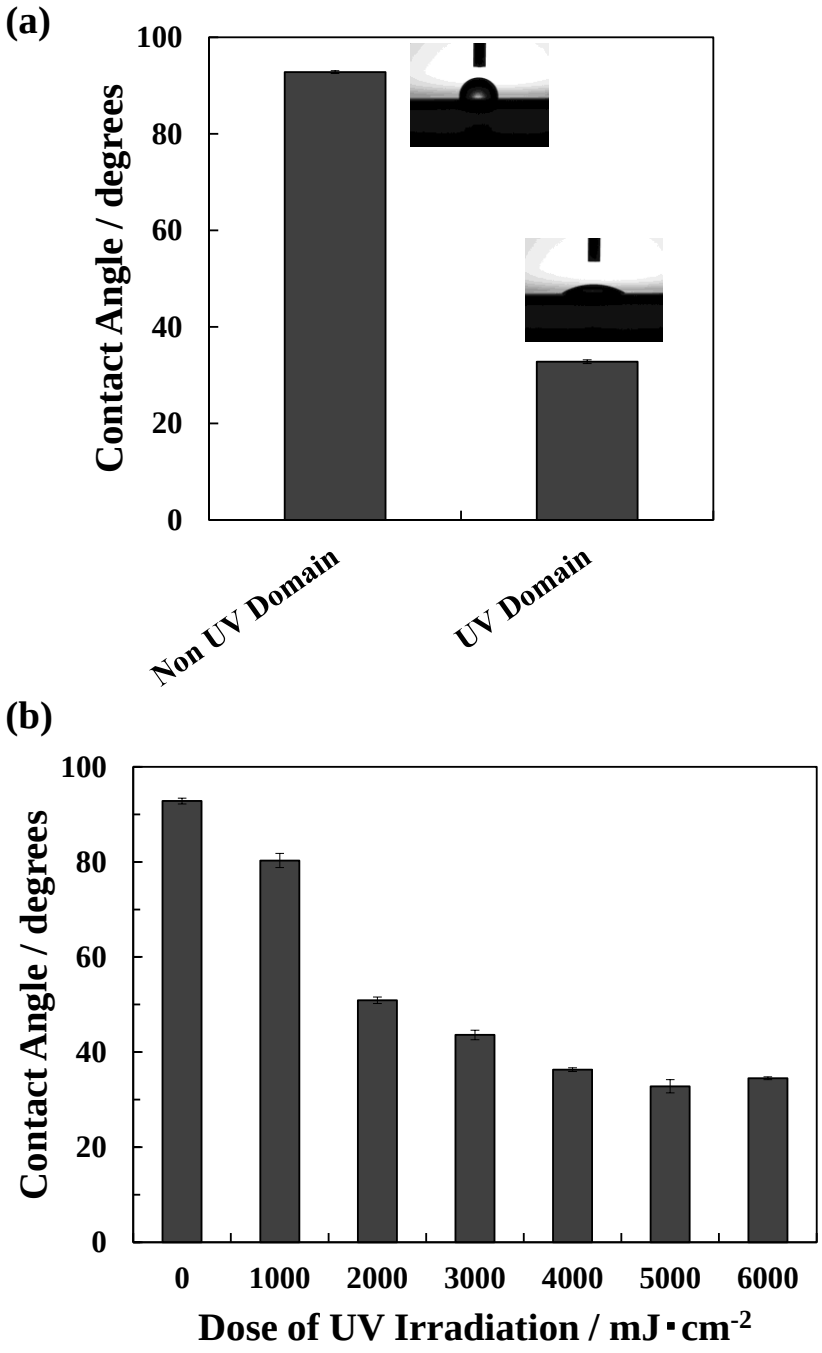

Figure 5-7. Contact angle of polymer brush (PEHMA-PCMB@BPE-EHT) which was prepared by sequential polymerization of EHT (SI-ATRP) and CMB (SI-RAT) on the BPE-EHT mixed SAM. (a) Non-irradiated and irradiated domains. (b) Effect of irradiation dose on the contact angle of binary polymer brush (PEHMA-PCMB@BPE-EHT) which was prepared by sequential polymerization of EHT (SI-ATRP) and CMB (SI-RAT) on the BPE-EHT mixed SAM.

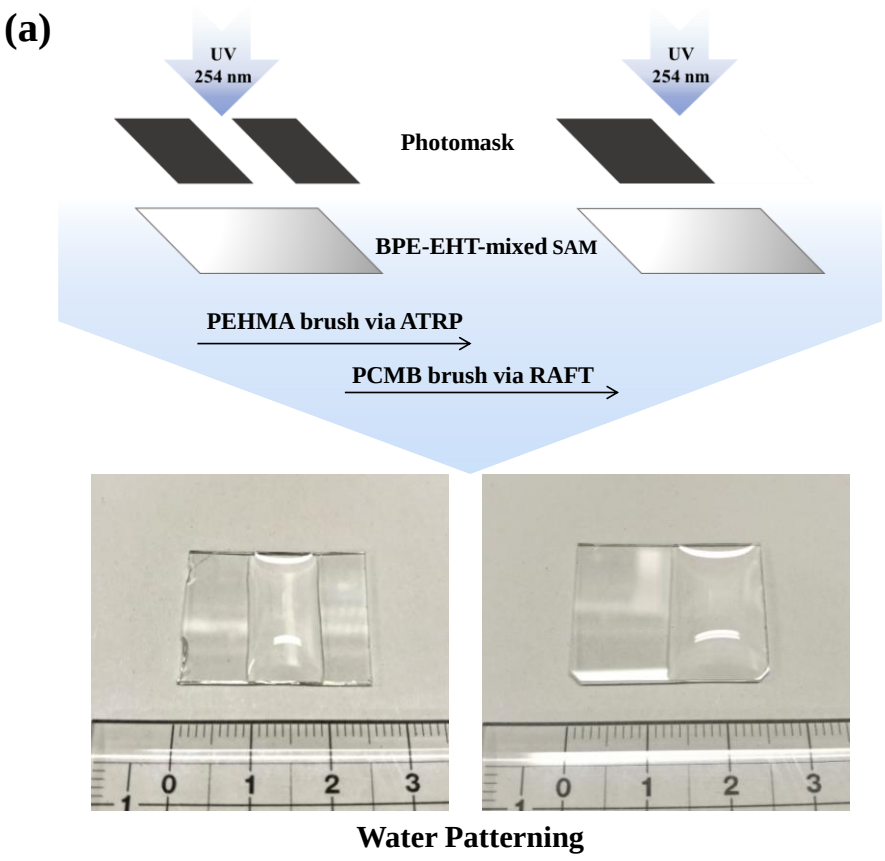

Figure 5-8. Water layer above the binary polymer brush.

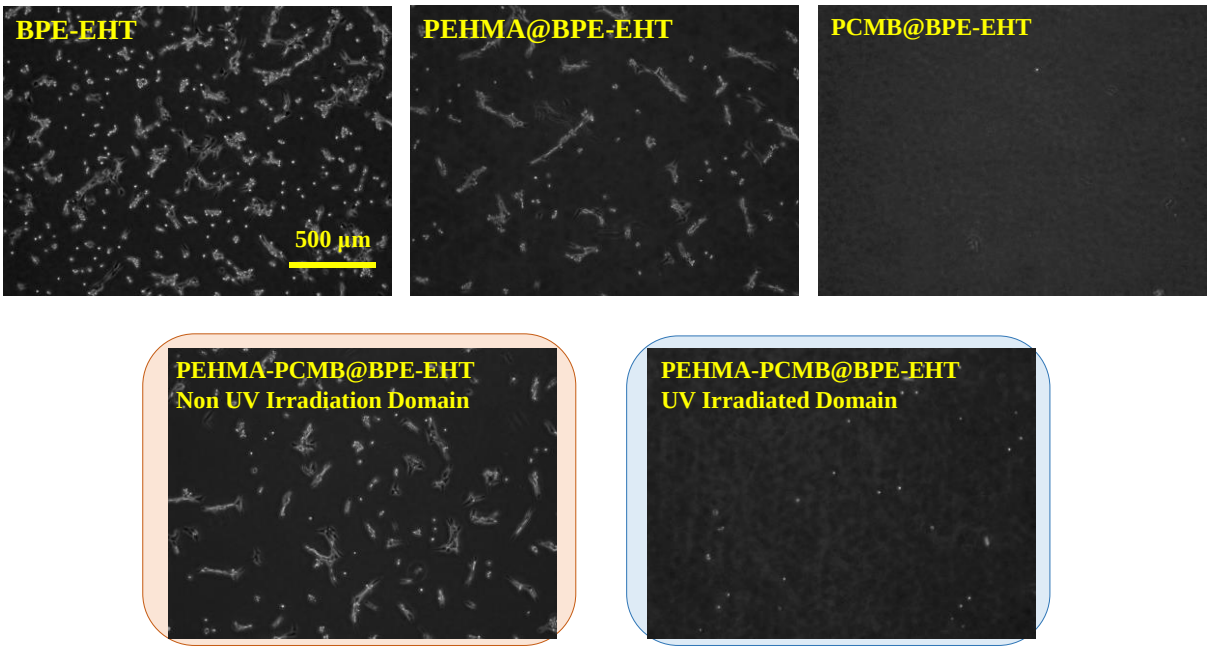

Figure 5-9. Micrographs of 3T3 cells adhered onto various surfaces. BPE-EHT: BPE-EHT-mixed SAM-modified surface. PEHMA@BPE-EHT: PEHMA brush constructed on non-irradiated BPE-EHT-mixed SAM. PCMB@BPE-EHT: PCMB brush constructed on non-irradiated BPE-EHT-mixed SAM. PEHMA-PCMB@BPE-EHT: Binary polymer brushes on non-irradiated and irradiated BPE-EHT-mixed SAM.

5.4 Conclusion

By the UV irradiation, a bromine atom at the end of ATRP initiator SAM introduced to the surface of glass and silicon wafer could be easily and selectively cleaved and the surface density of PEHMA brush produced by the SI-ATRP could be controlled by the regulation of irradiation time. By the subsequent RAFT polymerization of CMB, the surface density of the cells adhered to the brush could be easily regulated, suggesting the control of the adsorbed amount of proteins to which cells adhered. By the sequential polymerization of EHMA by SI-ATRP and CMB by SI-RAFT polymerization after UV irradiation through a photomask, the author could construct the patterned binary polymer brush composed of anti-biofouling PCMB domain (UV-irradiated region) and fouling PEHMA domain (non-irradiated region), indicating practical usability of the adopted procedures in biomedical fields.

5.5 References

[1] Ishihara, K.; Aragaki, R.; Ueda, T.; Watanabe, A.; Nakabayashi, N. *J. Biomed. Mater. Res.* **1990**, *24*, 1069.

[2] Kitano, H.; Suzuki, H.; Matsuura, K.; Ohno, K. *Langmuir* **2010**, *26*, 6767.

[3] Fujishita, S.; Inaba, C.; Tada, S.; Gemmei-Ide, M.; Kitano, H.; Saruwatari, Y. *Biol. Pharm. Bull.* **2008**, *31*, 2309.

[4] Tada, S.; Inaba, C.; Mizukami, K.; Fujishita, S.; Gemmei-Ide, M.; Kitano, H.; Mochizuki, A.; Tanaka, M.; Matsunaga, T. *Macromol. Biosci.* **2009**, *9*, 63.

[5] Nishida, M.; Nakaji-Hirabayashi, T.; Kitano, H.; Matsuoka, K.; Saruwatari, Y. *J. Biomed. Mater. Res. Part A.* **2016**, *104A*, 2029.

[6] Kitano, H.; Sudo, K.; Ichikawa, K.; Ide, M.; Ishihara, K. *J. Phys. Chem. B.* **2000**, *104*, 11425.

[7] Kitano, H.; Imai, M.; Sudo, K.; Ide, M. *J. Phys. Chem. B* **2002**, *106*, 11391.

[8] Kitano, H.; Imai, M.; Mori, T.; Gemmei-Ide, M.; Yokoyama, Y.; Ishihara, K. *Langmuir* **2003**, *19*, 10260.

[9] Kitano, H.; Tada, S.; Mori, T.; Takaha, K.; Gemmei-Ide, M.; Tanaka, M.; Fukuda, M.; Yokoyama, Y. *Langmuir* **2005**, *21*, 11932.

[10] Kondo, T.; Nomura, K.; Murou, M.; Gemmei-Ide, M.; Kitano, H.; Noguchi, H.; Uosaki, K.; Ohno, K.; Saruwatari, Y. *Colloids Surfaces B: Biointerfaces* **2012**, *100*, 126.

[11] Kitano, H. *Polym. J.* **2016**, *48*, 15.

[12] Brittain, W. J.; Minko, S. *J. Polym. Sci. A: Polym. Chem.* **2007**, *45*, 3505.

[13] Kato, M.; Kamigaito, M.; Sawamoto, M.; Higashimura, T. *Macromolecules* **1995**, *28*, 1721.

[14] Wang, J. S.; Matyjaszewski, K. *J. Am. Chem. Soc.* **1995**, *117*, 5614.

[15] Matyjaszewski, K.; Xia, *J. Chem. Rev.* **2001**, *101*, 2921.

[16] Barner-Kowollik, C. *Handbook of RAFT Polymerization*. (**2008**) Weinheim: Germany.

[17] Mitsukami, Y.; Donovan, M. S.; Lowe, A. B.; McCormick, C. L. *Macromolecules* **2001**, *34*, 2248.

[18] McCormick, C. L.; Lowe, A. B. *Acc. Chem. Res.* **2004**, *37*, 312.

[19] Hawker, C. J.; Bosman, A. W.; Harth, E. *Chem. Rev.* **2001**, *101*, 3661.

[20] Ohno, K.; Izu, Y.; Tsujii, Y.; Fukuda, T.; Kitano, H. *Eur. Polym. J.* **2004,** *40*, 81.

[21] Ahmada, S. A.; Leggetb, G. J.; Hucknal, A.; Chilkoti, A. *Biointerfaces* **2011**, *6*, 8.

[22] Matsuura, K.; Ohno, K.; Kagaya, S.; Kitano, H. *Macromol. Chem. Phys.* **2007**, *208*, 862.

[23] Kitano, H.; Kawasaki, A.; Kawasaki, H.; Morokoshi, S. *J. Colloid Interface. Sci.* **2005**, *282*, 340.

[24] Suzuki, H.; Murou, M.; Kitano, H.; Ohno, K.; Saruwatari, Y. *Colloids Surfaces B: Biointerfaces* **2011**, *84*, 111.

[25] Kitano, H.; Tokuwa, K.; Ueno, H.; Li, L.; Saruwatari, Y. *Colloid Polymer Sci.* **2015**, *293*, 2931.

[26] Nakamura, M.; Mir, T. A..; Arai, K.; Ito, S.; Yoshida, T.; Iwanaga, S.; Kitano, H.; Obara, C.; Nikaido, T. *Intl. J. Bioprinting* **2015**, *1*, 39.

[27] Quan, H.; Zhang, X.; Lu, H; Huang, Z. Centr. *Eur. J. Chem.* **2012,** *10*, 1624.

[28] Draper, J.; Luzinov, I.; Minko, S.; Tokarev, I.; Stamm, M. *Langmuir* **2004**, *20*, 4064.

[29] Serrano-Ruiz, D.; Rangou, S.; Avgeropoulos, A.; Zafeiropoulos, N. E.; López-Cabarcos, E.; Rubio-Retama, J. *J. Polym. Sci. Part. B.* **2010**, *48*, 1668.

[30] Julthongpiput, D.; Lin, Y. H.; Teng, J.; Zubarev, E. R.; Tsukruk, V. V. *Langmuir* **2003**, *19*, 7832.

[31] Berger, S.; Synytska, A.; Ionov, L.; Eichhorn, K. J.; Stamm, M. *Macromolecules* **2008**, *41*, 9669.

[32] Jiang, X.; Zhao, B.; Zhong, G.; Jin, N.; Horton, J. M.; Zhu, L.; Hafner, R. S.; Lodge, T. P. *Macromolecules* **2010**, *43*, 8209.

[33] Ye, P.; Dong, H.; Zhong, M.; Matyjaszewski, K. *Macromolecules* **2011**, *44*, 2253.

[34] Kitano, H.; Suzuki, H.; Kondo, T.; Sasaki, K.; Iwanaga, S.; Nakamura, M.; Ohno, K.; Saruwatari, Y. *Macromol. Biosci.* **2011**, *11*, 557.

[35] Kitano, H.; Kondo, T.; Kamada, T.; Iwanaga, S.; Nakamura, M.; Ohno, K. *Colloids Surfaces B: Biointerfaces* **2011,** *88*, 455.

[36] Suzuki, H.; Li, L.; Nakaji-Hirabayashi, T.; Kitano, H.; Ohno, K.; Matsuoka, K.; Saruwatari. Y. *Colloids Surfaces B: Biointerfaces* **2012**, *94*, 107.

[37] Kamada, T.; Yamazawa, Y.; Nakaji-Hirabayashi, T.; Kitano, H.; Usui, Y.; Hiroi, Y.; Kishioka, T. *Colloids Surfaces B: Biointerfaces* **2014**, *123*, 878.

[38] Okuda, Y. (**2000**) Japan Patent 3032155.

[39] Mukaiyama, T.; Ninoi, T.; Okuda, Y.; Uchiyama, Y. (**2006**) Japan Patent 3878315.

[40] Ohno, K.; Akashi, T.; Huang, Y.; Tsujii, Y. *Macromolecules* **2010**, *43*, 8805.

[41] Ohno, K.; Ma, Y.; Huang, Y.; Mori, C.; Yahata, Y.; Tsujii, Y.; Maschmeyer, T.; Moraes, J.; Perrier, S. *Macromolecules* **2011**, *44*, 8944.

[42] Ohno, K.; Morinaga, T.; Koh, K.; Tsujii, Y.; Fukuda, T. *Macromolecules* **2005**, *38*, 2137.

[43] Tsujii, Y.; Ejaz, M.; Sato, K.; Goto, A.; Fukuda, T. *Macromolecules* **2001**, 34, 8872.

[44] Brandrup, J.; Immergut, E. H.; Grulke. E. A.; Abe, A.; Bloch, D. R. *Polymer Handbook-4th Edition*, **2003**, Wiley-Interscience.

[45] Iwata, R.; Suk-In, P.; Hoven, V. P.; Takahara, A.; Akiyoshi, K.; Iwasaki, Y. *Biomacromolecules* **2004**, 5, 2308.

Chapter 6

Conclusion

In this thesis, it was shown that various functions (highly hydrophilic, suppression ability of protein adsorption and cell adhesion) required as medical materials, can be introduced into the surface of solid material by the surface modification with the biocompatible polymer（poly[2-deoxy-2-*N*-(2-methacryloyloxyethyl)aminocarbamyl *D*-glucose] (PGUMA) or poly[1-carboxy-*N*,*N*-dimethyl-*N*-(2-methacryloyloxyethyl)methanaminium hydroxide inner salt] (PCMB)). Further, by combining these surfaces with the technology of surface micro-fabrication by the irradiation of ultraviolet (UV) or ion beam (IB), the construction of the specific patterning/gradation of biological substance like proteins and cells could be pursued.

In **Chapter 2**, a polymer brush with pendent PGUMA was obtained by surface-initiated reversible addition-fragmentation chain transfer (SI-RAFT) polymerization of GUMA on the substrate. The linear relationship between the loge ($[M]_o/[M]$) value and the reaction conversion, and the small polydispersity in *M*w/*M*n value of PGUMA produced in liquid phase at the same time suggested that the polymerization proceeded in a living manner. The bicinchoninic acid method indicated that the PGUMA brush was significantly resistant against non-specific adsorption of bovine serum albumin (BSA) and lysozyme (egg white). Furthermore, the adhesion of cells such as HepG2, and HEK293 cells was strongly suppressed by the presence of PGUMA brush. Such glucosylurea group-carrying polymer brush prepared here might be quite useful to provide a ‘‘bio-inert (anti-biofouling)’’ surface in bio-medical fields.

Subsequently, IB irradiation was used to prepare a heart-shaped patterning of PGUMA brush surface. By performing the experimentals of cell adhesion, a patterning of cells that the

irradiated area was covered with cells while no cells attached to other area was observed, and anti-biofouling properties of the PGUMA brush was definitely indicated.

A similar approach of IB irradiation is also used on the copolymer (poly(CMB-r-MPTMS))-modified surface to prepare a heart-shaped patterning of cells, as reported in our research group previously. The reforming and cell patterning of poly(CMB-*r*-MPTMS)-modified surface was easily realized by the IB irradiation, but a problem that IB irradiation is not suitable as a method to reform large area still remained. In contrast, the surface reforming by UV irradiation showed that, although the photomask pattern is necessary for the purpose, it is advantageous in convenience that a large area can quickly reforming in one shot.

Therefore, in **Chapter 3**, the author carried out the UV irradiation at 193 nm (an excimer laser, ArF) into copolymer layer-modified surface and observed a patterning of the fluorophore-labeled protein. The thin layer composed of random copolymer of CMB monomers and *p*-trimethoxysilylstyrene (STMS) monomers (or 3-methacryloxypropyltrimethoxysilane (MPTMS)) (9:1) was easily constructed on a glass substrate or a silicon wafer by covalent bonding (silane-coupling reaction). The copolymer layer was highly resistant against non-specific adsorption of BSA. However, on ArF-UV irradiation at 193 nm, the layer became hydrophobic and BSA was significantly adsorbed on the substrate. Therefore, upon UV irradiation through a photomask, a patterning of the fluorophore-labeled protein with a resolution of about 1 μm could be clearly observed. On the other hand, the copolymer layer of CMB and 3-methacryloxypropyltrimethoxysilane (MPTMS) (9:1) without an aromatic group exhibited less distinct pattern. Further, the poly(CMB-*r*-STMS) layer decomposed more quickly compared with the poly(CMB-*r*-MPTMS) layer at low irradiation dose. Hence, the efficient cleavage of the layer upon UV-irradiation makes poly(CMB-*r*-STMS) highly useful in diverse biomedical applications.

In **Chapter 4**, an approach by the UV irradiation at 254 nm was applied on the surface that was covered with a self-assembled monolayer (SAM) of a 2-bromoisobutyryl end group-

carrying initiator for atom transfer radical polymerization (ATRP) via the silane-coupling reaction. When the initiator SAM was irradiated with UV light at 254 nm, the surface density of bromine atoms was reduced by the scission of C-Br bonds as observed by XPS. With the surface-initiated ATRP of the CMB monomer, the surface density of PCMB brushes could be easily varied by changing the irradiation period of UV light prior to the polymerization. Furthermore, by using a UV-cut shutter sliding above the initiator SAM-modified substrate at a constant speed, the degree of bromine atom removal could be linearly varied along the direction of movement of the shutter.

This approach does not require the high-energy light/beams sources such as ArF-excimer laser and focused ion beams, there is a great advantage that normal UV light source is sufficient for surface fabrication. Although the irradiation takes time, it is rather advantageous to produce the gradient with a good reproducibility by the movement of the shutter. Consequently, the amount of both proteins adsorbed and cells adhered to the PCMB brush-covered substrate could easily be controlled by the gradation of the surface density of PCMB brushes, which suppressed protein adsorption and cell adhesion. Such a technique is very simple and useful for the regulation of the surface density of adsorbed proteins and adhered cells on an originally bio-inert surface.

Based on the results of **Chapter 4**, the author tried a patterning with two kinds of polymer brush domain on mixed SAM by using the 254 nm-UV irradiation, and introduced in **Chapter 5**.

In **Chapter 5**, a mixed SAM of an initiator (3-(2-Bromo-2-isobutyryloxy)propyl triethoxysilane, BPE) for ATRP and an agent (6-(triethoxysilyl)hexyl 2-(((methylthio)carbonothioyl)thio)-2-phenylacetate, EHT) for RAFT polymerization was constructed on a surface of silicon wafer or glass substrate. Then, the 254 nm-UV was irradiated at the mixed SAM through a photomask to selectively decompose the C-Br bond of BPE. At the surface-initiated ATRP of 2-ethylhexyl methacrylate (EHMA), consequently, the shape and

size of PEHMA brush domain could be very easily modulated. Subsequently, surface-initiated RAFT polymerization of CMB monomer, was carried out. Using the sequential polymerization, a patterning of PCMB and PEHMA brush domains on the solid substrate could be very easily pursued. Since the PCMB brush indicated anti-biofouling properties and the PEHMA brush had non-polar properties, the patterning with biocompatible (hydrophilic) domain and adhesive (hydrophobic) domain could be realized. Such a micro-fabrication technique is very simple and useful for the construction of complex surface including different domain of polymer brush.

Thus, this thesis showed the construction of surface having ability suppressing the adhesion of the biological substance, by combining the biocompatibility polymer with various surface reforming methods/techniques. Also, the biocompatibility polymer surface is expected to be applied as biomaterial. Further, it showed that is possible to construct specific patterning and concentration gradient (gradation) of biological materials such as proteins and cells. These techniques could be very useful for the macro-fabricating patterned surfaces that could be suitable as cell arrays for the screening of novel drugs and the evaluation of cell migration and chemotaxis. Therefore, the author believes that they can contribute to the further development of biomaterial/cell biology/molecular biology in the future.

List of Publications

1. Hiromi Kitano, Yan Liu, Ken-ichi Tokuwa, Lifu Li, Shintaroh Iwanaga, Masato Nakamura, Naoki Kanayama, Kohji Ohno, Yoshiyuki Saruwatari

"Polymer Brush with Pendent Glucosylurea Groups Constructed on a Glass Substrate by RAFT Polymerization"

European Polymer Journal, **2012**, *48*, 1875-1882.

2. Lifu Li, Tadashi Nakaji-Hirabayashi, Ken-ichi Tokuwa, Hiromi Kitano, Kohji Ohno, Yuki Usui, Takahiro Kishioka

"UV-Patterning of Anti-Biofouling Zwitterionic Copolymer Layer with an Aromatic Anchor Group"

Macromolecular Materials and Engineering, **2016**, DOI: 10.1002/mame.201600374.

3. Lifu Li, Tadashi Nakaji-Hirabayashi, Hiromi Kitano, Kohji Ohno, Takahiro Kishioka, Yuki Usui

"Gradation of Proteins and Cells Attached to the Surface of Bio-Inert Zwitterionic Polymer Brush"

Colloids and Surfaces B: Biointerfaces **2016**, *144*, 180-187.

4. Lifu Li, Tadashi Nakaji-Hirabayashi, Hiromi Kitano, Kohji Ohno

"A Novel Approach for Patterning with Binary Polymer Brushes"

In preparation.

Other Publications

Article

1. Hisatomo Suzuki, Lifu Li, Tadashi Nakaji-Hirabayashi, Hiromi Kitano, Kohji Ohno, Kazuyoshi Matsuoka, Yoshiyuki Saruwatari

"Carboxymethylbetaine Copolymer Layer Covalently Fixed to a Glass Substrate"

Colloids and Surfaces B: Biointerfaces **2012**, *94*, 107-113.

2. Hiromi Kitano, Ken-ichi Tokuwa, Haruka Ueno, Lifu Li, Yoshiyuki Saruwatari,

"Zwitterionic Polymer-Grafted Microspheres Prepared by RAFT Polymerization"

Colloid and Polymer Science **2015**, *293*, 2931-2939.

Book

1. 北野 博巳、李 黎夫、中路 正,

「双性イオン型高分子シランカップリング剤と応用」,

『シランカップリング剤の効果と使用方法』,

サイエンス&テクノロジー株式会社, 2012 年 11 月 15 日発刊.

Acknowledgements

First and foremost, I would like to express my sincere gratitude to Professor Hiromi Kitano not only for his constant guidance, encouragement, valuable discussion and detailed criticism on the manuscript throughout this study but also for guidance of the exotic life.

I also would like to convey my appreciation to Associate Professor Tadashi Nakaji-Hirabayashi for his constant guidance, intimate suggestions, significant advice, devoted leading and encouragement throughout the present work. The completion of the present research has been an existing project and one which would not have been possible without his guidance.

I am sincerely wish to express appreciation to Dr. Kohji Ohno, Associate Professor of the Institute for Chemical Research, Kyoto University, for his constant guidance and provision of the ATRP initiator BPE and the RAFT agents EHT.

I wish to thank Professor Koji Tohda, Professor Hitoshi Abe, Professor Hiroyuki Higuchi, Associate Professor Hajime Abe, and Associate Professor Makoto Gemmei-Ide in Department of Advanced Nano- and Biosciences, Graduate School of Innovative Life Sciences, University of Toyama, for their constant advice and encouragement.

I would like to thank Associate Professor Kensaku Itou in Graduate School of Science and Engineering for Education, University of Toyama, for his constant advice and encouragement.

I also would like to thank Dr. Hisatomo Suzuki, Mr. Masanobu Murou, Miss Yan Liu, Mr. Tomohiro Kamada, Mr. Sho Saito, Mr. Koutaro Miyajima, Mr. Kouji Nomura, Mr. Ken-ichi Tokuwa, and other members of Professor Kitano' laboratory and of the Graduate School of Science and Engineering for Education, University of Toyama for their kind help.

I am grateful to Osaka Organic Chemical Industry and ShinEtsu Chemicals for their kind provision of CMB (GLBT®) and EHMA, and STMS (KBM1403®), respectively.

I greatly would like to express my gratitude to the Kobayashi International Scholarship Foundation for the support of scholarship (2011~2014).

I also would like to thank Dr. Noritatsu Tsubaki, Professor of Science and Engineering for Education, University of Toyama, for his help and constant advice, when I came to Japan.

I wish to express deep appreciation to my uncle, Dr. Ruixue Li, Professor of Graduate School of Business Administration, Hosei University for his constant guidance and encouragement.

I express my deep gratitude to my father, Ruimin Li, my mother, Quanqin Jia, my younger brother, Dr. Kun Li, and other members of my big family for their cordial support and continuous encouragement.

Finally, my pretty wife Qi Wan, my sweet daughter Yinuo, my love for you two is beyond words!

March, 2017

Toyama

"To change the world ~"

Lifu Li

李　黎夫

リ　レイオ